

THESIS FOR THE DEGREE OF DOCTOR OF PHILOSOPHY (PhD)

The functional role of Ca²⁺-and voltage-gated potassium channels in activated human T cells and fibroblast-like synoviocytes

by Zoltán Dénes Pethő

Supervisor: Zoltán Varga, PhD



UNIVERSITY OF DEBRECEN

DOCTORAL SCHOOL OF MOLECULAR MEDICINE

Debrecen, 2017

TABLE OF CONTENTS

LIST OF ABBREVIATIONS.....	3
1. PREFACE.....	5
2. SCIENTIFIC BACKGROUND	6
2.1. General characteristics of ion channels	6
2.1.1. <i>Overview of potassium channels</i>	6
2.1.2. <i>The Ca²⁺ release- activated Ca²⁺ channel</i>	8
2.1.3. <i>Specific regulatory subunits of ion channels</i>	9
2.1.4. <i>Modes of ion channel inhibition</i>	12
2.2. Ion channels as key regulators of the immune system	16
2.2.1. <i>Ion channels regulate the T cell mediated immune response</i>	18
2.2.2. <i>Role of potassium channels in autoimmunity</i>	20
2.3. Modes of physiological and <i>in vitro</i> T lymphocyte activation	22
2.3.1. <i>Ion channel inhibitors and rapamycin impair the T cell-mediated immune response</i>	24
2.4. Fibroblast-like synoviocytes are key effectors in rheumatoid arthritis.....	27
2.4.1. <i>Ion channels influence the phenotype of RA-FLS</i>	28
2.4.2. <i>KCa1.1 as a possible therapeutic target</i>	30
3. AIMS OF THE STUDY	32
4. MATERIALS AND METHODS.....	33
4.1. Reagents	33
4.2. Isolation and culture of peripheral blood mononuclear cells	33
4.2.1. <i>Selective stimulation of T lymphocytes</i>	33
4.2.2. <i>Applying pharmacological inhibitors of T lymphocyte ion channels</i>	34
4.3. CFSE dilution assay and PI staining	35
4.4. Flow cytometry experiments	35
4.5. Measurement of secreted cytokine concentration	38
4.6. Culturing RA-FLS.....	38
4.7. Reverse transcription (RT) and quantitative polymerase chain reaction (qPCR).....	40
4.8. SDS-PAGE and Western blotting	41
4.9. Transfection of small interfering RNA (siRNA).....	41
4.10. Transwell invasion assay	41
4.11. Electrophysiology	42
4.11.1. <i>Whole-cell patch-clamp</i>	42
4.11.2. <i>Activation and inactivation kinetics of the K⁺ current</i>	43

4.11.3. Test substances.....	43
4.12. Statistical evaluation and plotting the results.....	44
5. RESULTS.....	45
5.1. The anti-proliferative effect of cation channel blockers in T lymphocytes depends on the strength of mitogenic stimulation.....	45
5.1.1. Dose-dependence of mitogen-induced proliferation.....	45
5.1.2. Ion channel blockers and rapamycin alone and in combination inhibit lymphocyte proliferation.....	47
5.1.3. Cell viability is not affected by the inhibitors of T cell proliferation.....	50
5.1.4. Cytokine production of T cells can be reduced by ion channel blockers.....	52
5.2. Different Expression of β Subunits of the KCa1.1 Channel by Invasive and Non-Invasive Human Fibroblast-Like Synoviocytes.....	53
5.2.1. RA-FLS express multiple β subunits at the mRNA and protein levels.....	53
5.2.2. RA-FLS express either $\beta 1$ or $\beta 3b$ subunits at their plasma membrane.....	54
5.2.3 Expression of KCa1.1 $\beta 3b$ is associated with higher levels of KCa1.1 α and CD44.....	57
5.2.4 Knocking down the $\beta 3$ subunit of KCa1.1 decreases cell surface expression of the pore-forming α subunit of KCa1.1.....	60
5.2.5 Knocking down the $\beta 3$, but not the $\beta 1$, subunit of KCa1.1 attenuates the ex vivo invasiveness of RA-FLS.....	61
6. DISCUSSION.....	62
6.1 The anti-proliferative effect of cation channel blockers in T lymphocytes depends on the strength of mitogenic stimulation.....	62
6.2 Different Expression of β Subunits of the KCa1.1 Channel by Invasive and Non-Invasive Human Fibroblast-Like Synoviocytes.....	65
7. SUMMARY.....	68
8. ÖSSZEFOGLALÁS.....	69
9. REFERENCES.....	70
10. LIST OF PUBLICATIONS.....	82
11. ORAL AND POSTER PRESENTATIONS.....	84
12. KEYWORDS.....	92
13. ACKNOWLEDGEMENTS.....	93

LIST OF ABBREVIATIONS

[Ca ²⁺] _i :	Intracellular calcium concentration
2-Apb:	2-Aminoethoxydiphenyl borate
AA:	Arachidonic acid
ANOVA:	Analysis of variance
AnTx:	Anuroctoxin
ASIC:	Acid-sensing ion channel
CD:	Cluster of differentiation
CFSE:	Carboxifluorescein succinimidyl ester
ChTx:	Charybdotoxin
CRAC:	Calcium release- activated calcium channel
cT:	Cycle treshold
DAG:	Diacyl glycerol
DI:	Division index
DMARD:	Disease-modifying anti-rheumatic drug
ELISA:	Enzyme-linked immunosorbent assay
ER:	Endoplasmic reticulum
FKBP:	FK506 binding protein
FLS:	Fibroblast-like synoviocyte(s)
GAPDH:	Glyceraldehyde 3-phosphate dehydrogenase
IP ₃ :	Inositol 1,4,5-trisphosphate
KCa:	Calcium-activated potassium channel
Kv:	Voltage-gated potassium channel
LCA:	Lithocholic acid
MMP:	Matrix metalloprotease
MS:	Multiple sclerosis
mTOR:	Mammalian target of rapamycin
NSAID:	Non-steroidal anti-inflammatory drug
OA:	Osteoarthritis
PBMC:	Peripheral blood mononuclear cell
PBS:	Phosphate buffer solution
PI:	Propidium iodide
PIP ₂ :	Phosphatidylinositol 4,5-bisphosphate

PLC- γ :	Phospholipase C gamma
PMA:	Phorbol 12-myristate 13-acetate
RA:	Rheumatoid arthritis
RA-FLS:	FLS from patients with RA
RCK:	Regulator of potassium conductance
RF:	Rheumatoid factor
STIM:	Stromal interaction molecule
T _C :	Cytotoxic T cell
T _{CM} :	Central memory T cell
T _{EM} :	Effector memory T cell
T _H :	Helper T cells
T _{reg} :	Regulatory T cell
τ_{act} :	Activation time constant
τ_{in} :	Inactivation time constant
VGKC:	Voltage-gated potassium channel
VGSC:	Voltage-gated sodium channel

1. PREFACE

Ion channels play a pivotal role in evoking and maintaining the physiological and pathological immune response and thus inflammation and autoimmunity. They affect multiple cellular functions, such as cell division or cell migration mainly through regulation of the membrane potential as well as through interaction with various intracellular molecular partners. In a healthy immune system, voltage- and Ca^{2+} -gated potassium channels are crucially important for the activation and proliferation of T lymphocytes, and thus, for the function of the immune system. These ion channels can also contribute to the development of autoimmune diseases such as rheumatoid arthritis, through their pathological overexpression in lymphocytes along with propagating tissue destruction mediated by effector cells.

The work presented here aims to provide insight into the involvement of K^+ channels in physiological T cell proliferation as well as into their contribution to the pathological activation of fibroblast-like synoviocytes in rheumatoid arthritis. The thesis is based on two international publications, but is greatly amended by previously unpublished and undiscussed insights.

Firstly, considering the previous studies focused on the effects of channel blockers on T cell proliferation, we noted variable effectiveness due to differing experimental systems. We approached this issue by investigating how the strength of the mitogenic stimulation influences the efficiency of cation channel blockers in inhibiting activation, cytokine secretion and proliferation of T cells under standardized conditions. In practice, this meant measuring the anti-proliferative effects of ion channel blockers and rapamycin on lymphocytes cultured under the same experimental circumstances at multiple levels of lymphocyte stimulation using carboxyfluorescein succinimidyl ester (CFSE) and propidium iodide (PI)-staining. Flow cytometry measurements were performed to determine the extent of cellular viability and proliferation, and ELISA experiments measured secreted levels of interferon- γ (IFN- γ) and interleukin 10 (IL-10).

To investigate the involvement of ion channels in autoimmune diseases, we turned our attention to fibroblast-like synoviocytes in rheumatoid arthritis (RA), which are responsible for damage to the cartilage and the surrounding tissue. These effector cells express KCa1.1 as their major plasma membrane K^+ channel. Blocking KCa1.1 reduces the invasive phenotype of fibroblast-like synoviocytes and attenuates disease severity in animal models of RA. As the pore-forming α subunit of KCa1.1 is widely distributed in the body and blocking it induces severe side effects, we aimed to characterize the tissue-specific accessory subunits of KCa1.1 channels to provide an opportunity for selective RA treatment.

2. SCIENTIFIC BACKGROUND

2.1. General characteristics of ion channels

The ion selective conductance of the cell membrane is mediated by ion channels and various carrier proteins. Ion channels are pore-forming transmembrane proteins that allow passive passage of ions through the cell membrane. Two key features distinguish ion channels from other transporters: the ion transport always follows the electrochemical gradient and the ion transport through the pore has a particularly high rate (3). Ion channels can be categorized based on the ions they conduct (e.g. H^+ , K^+ , Ca^{2+} , Cl^-), their selectivity (highly-, partially- or non-selective), their gating (voltage-gated, ligand-gated, light-gated, mechanosensitive, etc.), the direction of ionic current (inward-, outward-, or non-rectifier) and their structural similarities (e.g. Shaker-type K^+ channels, TRP channels) (4). This work mainly focuses on voltage- and Ca^{2+} -gated K^+ channels and the Ca^{2+} release- activated Ca^{2+} channel (CRAC), as well as accessory subunits of ion channels, hence these will be introduced below.

2.1.1. Overview of potassium channels

K^+ channels have been classified into several families according to their amino acid sequences, including those with six (6TM), four (4TM), or two (2TM) putative transmembrane segments per subunit. The main families of K^+ channels are represented in Fig. 2.1. Every K^+ channel subunit contains one or more pore (P-) loops that comprise a selectivity filter responsible for selective K^+ permeation. The 6TM channels include the voltage-gated K^+ channels (VGKC or K_v) as well as the Ca^{2+} -activated K^+ channels (KCa). Among KCa, $KCa_{1.1}$ contains an extra S_0 helix as shown in Fig. 2.1. Moreover, inward rectifier K^+ channels (Kir) allow flow of K^+ into the cell and consist of tetramers containing two transmembrane segments (M1 and M2) and a pore loop. The K2P family of channels (leak or background channels) contain four transmembrane segments and two pore domains.

VGKC assemble from four distinct, approximately 60-60 kDa polypeptide chains, arranged around the central ion conducting pore in a fourfold symmetrical manner as indicated by Fig. 2.1. This complex is also known as the α subunit of the channel, which can be associated to one or more ancillary β subunits. The polypeptide chains of the α -subunit contain typically six alpha transmembrane helices S_1 through S_6 with a membrane re-entrant pore loop intervening the S_5 and S_6 helices. The voltage-sensing domain is formed by the S_1 - S_4 helices, with the S_4 segment being highly conserved and containing multiple gating charges in a

repeating RXXR motif. The ion conducting pore domain consists of the S5 and S6 segments of the four peptides and the pore loop between them. As membrane potential changes, the arginines on the S4 interact with negative charge clusters on the S1-S3 helices, facilitating S4 movement in response to the electric field. Thus, the S4 exerts force on the S4-S5 linker and this sophisticated electromechanical coupling propagates to the subsequent segments of the channel ultimately leading to channel opening. In VGKC, the pore loop between the S5 and S6 segments contains an emblematic selectivity filter, consisting of four amino acids (almost exclusively GYGD) that is responsible for K^+ selectivity (1).

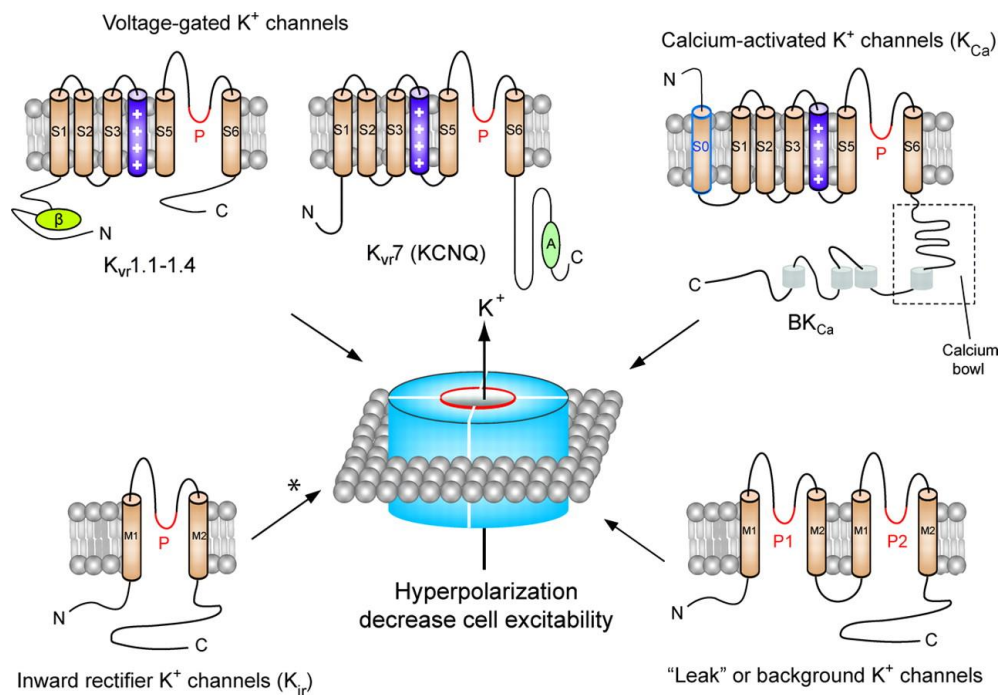


Figure 2.1.: General structure of the four major K^+ channel families (2)

Columns S0-S6 and M1-M2 represent transmembrane domains of respective channels, the blue column indicates the positive charge centers in the S4 domain, the red lines imply the pore (P-) loop. The green circles β and A represent the accessory β subunit- and ankyrin binding sites, respectively.

VGKC can be categorized based on sequence homology, ranging from Kv1.x to Kv12.x channels. The so-called *Shaker*-type channels are homologous to the Shaker channel of the *Drosophila melanogaster*, and are termed Kv1.1-Kv1.8. According to the classical nomenclature, Shaker type channels are termed delayed rectifying channels as they open slowly compared to sodium or calcium channels and show little time-dependent inactivation, similar to other Kv channels such as the Kv2 or Kv7 families (5).

Ca^{2+} -gated K^+ channels are structurally homologous to VGKC in their transmembrane domains and the selectivity filter, however they contain intracellular Ca^{2+} -sensing segments. In contrast to Kv channels, KCa channels are voltage-independent except for the KCa1.1. The members of this family can be distinguished by their different unitary K^+ conductance, with KCa1.1 (MaxiK, Slo1, BK, BK_{Ca}) having an impressive single channel conductance of 100-300 pS, KCa3.1 (IKCa1) having a 20-60 pS conductance, and the KCa2.x channels (SK1-4) having a conductance of 10 pS (1, 6). These channels also differ in their site of expression. KCa1.1 is quite ubiquitously expressed, and its tissue-specific expression mainly relies on the regulatory subunits it is associated with. The KCa2 family channels almost exclusively reside in the nervous system, whereas the KCa3.1 is expressed in peripheral tissues such as the pancreas, lung, placenta, erythrocytes and lymphocytes (7). These channels also differ in the way they sense calcium. Each KCa1.1 α subunit contains two regulators of K^+ conductance (RCK1 and RCK2) domains, which are accountable for calcium binding, and altogether eight RCK domains from the four subunits assemble as a ring-like structure known as the gating ring (1). The Ca^{2+} -sensitivity of KCa3.1 is conferred by the Ca^{2+} -binding protein calmodulin (CaM), with constitutively binding the CaM C-lobe to the intracellular C-terminal domain of the channel (8). In case of the KCa2 channels, calcium does not directly bind to the channel, but through a calmodulin binding site that can recognize Ca^{2+} -bound calmodulin with high affinity. Among the KCa channels, the KCa1.1 is structurally unique as it contains an extra transmembrane domain S0, rendering the N terminus of the channel to be localized extracellularly (6). Also, this channel is gated by both voltage and Ca^{2+} . Voltage can activate KCa1.1 channels in the absence of Ca^{2+} binding, and likewise, Ca^{2+} can also activate KCa1.1 channels when the voltage sensors are at the resting state (1, 9).

2.1.2. The Ca^{2+} release- activated Ca^{2+} channel

CRAC channels are formed by a complex of a plasma membrane-spanning ORAI and endoplasmic reticulum (ER) membrane-resident STIM proteins. The first step of CRAC channel activation is mediated by the stromal interaction molecules (STIM) 1 and its homolog, STIM2. Upon depletion of Ca^{2+} from the smooth ER, Ca^{2+} dissociates from STIM, namely from its paired EF-hand domain in the lumen. This results in conformational changes, first in the N-terminus and ultimately in the cytoplasmic C-terminus of STIM (10, 11). These changes expose the so-called oligomerization domains allowing STIM1 and STIM2 to oligomerize and migrate to the ER-plasma membrane junctions, where they form large clusters, or puncta. The calcium channel ORAI consists of six subunits and is recruited by STIM to these junctions, resulting in

localized Ca^{2+} -influx. ORAI1 has two known homologs, ORAI2 and ORAI3. The first transmembrane domain of ORAI1 is critical in terms of pore lining and contains several amino acid residues, including a crucial glutamate, E106, that is responsible for Ca^{2+} -binding and the high Ca^{2+} -selectivity of the CRAC channel (11). Thus, the S1 domain of ORAI1 defines the key biophysical properties of the channel, and S2-S4 are hypothesized to shield S1 from the surrounding phospholipid bilayer and provide structural support for the channel (12).

2.1.3. Specific regulatory subunits of ion channels

The human genome encodes over 230 pore-forming subunits of ion channels, from which at least 70 are mainly voltage-dependent that have unique unitary conductances, voltage sensitivities, and activation/deactivation/inactivation gating kinetics (5, 13-18). Despite this diverse range of ion channels, most need to co-assemble with intracellular, extracellular or membrane-spanning accessory subunits to be functional in different tissues. This section will only cover ion-channel-exclusive auxiliary subunits, disregarding non-specific interaction partners that modify ion channel function, such as calmodulin, ankyrin or caveolin (19). The accessory subunits, traditionally labeled in the literature as Greek letters β , γ or δ are essential for proper physiological function, and their mutations cause severe human diseases (1). In total, there are more than 50 ion channel-specific regulatory subunits of ion channels known in the literature, and taking their numerous transcript variants into account they are the reason for the remarkable functional heterogeneity of ion channels (14-18). Considering the astonishing diversity of ion channel accessory subunits, after a brief overview this chapter will mainly focus on the regulatory subunits of voltage-gated potassium channels.

Structurally, regulatory subunits are usually profoundly smaller than their corresponding channels, but apart from that they are surprisingly diverse. Some membrane-spanning auxiliary subunits bind to the voltage sensor domain of their channels with non-covalent bonds. Other regulatory subunits interact directly with the pore of the channel e.g. through a ball-on-chain mechanism. Moreover, intracellular accessory subunits, such as the $\text{Kv}\beta$ on Shaker-type potassium channels, can bind to cytoplasmic domains of the channels (18).

Functionally, regulatory subunits can be interpreted as metaphoric reins on the neck of the channel horses. Through selective interaction with the channels, accessory subunits may modify the single channel conductance of the respective channels, and impair or enhance their voltage sensing, enabling a voltage-gated channel to function in both excitable and non-

excitable cells (1). They can also influence the membrane expression of the channel, and can have a significant impact on channel kinetics. It is also known that accessory subunits may bind to cytoplasmic interaction partners such as anchoring proteins of secondary messengers. For example, Kv β extends Shaker-type Kv channels by an impressive 10 nm towards the intracellular space thus possibly forming a large area for interaction partners (18). To make the picture even more complex, it has been shown that Nav β , which has originally been known as an accessory subunit of sodium channels, can alter neuronal voltage-gated potassium channels as well (20).

It is also worth mentioning that as ion channels are usually multimeric proteins, multiple regulatory subunits can bind to a single ion channel. In case of the homotetrameric KCa1.1 for example, the β 2 subunit can alter the inactivation kinetics of the channel through a ball-on-chain mechanism in a manner that depends on how many monomers of the channel are coupled to β 2. If the β 2 to KCa1.1 ratio is 1:4, only slight inactivation of the KCa1.1 can be observed, however, if the ratio of β 2 to KCa1.1 increases, the rate of inactivation becomes significantly faster and ultimately complete inactivation can be observed (21, 22).

The ancillary subunits of voltage-gated potassium channels have been extensively reviewed by Pongs et al. (18). Kv channels have altogether nearly 20 auxiliary subunits. The first Kv β , now known as Kv β 2 was originally described by pull down assays and was subsequently cloned (23-25). Since then, the literature acknowledges Kv β 1 and Kv β 3 as additional members of the Kv β family. All members of this family are coupled to Shaker-type potassium channels, and have a conserved C-terminal domain. In contrast, the N-terminus is highly variable amongst the Kv β s: Kv β 1 and Kv β 3, but not Kv β 2 have an N-terminal ball-on-chain domain. These structural variances at the N-terminus lead to substantial functional differences regarding the different Kv β isoforms. Most prominently, Kv β 1 and Kv β 3 lead to inactivation of the Kv currents whereas Kv β 2 does not induce inactivation (26-28).

The minK (KCNE1-5) family are small, single transmembrane domain-containing proteins of utmost physiological relevance that mostly interact with members of the KCNQ family. The most prominent member of the family, KCNE1 is known to assemble with KCNQ1 to give rise to the cardiac IKs current that is responsible for cardiac repolarization. Mutations in the KCNE1 gene can lead to hereditary cardiac diseases, mainly long QT syndrome (29). Interestingly, the typical stoichiometry between KCNE and KCNQ is 1:2, and each KCNE family member has only one functional splice variant in the human tissues (18).

Lastly, other K^+ channel interacting proteins known as KChIP and DPPL can interact with the intracellular and extracellular domains of Kv4 channels, respectively, thereby forming gigantic molecular complexes. Alternative splicing of KChIPs lead to altogether 18 functional isoforms with highly variable N-terminal regions (18). KChIPs are crucial as they can ultimately modify cardiac and neuronal Kv4 channels and knock-out animals lacking KChIP1 and KChIP2 exhibit higher susceptibility to seizures and arrhythmias. DPPL subunits associate to Kv4 channels in the brain and silencing DPPL results in a reduction of subthreshold excitability of CA1 pyramidal neurons (18).

KCa1.1 channel accessory subunits are important for the association of the KCa1.1 channel with the L-type Ca^{2+} channel in a multi-ion-channel protein complex. Also, the presence of β or γ subunits affects the kinetics of the channel as well as the selectivity and affinity of various KCa1.1 channel modulators (Fig. 2.2).

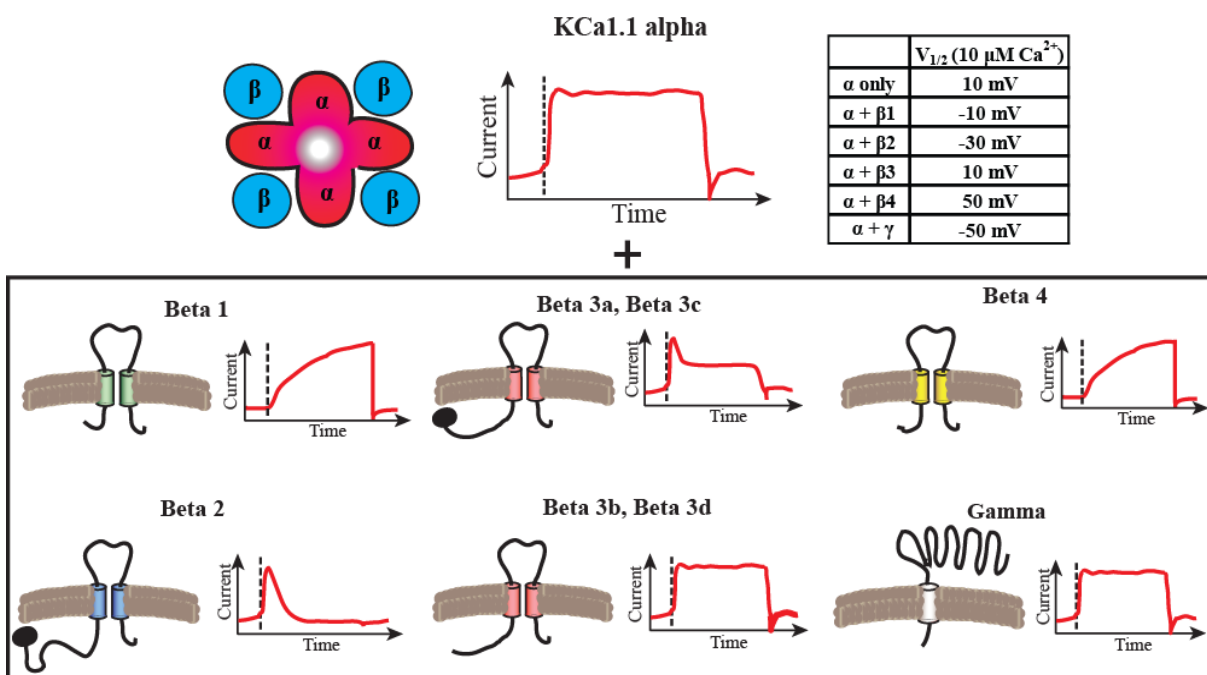


Figure 2.2.: Auxiliary subunits alter KCa1.1 currents

The diagram above shows activation and inactivation kinetics in KCa1.1 alone and associated to diverse β subunits. As the schematic diagram on the top left shows, up to 4 β subunits can accompany a channel. $\beta 1$ and $\beta 4$ slow activation kinetics, whereas $\beta 2$ and $\beta 3$ cause inactivation. The table on the top right shows that the γ , $\beta 1$ and $\beta 2$ subunits cause a left shift whereas $\beta 4$ causes a right shift in the voltage-dependence of the channel.

In KCa1.1, four β subunits with distinct amino acid sequences have been described: β 1 (KCMB1) is found in smooth muscles, β 2 (KCMB2) is prevalent in the adrenal gland and brain, β 3 (KCMB3) is expressed mainly in the testis, and β 4 (KCMB4) is specifically expressed in the central nervous system (30-35). These β subunits display similar topology containing short N- and C-termini both on the intracellular side, two TM helices, and a large extracellular loop. Also, KCa1.1 can be associated to four types of γ auxiliary subunits (γ 1– γ 4, encoded by the LRRC26, LRRC52, LRRC55, and LRRC38 genes, respectively). The four γ subunits have similar molecular weights of about 35 kDa. They are type I single-span membrane proteins containing a classic N-terminal cleavable signal peptide for extracellular localization of the N-terminal LRR domain in the mature proteins (35-37). They have unique expression profiles, as the γ 1 subunit is highly expressed in the salivary glands, prostate, and trachea, whereas γ 2 is localized mainly in the testes, and γ 3 is found mostly in the nervous system (35). Also, the γ 1 subunit can inhibit the effect of some KCa1.1 activators, such as mallotoxin (38).

The changes induced by auxiliary subunits on KCa1.1 currents are summarized on Fig.2.2. The β 1 and β 4 subunits overall induce slowing of the macroscopic current kinetics and an increase in apparent calcium and voltage sensitivity. In addition, the β 1, β 2, and β 4 subunits modulate membrane expression of the KCa1.1 conducting α subunit (33, 34, 39). The β 2 and some splice variants of β 3 subunits also cause rapid inactivation through their intracellular N-termini. Steroid compounds, such as lithocholic acid (LCA), selectively enhance KCa1.1 currents only if the channel contains the β 1 subunit (40, 41). In contrast, arachidonic acid (AA) amplifies currents in presence of β 2 or β 3, but not β 1 or β 4 subunits whereas the scorpion toxins iberiotoxin and ChTx fail to inhibit KCa1.1 in presence of the β 4 subunit (31, 42).

2.1.4. Modes of ion channel inhibition

Ion channel inhibitors or blockers are molecules that interact with ion channels in a manner that results in a net decrease of ionic current. Channel inhibitors can be used to assess the physiological function of ion channels, and due to their specific binding to the channel, they are also suitable for testing the structural properties of the binding site. Using ion channel inhibitors, it became possible to accomplish significant advances in understanding channel function and gating mechanisms. The two major mechanisms of ion channel inhibition are pore block, where the inhibitor directly occludes the ion conduction pathway, and allosteric inhibition (1, 3) (Fig. 2.3.).

Pore blockers occlude the passage of permeant ions through the channel and are the most commonly applied type of inhibitors. Chemically, they can be either competing ions, such as Cd^{2+} , Ba^{2+} , Cs^+ , or small molecule inhibitors usually ranging from 200-1000 Da, or peptide toxins, that are usually composed of 20-70 amino acids. As the pore of an ion channel connects to the extracellular side as well as to the intracellular vestibule of the channel, it is plausible that many pore blockers usually only act from one side of the cell membrane (1, 43-45).

The fundamental idea of allosteric inhibition is that a modulatory chemical can selectively stabilize protein conformation by shifting the equilibrium between functional states (1, 37, 46). Translating this phenomenon to ion channels, allosteric inhibitors (or negative allosteric modulators) act by closing channels as they induce channel proteins to assume nonconducting conformations, such as an inactivated or closed state. By shifting the equilibrium of a channel to a nonconducting state, the channel will open less frequently and more likely be inhibited. Allosteric inhibitors can act by various mechanisms, such as surface charge screening, membrane perturbation, or direct binding to the ion channel. Due to this fact, the exact mechanisms of action of many allosteric inhibitors remains a mystery. One fitting example of such a poorly understood allosteric blocking mechanism is paxilline, a fungal alkaloid, which has been known to inhibit KCa1.1 channel for more than 20 years (47, 48). Recently, it has been shown that it acts almost exclusively on closed channels, but the exact location of the channel-blocker interaction still remains to be elucidated (49).

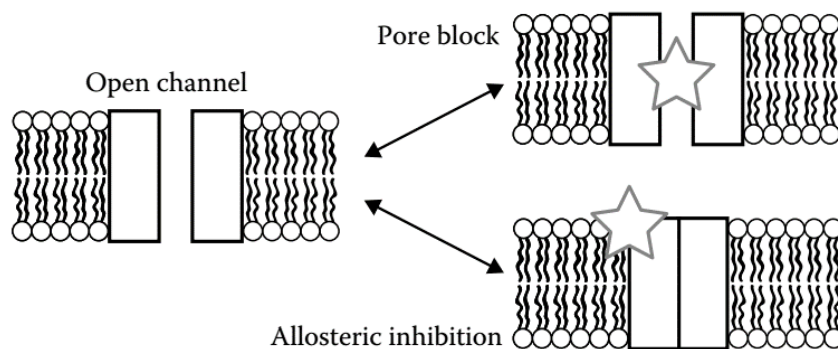


Figure 2.3.: Types of ion channel blockers

Pore block results from inhibitors binding in the pore to occlude ion permeation. Allosteric inhibition results from inverse agonists that cause an open channel to close (1).

Quantification of ion channel inhibition is necessary to precisely describe the dose-response relationship. As binding of a molecule to the channel can be understood as a chemical equilibrium in a system, it can be described as follows:



where L is the ligand, R is the receptor and k_{on} and k_{off} are the association and dissociation rate constants, respectively (3, 44). Based on Eq. 1., it is possible to calculate the ratio of the dissociation and association rate constants, that ultimately yields the dissociation constant, K_d :

$$\text{Eq. 2.} \quad \frac{[L][R]}{[LR]} = \frac{k_{off}}{k_{on}} = K_d$$

where [L] is the concentration of the free ligand, [R] is the concentration of the receptor, and [LR] is the concentration of the ligand-receptor complex. Eq. 2. implicates that K_d can be determined by two means, thermodynamically, by studying concentrations of [L], [R] and [LR], and kinetically, by determining the two kinetic parameters. The K_d has units of concentration and is suitable to obtain intuition about dose dependence of a molecule. If an ion channel blocker that binds the channel in a 1:1 stoichiometry, the K_d can be practically understood as the concentration where 50% of channels are blocked, making it a straightforward measurable quantity. The K_d is sufficient to describe the dose-response of a system at equilibrium (3, 44). Fractional inhibition of ion currents depending on the concentration of the blocker can be fit by a sigmoidal Hill equation that reaches saturating effect at very high concentrations. This means that if $10 \times K_d$ concentration is applied, about 90% of the channels are blocked, whereas at $100 \times K_d$ concentration more than 99% of the channels are inhibited. However, applying ion channel inhibitors in increasing concentration one must take care that the interaction between inhibitor and channel remains specific and no additional targets are affected by the blocker.

For the peptide-channel interaction it is typical that the toxins bind to the extracellular region of the channels, consequently inhibiting ionic flux through the pore (50). Since the voltage-gated potassium channels exhibit high sequence similarity, natural venoms that contain multiple toxins generally block more channel types thus they have low selectivity for a given channel. In the last decades an abundance of peptide toxins has been isolated from animal venoms, which

selectively inhibit diverse K⁺ channels including Kv1.3 or KCa1.1 with high affinity. Their striking potency and specificity can lead to the fact that the most potent peptide blockers work in an impressive pM (10⁻¹² M) concentration range. Through mutation studies of both ion channels and their respective toxins with a known structure (e.g. ChTx), it was possible to clarify the channel pore topology and identify the residues that play a role in the interaction between the toxin and the channel (51-53). Also, in recent years, cryo-EM studies have revealed 3D structures of numerous ion channels, further confirming previous topological results (54-58). For example, by 2017 we know the atomic structure of Kv1.2 alone, with accessory subunit Kvβ and with the inhibitor ChTx, as well as the full atomic structure of the *Aplysia* KCa1.1 (54, 59-61). ChTx, discovered in scorpion venom was the first polypeptide blocker of Kv1.3 with nanomolar affinity. Our workgroup is actively involved in characterizing and modifying polypeptide inhibitors isolated from various scorpion venoms (e.g. Vm24, Tst26, anuroctoxin) that have low-nanomolar and picomolar affinities for the Kv channels (62-66). Anuroctoxin (AnTx) was characterized and subsequently synthesized by our workgroup in 2014 using recombinant technique and solid phase chemical synthesis (62, 63). With site directed mutations our workgroup could design and synthesize a variant of AnTx, which is a high affinity and selective inhibitor of the Kv1.3 channel (62).

Small molecule inhibitors have a simpler structure, and are quite heterogeneous in their blocking mechanisms as well as in their binding sites. Small molecule blockers are usually far less potent than peptide inhibitors due to their smaller interaction surface, blocking ion channels in the nM or μM range (10⁻⁹ -10⁻⁶ M). These inhibitors are mainly hydrophobic or at least amphipathic, so they can diffuse through the cell membrane, and target the channels from every imaginable site, extra- and intracellularly, or even from inside the phospholipid bilayer. As some of these compounds can reside in the membrane itself, even washing out the inhibitor using perfusion in patch-clamp may not reverse the channel inhibition (e.g. in case of paxilline inhibition of KCa1.1) (1).

One of the best characterized small molecule inhibitors of K⁺ channels is tetraethylammonium (TEA), active in mM (10⁻³ M) concentration range, which has both an extra- and intracellular binding site in Shaker channels (67, 68). When bound to the extracellular binding site, TEA slows down inactivation because the TEA-bound ion channel cannot become inactivated. TEA locks a K⁺ ion in the selectivity filter at a site that controls inactivation. Therefore, the channel first needs to release TEA and the K⁺ ion before it can inactivate. This mechanism of action is metaphorically described as a “foot-in-the-door” mechanism.

Intracellularly, when approaching from the inner vestibule of the channel, it binds to specific amino acids near the pore. When bound to the intracellular binding site, TEA competes with a ball-on-chain mechanism responsible for the so-called N-type inactivation, thus slowing inactivation kinetics. As noted above, most small molecule inhibitors have a far less clearly described mechanism of action than TEA, but nevertheless, several are used routinely in the clinical practice. Local anesthetics, such as lidocaine are small molecule inhibitors used clinically to block sodium channel pores. The vasodilator verapamil is a calcium channel pore blocker and is applied in a variety of cardiovascular diseases (1).

2.2. Ion channels as key regulators of the immune system

Sustaining a proper immune response requires a coordinated interaction between several types of immune cells, including lymphocytes and antigen presenting cells (APCs). Cells of the innate and adaptive immune systems need to be activated precisely at the right moment to strike effectively against internal or external threats, as well as to avoid unnecessary activation of these cells possibly leading to autoimmunity. Like all other excitable and non-excitable cells, immune cells express ion channels to control their membrane potential (V_m) and regulate Ca^{2+} signaling as well as physiological cell functions, such as gene expression, proliferation, migration and differentiation. The following section aims to provide a brief introduction about ion channels that play key physiological roles in various immune cells focusing on T cells, which were the primary subjects of our studies.

To date numerous ion channels have been discovered in T lymphocytes (summarized in (69, 70)): the Ca^{2+} -release- activated Ca^{2+} channel (CRAC) (71); the *Shaker*-type voltage-gated K^+ channel Kv1.3 (72), the Ca^{2+} -activated K^+ channel KCa3.1, also known as IKCa1 or KCNN4 (73, 74); the non-selective TRPM7, that is proposed to be involved in the magnesium homeostasis of the cell; TRPM2, which is reported to play a role in T cell activation and proliferation (75), TRPV2, that has been implicated in T cell development, the two-pore potassium leak channels K2P3.1 (TASK1), K2P5.1 (TASK 2), and K2P9.1 (TASK3), that are involved in setting the resting V_m , and finally the swelling-activated chloride channel Cl_{swell} , encoded by the SWELL1 gene, which plays a role in volume regulation (76, 77). As CRAC, Kv1.3 and KCa3.1 channels co-localize in the immune synapse and are up-regulated in different T-cell subtypes (78, 79), it is widely accepted that these channels are indispensable early factors in the Ca^{2+} -dependent activation pathways of the T cell (80). Moreover, pharmacological

inhibition of Kv1.3 and KCa3.1 channels or genetic silencing of KCa3.1 also reduces calcium entry from CRAC channels.

During B lymphocyte activation, CRAC mediates calcium influx from the extracellular environment upon emptying of ER calcium stores. As in T cells, calcium influx by TRPV2 mediates B cell development, activation and proliferation (81). TRPM6 and TRPM7 are also present in B cells, and are accountable for maintaining Mg²⁺ homeostasis and activation of B cells (82, 83). Kv1.3 and KCa3.1 in B lymphocytes are involved in the maintenance of the membrane potential and play a role in B cell proliferation and the so-called isotype switching of memory cells (84). Finally, influx of K⁺ through VGKC such as Kv1.3 induces mitosis in B cells as well as DNA synthesis in S phase (85, 86).

The prominent professional APCs known as dendritic cells (DCs) are prevalent primarily in tissues that keep close contact with the environment, such as in external tissues like skin as well as in internal structures such as the lung and the gut. In these tissues, the DCs upon engulfing pathogens, migrate to lymphoid tissues to stimulate respective immune responses by presenting the antigen to naïve lymphocytes. During DC maturation, it has been shown that voltage-gated sodium channels, mainly Nav1.7 become down-regulated whereas VGKCs become markedly up-regulated (87, 88). It could thus be said that the sodium channels may account for the immature state and VGKC such as Kv1.3 may be overexpressed to regulate the secretion of cytokines and cell adhesion molecules of mature DC by modulating membrane potential and Ca²⁺ signaling (89). Also, maturation can be suppressed by Kv1.3 inhibition as Kv1.3 blockers reduce the expression of maturation markers, cell surface MHC II molecules, chemotaxis and cytokine production (88). Also, DC functions such as migration and proliferation have been shown to be supplemented by other ion channels (90), such as TRMP2 (91), TRPM4 (92), TRPV1 (93), aquaporins (94, 95), P2X7 receptors (96), the calcium-activated chloride channel ANO6 (97), voltage-gated proton (Hv1) channels (98) as well as acid-sensing ion channels (ASICs) (99).

Typical phagocytic cells such as macrophages and the related microglia have marked voltage-gated sodium currents (e.g. Nav1.6), and inhibiting these channels ameliorates cell infiltration and phagocytic function in a model disease of multiple sclerosis (MS) (100). CRAC channel-induced Ca²⁺ influx is essential for producing reactive oxygen species in macrophages (101, 102). Furthermore, KCa3.1 is responsible for the maintenance of hyperpolarization induced sustained calcium influx from CRAC in macrophages (86). Neutrophil granulocytes, the most prevalent phagocytotic white blood cells in the blood rapidly respond to tissue damage

by degranulation, release of reactive oxygen species and subsequently phagocytosis of potential hazards. Upon tissue injury, activation of NADPH oxidase is followed by the production of superoxide anion and hydrogen peroxide, and subsequent degranulation and cell migration is regulated in a considerable extent by calcium. The intracellular calcium concentration $[Ca^{2+}]_i$ is mediated by TRPM2, TRPV channels and CRAC and dysfunction of these channels impairs effector functions of neutrophils (86). Besides the channels involved in Ca^{2+} signaling, other channels also influence neutrophil function. CFTR, a cAMP activated chloride channel is likely to be involved in the neutrophil bactericidal activity and consequently down-regulation of this channel affects neutrophil microbicidal function (103). The voltage-gated H^+ channel Hv1 acts as a key regulator for cytosolic acid and superoxide anion production in neutrophils by regulating pH and so inhibition of this channel reduces phagocytic function (104).

2.2.1. Ion channels regulate the T cell mediated immune response

T cells express CRAC, Kv1.3 as well as KCa3.1 channels, which, during activation, co-localize in a structure that forms between an antigen-presenting cell (APC) and a lymphocyte, namely in the immune synapse (IS) (78, 79). In the IS, specific membrane proteins of APCs and T cells rearrange and segregate into the contact area between the two cells (105), creating the so called supramolecular activation cluster consisting of two concentric rings of molecule complexes. It is widely accepted that upon successful formation of the immune synapse, these channels are indispensable early factors in the Ca^{2+} -dependent activation pathways of the T cell (Fig. 2.4.) (80). In non-excitable cells, probably the most studied event involving ion channels is the Ca^{2+} signal occurring subsequently to the T cell receptor (TCR) activation. Ca^{2+} influx is associated with oscillations $[Ca^{2+}]_i$ that are generated by an intricate interplay of multiple channels, including K^+ , Na^+ , and Cl^- channels, that regulate V_m (85, 106). This initial signaling step of TCR activation results in the activation of phospholipase C- γ (PLC- γ). This enzyme catalyzes the cleavage of phosphatidylinositol 4,5-bisphosphate (PIP_2) into diacyl glycerol (DAG) and inositol 1,4,5-trisphosphate (IP_3). DAG is responsible for the activation of protein kinase C (PKC), which in turn phosphorylates several intracellular substrates. The other crucial component of this signaling cascade is the two-phase elevation of the intracellular Ca^{2+} concentration. IP_3 is the key element in the initial Ca^{2+} influx: binding of IP_3 to its receptors on the ER results in Ca^{2+} release from the endoplasmic stores. This in turn activates STIM1 on the membrane of the ER, which translocates to a region of the endoplasmic membrane where it can

activate Orai1 molecules. Orai1, as mentioned earlier forms the pore of CRAC channels, through which Ca^{2+} ions can flow into the cell, creating the second, prolonged increase in the cytosolic Ca^{2+} concentration (107, 108).

One of the consequences of the increased $[\text{Ca}^{2+}]_i$ following TCR activation is membrane depolarization, which limits further Ca^{2+} influx by impairing the favorable electrochemical gradient to drive Ca^{2+} into the cytoplasm. Thus, lymphocytes as well as other immune cells require K^+ channels that, by the efflux of K^+ , maintain a hyperpolarized membrane potential critical for sustaining the gradient for Ca^{2+} entry via Ca^{2+} release-activated Ca^{2+} (CRAC) channels. CRAC channels are responsible for the generation of Ca^{2+} currents in these cells (107, 109, 110), and the negative membrane potential is ensured by the two potassium channels.

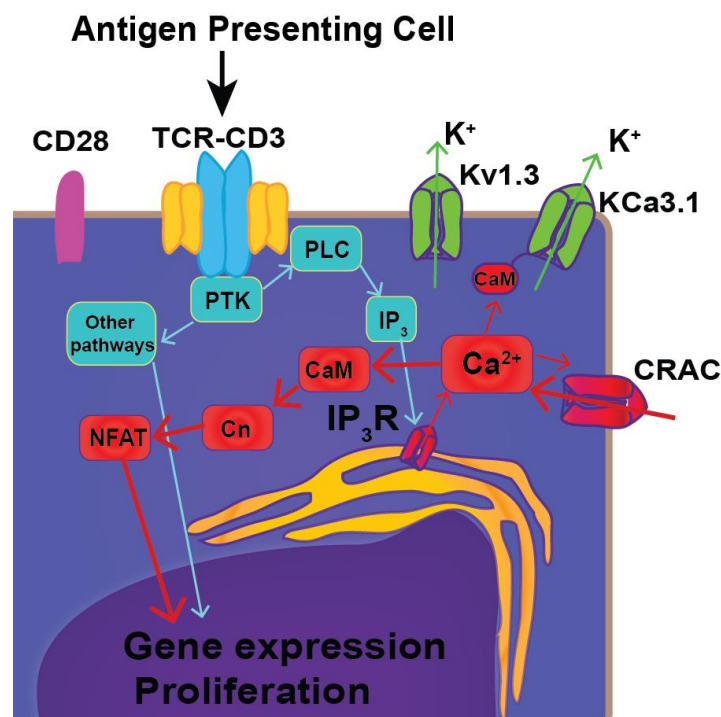


Figure 2.4.: T cell activation is coupled to ion channel function

Upon antigen presentation from the APC, the orchestrated signaling cascade originating from the T cell receptor leads to opening ion channels as well as activation of secondary messengers. Ultimately, through calcium bursts, NFAT becomes active and gene transcription can be initiated (see details in text). TCR: T cell receptor; PTK: phosphotyrosin kinases; PLC: phospholipase C; IP₃: inositol-1,3-triphosphate; CaM: calmodulin; Cn: calcineurin; NFAT: nuclear factor of activated T cell.

Interestingly, while the membrane potential of resting T cells is controlled primarily by Kv1.3 channels (~200-400 channels/cell), this function is partially taken over by KCa3.1 channels in activated cells (111).

Increase in $[Ca^{2+}]_i$ may activate intracellular pathways involving calmodulin as well as additional secondary messengers such as calcineurin. This phosphatase removes the inhibitor phosphates from the nuclear factor of activated T-cells (NFAT), allowing its dimerization and subsequently, nuclear translocation. This transcription factor can then bind to the promoter region of target genes (e.g. IL-2 gene) involved in cytokine production and proliferation of T lymphocytes (72, 80).

2.2.2. Role of potassium channels in autoimmunity

The first autoimmune disease that was described as being related to ion channels was myasthenia gravis (112, 113). Since then, as summarized recently by RamaKrishnan et al. (114), several other autoimmune syndromes have been credited to malfunction of ion channels. During autoimmune diseases, ion channels can become the targets of auto-antibodies (115, 116) that inhibit channel function. In contrast, in some disorders K^+ channels can become overexpressed on the surface of autoreactive effector cells. Taken together, ion channels may play a direct role in the autoimmune reaction itself, rather than only being the target molecules. Inhibitor auto-antibodies against ion channels have been observed in numerous diseases. It has been shown that in Guillain-Barré syndrome, antibodies against VGKC lead to prolonged action potential and ultimately disorders in neurotransmission in the peripheral nervous system (117). In MS, antibodies targeting the inward-rectifier channel Kir4.1 contribute to demyelination (118). In myasthenia gravis, antibodies are produced affecting the Kv1.4 channels in cardiomyocytes (119). Physiologically, these channels are regulators of the cardiac action potential and their prolonged inhibition leads to arrhythmia as well as heart failure. Lastly, auto-antibodies against both Kv1.3 and KCa3.1 have been described in primary biliary cirrhosis where they contribute to the abnormal B cell-mediated immune reaction (120).

Diseases traditionally considered autoimmune can also be triggered by mutations of certain ion channels. Probably the most notorious mutation of an ion channel in such context is the loss-of-function mutation of Kir6.2 in the neonatal form of type 1 diabetes mellitus. The regulatory SUR1 subunit of the channel is involved in the sensing of blood glucose levels in form of ATP, as ATP binding leads to closure of Kir6.2, which leads to depolarization, followed by opening of voltage-gated calcium channels and ultimately secretion of insulin. Mutations in the ATP-binding site of SUR1 lead to inability of closing the potassium channel, and thus ineffective insulin secretion (121, 122).

Upon stimulation of naïve T lymphocytes, they differentiate into central memory T cells (T_{CM}), and in case of prolonged antigen stimulation, into effector memory T cells (T_{EM}). Auto-reactive effector T cells that display T_{EM} phenotype have been implicated in diseases such as rheumatoid arthritis (RA), type 1 diabetes mellitus and MS (114). As mentioned in section 2.1.1.2, Kv1.3 and KCa3.1 are the two potassium channels expressed in T cells. Both channels can be overexpressed in type 1 diabetes, leading to abnormal T cell activation patterns and eventually destruction of β cells of the Langerhans islets (123). Resting naïve, T_{CM} and T_{EM} cells independently of $CD4^+$ or $CD8^+$ phenotype express 200-300 Kv1.3 and 30 KCa3.1 channels per cell in average in their plasma membrane. Following activation, the number of Kv1.3 channels increases twofold while the number of KCa3.1 channels rises tenfold reaching an average of 500 channels per cell in naïve and T_{CM} cells. On the contrary, in T_{EM} cells the number of Kv1.3 reaches 1500 channels per cell after activation without any significant changes in the level of KCa3.1 (124). It was demonstrated that effector T_{EM} cells isolated from patients with autoimmune diseases show a K^+ channel expression pattern can be regarded as Kv1.3-dominant compared to KCa3.1, whereas naïve or activated T_{CM} cells express slightly more KCa3.1 and less Kv1.3. (125, 126). Interestingly, the same Kv1.3 dominant channel phenotype has been shown in psoriasis and rheumatoid arthritis (127, 128). Because of this unique expression pattern, the activity of these autoreactive T_{EM} cells can be manipulated by the application of specific Kv1.3 channel blockers. Therefore, it is not surprising that selective targeting of Kv1.3 has attracted significant attention as a potential novel treatment strategy for autoimmune diseases (124).

KCa3.1 is postulated to play a substantial role in inflammatory bowel diseases as well, as $KCa3.1^{-/-}$ as well as KCa3.1 inhibitor-treated mice exhibit more favorable disease conditions compared to wild-type mice (129, 130). However, human clinical trials involving KCa3.1 blocker Senicapoc® have failed in the recent years, as patients developed severe side effects such as exercise-induced asthma (130, 131).

Apart from Kv1.3 and KCa3.1, other potassium channels can also play a role in pathogenesis of autoimmune diseases. The two-pore potassium channels TASK1-3 are important for the activation and effector functions of T lymphocytes in vitro and in animal models of MS. Targeting this channel using inhibitors or knocking out the respective gene resulted in a significantly ameliorated course of disease, that was accompanied by a decreased activation of immune cells and less axonal damage compared to wild-type mice (114). KCa1.1 has been postulated to play a role in multiple diseases, which are collectively described in section 2.4.1.

2.3. Modes of physiological and *in vitro* T lymphocyte activation

The essential functions of adaptive immunity are to differentiate between the own antigens of the host and the foreign antigens through antigen presentation, to generate effective immune responses to counter pathogens and to create an effective immunological memory. T lymphocytes are highly potent cells of the adaptive immune system and are crucially important in the maintenance of immunological homeostasis. Rapid and specific activation through the TCR and its co-receptors CD4 and/or CD8 lead to the recruitment of numerous down-stream pathways, that ultimately result in T cell activation and proliferation, and subsequently lead to the differentiation into effector or memory cells (132, 133). Based on the TCR structure, it is possible to distinguish $\alpha\beta$ T cells with α and β heterodimer TCR and $\gamma\delta$ T cells with γ and δ subunits, that are considerably less common in the bloodstream than the $\alpha\beta$ T cells. The $\alpha\beta$ T cells can be further divided into subtypes based on their cell surface CD markers and their effector functions, the most important ones being CD4⁺ CD8⁻ helper (T_H) T cells, and CD4⁻ CD8⁺ cytotoxic (T_C) cells. In addition, there are regulatory or suppressor (T_{reg}) T cells, which most commonly express a phenotype of CD4⁺CD25⁺, but less prevalently CD8⁺CD25⁻ T_{reg} cells also exist. Depending on the cytokines produced, T_H cells can be classified into further subpopulations. T_H1 type cells produce vital cytokines such as interferon- γ (IFN- γ) and tumor necrosis factor α (TNF- α) and augment mainly inflammatory and cytotoxic cell mediated immune processes. T_H2 cells mainly produce IL-4, IL-5, IL-6 and IL-10, which are essential for the activation of B lymphocytes, and thereby primarily facilitate humoral immune responses (134). Various other T cell subtypes, such as T_H3, T_H9 and T_H17 cells have also been described. T_H3 cells include induced regulatory T cells, originating from naïve T cells, usually after oral consumption of antigens. They produce TGF- β that can inhibit activation of T_H1 and T_H2 cells (135). T_H9 effector cells produce IL-9 while T_H17 cells produce IL-17 physiologically, additionally they can play a significant role in autoimmune diseases (136-138).

Physiological T cell activation occurs upon contact with professional antigen presenting cells. The consequence of antigen presentation depends on the age and the stage of differentiation of the T cell, and also on the intensity and the duration of the stimulus (139). As mentioned above, it is well established that the co-localization of different signaling molecules forms an immunological synapse, which enhances the subsequent cellular response (79, 140). The molecules forming the immunological synapse on the T cell side include the TCR-CD3 complex together with co-activator molecules such as CD28 (141) and cell adhesion molecules such as CD40 ligand (142) or the CD-2 (143).

In concert with the Ca^{2+} -dependent mechanisms detailed in section 2.2.1., signaling pathways not involving NFAT also induce the proliferation of T cells. The main signaling pathways involve secondary messenger molecules such as MAP kinase or Ras that can induce gene expression of transcription factors and messenger molecules that facilitate pathways resulting in cell proliferation (144, 145). Such pathways include the mammalian target of rapamycin (mTOR), which contributes to the activation of both translational and metabolic pathways, and also influences DNA synthesis (146, 147). The mTOR can be blocked indirectly using rapamycin, also known as sirolimus. Rapamycin, originally described as a macrolide type antibiotic, can effectively inhibit the FK506 binding protein (FKBP12), which in turn interacts with mTOR. Thus, rapamycin is a highly effective immunosuppressive drug, that is currently widely used in the treatment of kidney graft rejection and graft versus host disease (148).

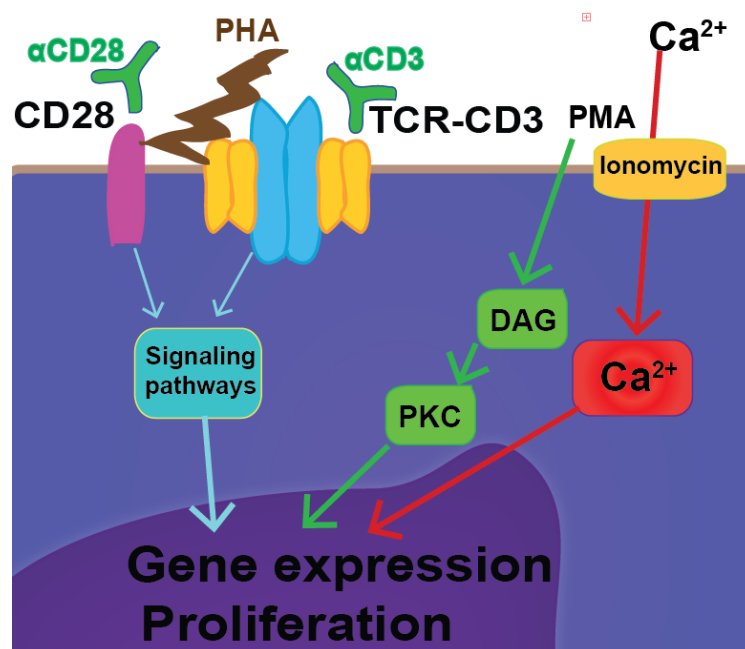


Figure 2.5: Mitogens are used to mimic physiological T cell activation

The illustration shows the mechanism of action of mitogens detailed in this work: Antibodies against cell surface markers are indicated with α ; PHA: phytohemagglutinin; PMA: phorbol-myristate acetate; DAG: diacylglycerol; PKC: protein kinase C

For modeling of lymphocyte proliferation *in vitro*, scientists commonly apply polyclonal T-cell activators, mitogens, which are capable of activating T-lymphocytes independently of TCR specificity (Fig. 2.5.). These are applied to lymphocytes either from blood or from lymphoid tissues. The most commonly used mitogens include plant lectins, activating antibodies, phorbol esters, and lipopolysaccharides (149).

Although there are lectin-type carbohydrate binding molecules on the surface of animal cells, e.g. on liver cells, and a pathway leading to the activation of the complement system is also lectin-mediated, the mitogenic lectins used in laboratories originate from plants, mainly from *Fabaceae*. Phytohemagglutinin (PHA) is isolated from *Phaseolus vulgaris*, while concanavalin A (Con A) is found in *Canavalia ensiformis*. These lectins cross-link with the carbohydrate moieties of membrane glycoproteins (including the TCR and the CD3 molecule).

Another family of mitogens are T cell activating antibodies. T-cell activation signals can be evoked using antibodies designed primarily against TCR and CD3, but complete activation of the actual T cell pool is not achieved without additional stimulus, e.g. combination with antibodies against costimulatory receptors such as anti-CD2 or anti-CD28 (150). For optimal T cell activation, antibodies are to be immobilized or fixed to solid surfaces, secondary antibodies or even beads (151).

Other characteristic mitogens used in combination are phorbol 12-myristate 13-acetate (PMA) and the Ca^{2+} ionophore ionomycin. These substances can activate the T cell independently of the presence of antigen. PMA, which is an analog of DAG, can penetrate the cell membrane and then intracellularly leads to PKC activation. The ionophore permeabilizes the cell membrane and the ER for calcium, so its effect is on Ca^{2+} influx from the extracellular space and further intracellular Ca^{2+} increase through the CRAC channel activation through the store-operated calcium entry mechanism. The two routes together are sufficient for T cell proliferation (149).

Increased level of activation can be achieved using bacterial superantigens and lipopolysaccharides. It is characteristic of them that although they activate numerous T lymphocytes, far more than an average antigen, they do not affect every subtype directly as the other mitogens mentioned above. This group includes enterotoxins isolated from *Staphylococci* or TSST (toxic shock syndrome toxins) (149).

2.3.1. Ion channel inhibitors and rapamycin impair the T cell-mediated immune response

As discussed in chapter 2.2., ion channels including the CRAC, Kv1.3, KCa3.1, and KCa1.1 have been implicated to contribute to the differentiation and maturation of immune cells, recognition of foreign antigens, initiation of immune responses and even inducing apoptosis. Therefore, it is not surprising that both inhibitors of Kv1.3 and several KCa3.1 and CRAC inhibitors have been shown to have effects on T lymphocyte proliferation (details on Fig. 2.6.). Experimental results and observations have been found since 1984 that inhibitors of

ion channels reduce the degree of T cell proliferation (152). The first such results were non-selective K⁺ channel inhibitors, tetraethylammonium (TEA), 4-aminopyridine (4-AP) and quinidine. However, the use of selective modulators of these channels could open the way for novel treatment modalities to relieve the “plague” of millions with autoimmune disorders, which currently have no definitive treatment.

Kv1.3 is an excellent candidate for immunotherapy, as it is expressed predominantly in astrocytes, T lymphocytes and oligodendrocytes (153) in contrast to CRAC and KCa3.1 channels, that are widely distributed and thus their blockers may have more side effects. Successful experimental trials employing Kv1.3 blockers have already been performed in animal models of autoimmune diseases such as MS (78), type 1 diabetes mellitus or rheumatoid arthritis (124). Dalazatide, which is a synthetic peptide derivative of the ShK toxin isolated from sea anemone *Stichodactyla helianthus*, is a specific inhibitor of the voltage-gated Kv1.3 potassium channel (124, 154). *In vivo* studies using dalazatide have shown that drug treatment inhibited the delayed-type hypersensitivity response by suppression of T_{EM} cells, but had no effect on naïve T cells or T_{CM} cells (155). In the current phase 1B study, dalazatide improved psoriatic skin lesions by inhibiting cytokine secretion and propagation of inflammation. It is also worth noting that treatment reduced mediators of inflammation in the blood and decreased the expression of T cell activation markers, and even more notably, was not accompanied by any serious adverse effects (156).

T lymphocyte activation can also be inhibited without profoundly affecting the Ca²⁺ signaling. Rapamycin, as mentioned in the previous chapter, binds to the mTOR (mammalian target of rapamycin) complex intracellularly through FKBP12 and inhibits its function (157). TOR is normally involved in cell growth, ribosomal synthesis, transcription and translation initiation processes, and is indispensable for the reorganization of actin cytoskeleton (158). Most of these processes are controlled by the activation of the S6- and the eIF-4E complexes. As opposed to tacrolimus (FK-506), a close structural homolog, rapamycin does not inhibit the function of calcineurin so Ca²⁺-mediated cell activation processes can largely remain intact.

The anti-proliferative effects of different ion channel blockers on T cells have already been described in several experiments and reviews. However, there is an obvious variability in the results of previous studies related to this topic. For example, the average blocker concentration necessary for 50% inhibition of cell proliferation ranged from $1 \times K_d$ concentration to $1000 \times K_d$ in case of Kv1.3 channel blockers, or from $1.5 \times K_d$ to $275 \times K_d$ in the case of the KCa3.1-blocker TRAM-34, where K_d is the drug concentration required to block half of the relevant channels in electrophysiological experiments (78, 159-162). A more detailed comparison can be appreciated on Fig 2.6., summarizing the proliferation inhibiting ion channel inhibitor concentrations for Kv1.3 KCa3.1 and CRAC channels, obtained by an extensive PubMed literature search (78, 123, 159-161, 163-179). Moreover, TRAM-34 inhibition alone had no effect on the proliferation of mixed T cell populations (163). The underlying mechanism responsible for this variability has not been systematically addressed before, but must be largely due to the different methods of T cell stimulation and different doses of mitogens applied in these studies.

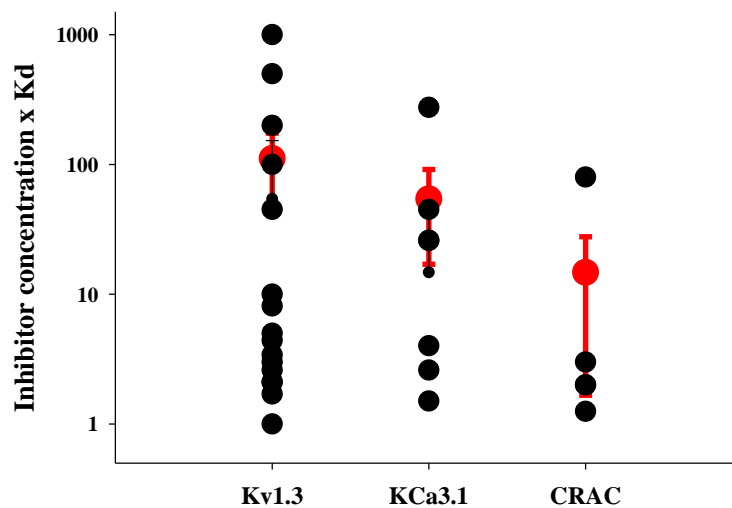


Figure 2.6.: Concentration of ion channel inhibitors needed for 50% inhibition of proliferation

The black dots show IC_{50} values from altogether 23 articles regarding ion channel inhibitors affecting T cell proliferation. The red dots show the mean concentration of Kv1.3, KCa3.1 and CRAC inhibitors, error bars indicate S.E.M. ($111.8 \times K_d \pm 63.38$; $54.3 \times K_d \pm 37.29$; $14.7 \times K_d \pm 13.07$, respectively).

2.4. Fibroblast-like synoviocytes are key effectors in rheumatoid arthritis

The previous sections have mainly covered ion channels in various immune cells under physiological and pathological conditions. However, ion channels of tissue effector cells can also be crucial for pathogenesis of certain autoimmune diseases. Normally, diarthrodial joints are characterized by the presence of a layer cartilage that lines the opposing bony surfaces, together with a lubricating synovial fluid within the synovial cavity. The capsule of a diarthrodial joint is divided into two main compartments: the supporting sub-intimal layer which contains vessels, nerves and a loose connective tissue as well as the superficial, thin intimal lining layer. The latter superficial layer is in contact with the intra-articular cavity and produces lubricious synovial fluid. The main cell types occupying the intimal lining are distributed in relatively equal proportions. Type A, or macrophage-like synovial cells are the main phagocytotic cells of this tissue and type B, or fibroblast-like synoviocytes (FLS) are involved in the secretion of extracellular matrix components such as hyaluronic acid, various collagens and aggrecan (Fig. 2.7.) (180-182).

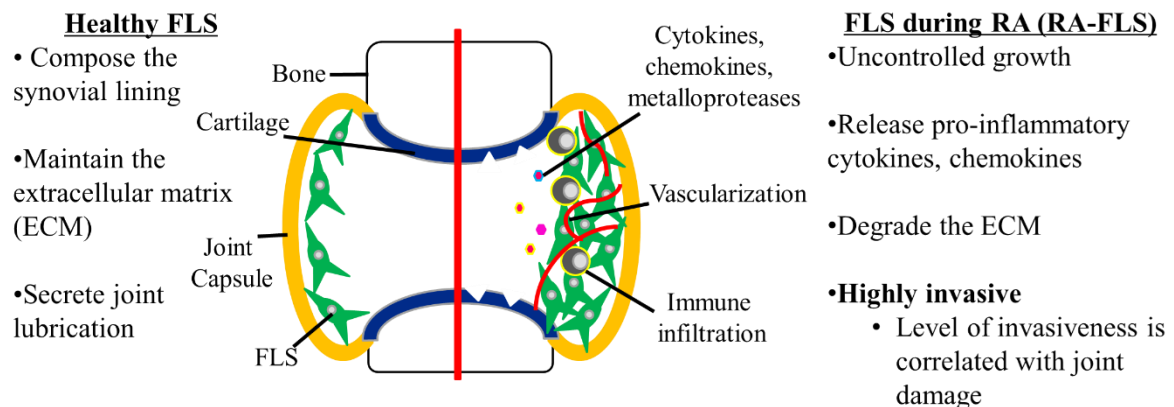


Figure 2.7.: *Fibroblast-like synoviocytes develop a pathological phenotype during rheumatoid arthritis*

The illustration above summarizes the properties of physiological FLS (left side) versus pathological “tumor-like” RA-FLS (right side).

Rheumatoid arthritis (RA) affects nearly 1% of the western population and is associated with reduced quality of living, disability, and reduced survival as it involves not only diarthrodial joints but can also target vital internal organs, including the heart and lungs (183-185). The hyperplastic synovial tissue in RA, also called pannus, has unique characteristics and like a

cancer invades and destroys cartilage and bone. While the RA synovial tissue degeneration is incompletely understood, the joint destruction mediated by it correlates with increased disease severity and unfavorable outcome. FLS that are normally nurturing the surrounding tissues and supporting the extracellular matrix can become highly invasive in RA. FLS in RA (RA-FLS) have been implicated in disease pathogenesis as they exhibit a transformed “tumor-like” phenotype (Fig. 2.7.) with increased invasiveness and production of proteases and of various pro-inflammatory and pro-angiogenic factors (180, 181, 186). FLS have a key role in the formation of the pannus from RA synovium (180), and the *in vitro* and *ex vivo* invasiveness of FLS correlate with the histological and radiographic damage in animal models of RA (187, 188).

In the last decades, management of RA has started to advance with the development of new treatments, however disease remission is rarely achieved and most patients only achieve mild to modest improvement (189). Furthermore, current therapies significantly impair immune responses rendering patients more susceptible to infections and cancer (190). Therefore, novel therapeutic options that lead to pronounced improvement or remission without inducing immunosuppression are needed.

2.4.1. Ion channels influence the phenotype of RA-FLS

RA-FLS and FLS from arthritic rats express functional KCa1.1 (detailed in section 2.1.1.) as the major K⁺ channel in their plasma membrane (191, 192). Blocking the function of KCa1.1 pore-forming α subunits in these FLS with paxilline inhibits their invasiveness and stops disease progression in animal models of RA (191, 192). However, paxilline is a lipophilic small molecule that blocks all KCa1.1 channels found in major organs, regardless of channel subunit composition (49, 193, 194), and can cross cell membranes as well as the blood-brain barrier; it therefore induces severe side effects such as tremors, incontinence, and hypertension (195-197). The molecular mechanism by which inhibiting KCa1.1 leads to inhibition of FLS invasiveness has remained unknown.

Besides KCa1.1, the literature so far demonstrated the presence of both an inward L-type calcium current and an outward voltage-gated delayed rectifier potassium current, of which KCa1.1 is a major constituent, in cultured rabbit intimal synoviocytes. The same channels, however, have not been described since in human FLS. FLS are known to express other ion channels, including a vast variety of members of the TRP family such as TRPV1, TRPV2,

TRPC1, TRPM3, and TRPM7, but their involvement in FLS function is still not fully understood (illustrated in Fig. 2.8.) (198). FLS expression of the extracellular matrix degradation enzyme matrix metalloproteases (MMPs) MMP-2 and MMP-3, two key mediators of invasion and joint damage, was significantly reduced by TRPV2 stimulation. These observations suggest that TRPV2 does not necessarily interfere with FLS migration but may instead disturb invasion and joint damage via interfering with an effector pathway such as MMP expression or cell activation (198). TRPM7 is also upregulated in RA-FLS compared to control and it was suggested that antagonists of TRPM7 channels may increase RA-FLSs apoptosis *in vitro* (199).

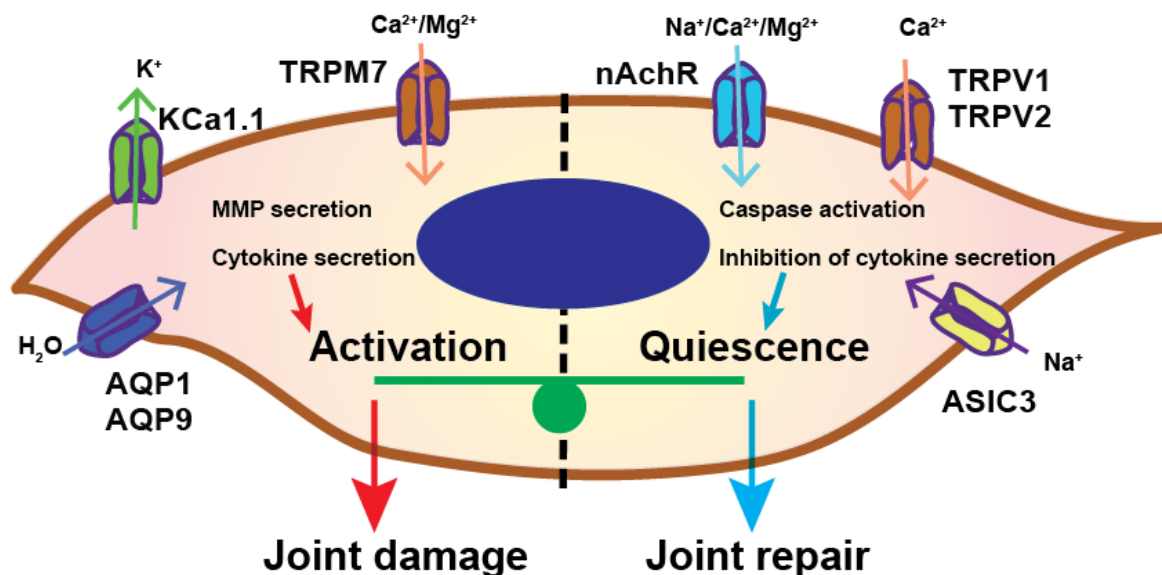


Figure 2.8.: The phenotype of FLS highly depends on ion channels

The diagram shows the key ion channels involved in regulation of FLS activation. The channels on the left side augment, whereas channels on the right side suppress FLS activation.

Also, $\alpha 7$ nAChR and its dup $\alpha 7$ variant are expressed in RA synovium, where they may play a critical role in regulating inflammation and $\alpha 7$ nAChR agonists reduced tumor necrosis factor α -induced IL-6 and IL-8 production by FLS (200, 201). Aquaporin 1 and 9 are expressed, too, in RA-FLS, and are involved in edema formation in osteoarthritis (OA) and RA. Lastly, ASIC3 is also expressed in RA-FLS, regulating pH responsiveness and controlling release of the extracellular matrix polysaccharide hyaluronan (202).

In conclusion, all the ion channels above may be potential therapeutic targets not only to treat the symptoms of pain associated with diseases of the joint, but more significantly, to attenuate the underlying causes of such diseases.

2.4.2. *KCa1.1 as a possible therapeutic target*

In many excitable cells, KCa1.1 channels are localized in plasma membrane complexes with voltage-gated Ca^{2+} channels; their activation via Ca^{2+} -entry causes cell hyperpolarization which prevents further Ca^{2+} -influx by closing proximal Ca^{2+} channels, thereby providing a negative feedback regulatory mechanism for Ca^{2+} -entry into the cell. In smooth muscle, proximity of KCa1.1 channels to sarcoplasmic reticulum Ca^{2+} release sites provoke a similar negative-feedback loop. However, in non-excitable cells, KCa1.1 channels supply positive-feedback regulation for Ca^{2+} -entry by providing K^{+} -efflux, thereby stimulating Ca^{2+} -influx. Moreover, they can provide K^{+} flux in epithelial cells that facilitates transmembrane flux of chloride along with water (1, 4, 203).

Because of their functional properties and extensive pattern of expression, KCa1.1 channels regulate a wide range of processes in animals: they control smooth muscle contractility, neuronal excitability, neurotransmitter release, endocrine secretion, epithelial function, and activation or migration of non-excitable cells like fibroblasts, among other putative physiologic roles (e.g. in cell migration). Therefore, it is expected that direct pharmacological modulation of KCa1.1 channels, either their activation or inhibition, would present a plethora of therapeutic opportunities (204).

Development of KCa1.1 channel agonists which target smooth muscle has been well explored, and clinical indications could include hypertension, erectile dysfunction, asthma, dysmenorrhea, and overactive bladder. In smooth muscles, KCa1.1 channels are coupled to ryanodine receptors (RyR) and often by the auxiliary $\beta 1$ subunits (7, 205, 206). Activation of KCa1.1 channels by RyR-mediated Ca^{2+} sparks potentiates a large outward K^{+} current that hyperpolarizes the membrane potential of smooth muscle cells, decreases Ca^{2+} -influx and relieves smooth muscle constriction. Direct and indirect KCa1.1 channel inhibition improves smooth muscle contractility both *in vivo* and *in vivo*, whereas activation of KCa1.1 channels in some smooth muscle tissues has a marked relaxing effect (204). Another potential application

of a KCa1.1 agonist would be activating channels in the nephrons of the kidney to stimulate K⁺ secretion and thus limit plasma hyperkalemia in certain conditions (207).

Obviously, using activators of KCa1.1 channels in neuronal tissue as a therapeutic approach must be approached with caution (208, 209). Mutations enhancing KCa1.1 activity can cause generalized epilepsy and paroxysmal dyskinesia, as well as spontaneous seizures and temporal lobe epilepsy. These potential side effects might be avoided by limiting blood-brain barrier penetration of the drug, or by focusing on activation of KCa1.1 channels assembled with unique beta subunit compositions in the target tissues that are different from KCa1.1 channels. The only possible benefit of a neuronal KCa1.1 agonist would be in the peripheral nervous system to reduce electrical activity of pain pathways and provoke analgesia. However, these therapeutics are still theoretical and require more robust pharmacological tools than currently available.

Development of KCa1.1 channel blockers could also be of therapeutic benefit in certain diseases, such as rheumatoid arthritis, glioblastoma multiforme, hypotensive crisis, and even glaucoma. However, a more cautious strategic approach is required than with a KCa1.1 channel agonist, to spare the countless physiological functions of this channel. For example, systemic exposure to the KCa1.1 channel inhibitor paxilline caused smooth muscle hyperexcitability, resulting in vasoconstriction and hypertension. Also, exposure in the central nervous system resulted in impaired motor functions and cerebellar ataxia, disrupted circadian rhythm, generalized and temporal epilepsy, seizures (210, 211). Moreover, disruption of KCa1.1 channel activity in the kidney could result in decrease of K⁺ secretion and subsequent hyperaldosteronism, further contributing to manifest hypertension. Lastly, a KCa1.1 inhibitor could also lead to spontaneous urinary bladder activity and thus uncontrolled urination.

Therefore, if KCa1.1 channels are to be targeted with an inhibitor, care must be taken to prevent broad exposure of KCa1.1 channel containing tissues to drug during dosing. Possible ways to overcome this hurdle would be application of an agent locally, directly onto the target, or synthesizing a small molecule modulator with metabolic liabilities to ensure fast metabolism and rapid clearance, or, using the drug in acute therapy rather than chronically (204). Finally, as the ancillary subunits of KCa1.1 are restricted to certain tissues, it may be possible to design inhibitors (e.g. antibodies) that only target the channel coupled to a certain regulatory subunit to minimize cross-reaction with different channel phenotypes in other tissues.

3. AIMS OF THE STUDY

As mentioned previously, voltage-gated ion channels play a key role in the regulation of different inflammatory cells, and thus in immune responses in general. We approached the functional aspects of potassium channels of the inflammatory cells from two directions.

Firstly, as detailed in the introduction, we approached the heterogeneity in the anti-proliferative effects of different ion channel blockers on T cells (Fig. 2.6.). The underlying mechanism responsible for this phenomenon was still unclear, although it could be accounted largely to the different methods of T cell stimulation. Therefore, *our aim was to elucidate this phenomenon by comparing the anti-proliferative effects of ion channel blockers and rapamycin on lymphocytes cultured and activated under identical experimental conditions.* Moreover, considering our results at various mitogen concentrations, we propose a theory to explain the underlying mechanisms of our observations.

Furthermore, we approached ion channel function in autoimmune diseases in regards of rheumatoid arthritis and more specifically RA-FLS. The RA-FLS express functional KCa1.1 as the major K⁺ channel at their plasma membrane. Paxilline, a lipophilic small molecule that blocks all KCa1.1 channels found in major organs, regardless of channel subunit composition, it therefore induces severe side effects such as tremors, incontinence, and hypertension. As detailed in section 2.4.2, despite the drawbacks of the unspecific block of KCa1.1 by paxilline, the channel remains an attractive target for therapy, partly because the regulatory subunits of KCa1.1 have restricted tissue distribution and affect channel pharmacology. To date, however, no KCa1.1 β subunit has been described in RA-FLS. Thus, *our aim was to elucidate whether RA-FLS express any accessory β subunits, and whether expression of these subunits have any functional implications in these cells.*

4. MATERIALS AND METHODS

4.1. Reagents

All reagents were purchased from Sigma-Aldrich (St. Louis, MO, USA), unless stated otherwise.

4.2. Isolation and culture of peripheral blood mononuclear cells

PBMCs were isolated from heparin-treated (heparin from TEVA Pharmaceutical Industries Ltd., Debrecen, Hungary) peripheral blood of healthy volunteers, under appropriate Ethical Committee approved protocol (DE OEC RKEB/IKEB 3989-2013). First, Hanks' Balanced Salt Solution (HBSS) was used to dilute the blood in 1:1 ratio, then the blood was centrifuged with the Ficoll-Hypaque density gradient (GE Healthcare Life Sciences, Little Chalfont, UK) at 1400 rpm for 30 minutes at room temperature. Next, the cloudy mononuclear cell layer was collected and washed two times using 50 ml HBSS, ultimately obtaining the PBMC population used in our experiments.

In n=4 preliminary experiments we used purified CD3⁺ T lymphocytes obtained by negative selection using RosetteSep™ (Stem Cell Technologies™, Vancouver, Canada) technique. This kit targets non-T cells for removal with antibodies recognizing specific cell surface markers, thus allowing negative selection of T lymphocytes. Using this technique, we could enrich CD3⁺ T cells to >95% in the population.

Following carboxyfluorescein succinimidyl ester staining (CFSE staining, see in section 4.5.3.) and activation, cells were cultured in 24 or 96 well plates at a cell density of 10⁶ cells/ml in standard RPMI-1640 medium (Sigma-Aldrich Co., Saint Louis, MO, USA) supplemented with 15% HEPES buffer (Sigma-Aldrich Co., Saint Louis, MO, USA), 10% FBS, 10 IU/ml penicillin, 0.1g/ml streptomycin and 2 mg/ml L-glutamine at 37°C in humid atmosphere with 5% CO₂. In each experiment, every plate was incubated for 5 days and was supplemented with fresh culture medium after 72 hours. After harvesting, cells underwent propidium iodide (PI) staining and subsequent FACS analysis.

4.2.1. Selective stimulation of T lymphocytes

At the beginning of the study, we performed preliminary experiments regarding our preferred method of stimulation. Four widely used and well-known lymphocyte stimulation techniques were compared using CFSE dilution assay on PBMCs: PHA stimulation; PMA

combined with ionomycin; soluble anti-CD3 antibody alone and in combination with anti-CD28. Moreover, we measured whole-cell K^+ currents, current density and biophysical characteristics of the Kv1.3 channel on representative populations of the stimulated T cells. We found the anti-CD3 and anti-CD28 stimulation was most reproducible (shown in 5.1.1.) and thus, we used this approach in our further experiments.

We applied 200 nM – 3 μ M soluble anti-CD3 antibodies combined with a constant amount of 1 μ g/ml soluble mouse anti-human CD28 in n=8 experiments for specific T cell stimulation in the PBMC and lymphocyte cultures. We enhanced the rate of stimulation by adding the soluble antibodies to the bottom of the culture well, left it to bind to the plate surface for 30 minutes at room temperature, then cells were added to the wells in culture medium suspension. In n=8 experiments we used superparamagnetic bead-conjugated anti-CD3 and anti-CD28 monoclonal antibodies (Life Technologies Co., Waltham, MA, USA), which we found more user-friendly than the soluble antibodies. The pairwise comparison of soluble mitogens and bead-mediated stimulation Student's t-test showed no significant difference between the divided cell populations with the two methods of stimulation ($p=0.336$). The beads are also known to provide adequate cross-linking, thus inducing a relatively high level of activation (151), in contrast to stimulation with soluble anti-CD3 and anti-CD28, that resulted in a higher amount of variability in our measurements (212). The bead-to-cell ratio in these cases was 1:200 - 1:1 (see Results).

4.2.2. Applying pharmacological inhibitors of T lymphocyte ion channels

To block the Kv1.3 channel, we used the peptide-type toxin AnTx, previously pharmacologically assessed by our lab (63). KCa3.1 channels were blocked using TRAM-34 (161) and the CRAC channels were inhibited by 2-Apb (213). We used the ion channel inhibitors at two different concentrations: the lower was equal to the dissociation constant, or $1 \times K_d$, of ion channel inhibition of the blockers and the higher was 10 times the K_d ($10 \times K_d$). In the case of AnTx, we used 500 pM ($1 \times K_d$) and 5 nM (63). In the case of 2-Apb, the K_d for lymphocytes is 5 μ M, and the other concentration used was 50 μ M ($10 \times K_d$). Finally, the KCa3.1 blocker TRAM-34 was used in 20 nM ($1 \times K_d$) and 200 nM ($10 \times K_d$) concentrations. In the case of rapamycin the lowest concentration reported in the literature (214, 215) to inhibit T cell proliferation by 50% ($1 \times IC_{50} = 20$ pM) was used as the lower dose and 200 pM ($10 \times IC_{50}$) was used as the higher dose.

4.3. CFSE dilution assay and PI staining

We applied the CFSE dilution assay, originally described in 1994 by Lyons et al (216-218), to measure the rate of cell proliferation. The staining procedure can be summarized as following: the membrane-permeable, but non-fluorescent carboxifluorescein diacetate succinimidyl ester (CFDA-SE) binds to structural proteins within the cell, and is subsequently cleaved by nonspecific esterases to become the membrane non-permeable and fluorescent CFSE. Upon cell division, the amount of CFSE is gradually halved in the daughter cells, thus the number of division cycles the cells have undergone can be determined. In our case, the lymphocytes divided usually every 24-48 hours, leading to 4-6 measurable cycles at the end of our experiments.

The final concentration of CFDA-SE (CellTrace™ CFSE Cell Proliferation Kit, Life Technologies Co., Waltham, MA, USA) in our experiments was 1 μM that led to a 100-to-1000-fold increase in the fluorescence intensity of the measured cells over the basal autofluorescence of unstained cells. After adding CFDA-SE, we incubated the PBMCs or T lymphocytes for 15 min at room temperature, then for 20 min at 37°C. Lastly, the cells were washed once with phosphate buffer solution (PBS). We took caution that the CFSE-stained cells remain hidden from excess light during our experiments. The cellular fluorescence after CFSE staining was ultimately recorded by flow cytometry.

PI staining was performed at the end of the 5-day incubation period. Therefore, we harvested and washed the cells once using HBSS, then added PI to the cell suspension to achieve 1 μg/ml final concentration. Cells were mixed gently with PI and then incubated in the dark for 5 minutes at room temperature.

4.4. Flow cytometry experiments

The flow cytometry measurements on PBMCs and T lymphocytes were performed on BD FACScan™ and FACS Array™ flow cytometers. We measured the light scatters, namely the forward scatter (FSC) and side scatter (SSC) and the fluorescence intensity on green and red channels. Gate setting for lymphocytes is shown in Fig. 5.2.A, and the gating of viable cells is represented in Fig. 5.4.A and B. The sheath fluid consisted of 1x PBS. Lymphocytes were selected from mixed cell populations of PBMC by their light scatter profile on FACS analysis.

Cell proliferation was measured based on the declining CFSE intensity in the green channel (Fig. 5.1B.). Division index (DI) was used as the indicator of proliferation and was calculated by the following formula:

Eq. 3.
$$DI = \left(\sum_{k=1}^n A_k \right) / \left(\sum_{k=0}^n A_k \right)$$

where k is the division cycle number (i.e. generation number) of cells, and A_k is the cell number in the k^{th} division cycle according to Fig. 5.1.B.

When performing the PI staining, the flow cytometer settings were adjusted to a negative control tube containing unstained cells. PI fluorescence intensity was measured in the red channel, because samples were co-stained with CFSE.

In case of RA-FLS, detection of the α subunit of KCa1.1 and of CD44, podoplanin, cadherin 11 and MMP-2 was performed as previously described (192, 219, 220) using antibodies listed in Table 1. Cells were treated with brefeldin A (eBioscience, San Diego, CA, USA) for 6 h before detection of intracellular MMP-2. Cells were permeabilized with 0.5% saponin for detection of intracellular epitopes. Data was acquired by a Canto II flow cytometer (BD Biosciences, San Jose, CA) using BD FACSDiva and analyzed using FlowJo (Treestar, Ashland, OR). Alternatively, live CD44^{high} and CD44^{low} cells were sorted under sterile conditions using a FACSARIAII flow cytometer (BD Biosciences) and immediately used for invasion assays.

Target	Host	Vendor (catalog number; manufacturer location)	Conjugation	Clone	Use
Primary antibodies					
Actin	Rabbit	Sigma-Aldrich (A2066; St. Louis, MO, USA)	–	–	WB
Actin	Mouse	Sigma-Aldrich (A3853)	–	AC-40	WB
Cadherin-11	Mouse	Thermo Fisher Scientific (MA1-06306; Rockford, IL, USA)	–	16A	FC
CD44	Mouse	Abcam (ab187571; Cambridge, MA, USA)	Alexa Fluor 488	MEM85	FC, EP
KCa1.1α	Mouse	Antibodies, Inc. (NeuroMab, 75-022; UC Davis/NIH NeuroMab Facility, Davis, CA, USA)	–	L6/60	WB
KCa1.1α	Rabbit	EMD Millipore (AB5228; Billerica, MA, USA)	–	–	FC
KCa1.1β1	Rabbit	Novus Biologicals (NBP1-33484; Littleton, CO, USA)	–	–	WB
KCa1.1β2	Mouse	Antibodies, Inc. (NeuroMab, 75-087; UC Davis/NIH NeuroMab Facility)	–	N53/32	WB
KCa1.1 pan-β3	Rabbit	Abcam (ab137041)	–	EPR9543(B)	WB
KCa1.1 β3a, βc, βd, βe	Mouse	Rockland Immunochemicals (200-301-E96; Limerick, PA, USA)	–	S40B-18	WB
KCa1.1β4	Mouse	Antibodies, Inc. (NeuroMab, 75-086; UC Davis/NIH NeuroMab Facility)	–	L18A/3	WB
MMP-2	Mouse	BioLegend (634802; San Diego, CA, USA)	–	F14P4D3	FC
Podoplanin	Rat	BioLegend (337003)	Phycoerythrin	NC-08	FC
Secondary antibodies					
Mouse IgG	Goat	LI-COR Biosciences (926-32210; Lincoln, NE, USA)	Infrared-800	–	WB
Mouse IgG1	Goat	Thermo Fisher Scientific (A-21127)	Alexa Fluor 555	–	FC
Rabbit IgG	Donkey	LI-COR Biosciences (926-68023)	Infrared-680	–	WB
Rabbit IgG	Goat	Abcam (ab150079)	Alexa Fluor 647	–	FC

Table 1. Characteristics of the antibodies used for this study.

EP electrophysiology, FC flow cytometry, IgG immunoglobulin G, KCa calcium-activated potassium channel, MMP matrix metalloproteinase, WB Western blot analysis

4.5. Measurement of secreted cytokine concentration

Culture supernatants of human peripheral blood mononuclear cells (n=3) were harvested five days after application of mitogens and ion channel blockers. Cytokine sandwich enzyme-linked immunosorbent assay (ELISA) was used to specifically detect and quantitate the concentration of soluble cytokines, namely IL-10 and IFN- γ . The level of these cytokines in the supernatant was measured by OptEIA kits (BD Biosciences, Franklin Lakes, NJ, USA), using duplicates, according to manufacturer's instructions.

4.6. Culturing RA-FLS

FLS from 14 patients with RA and 4 patients with osteoarthritis (OA), defined according to the criteria of the American College of Rheumatology (221), were purchased from Asterand (Detroit, MI) or collected as described (222, 223) under the appropriate Institutional Review Board (IRB) approved protocols (Table 2.). Cells were harvested for future experiments between passages 4 and 11; the FLS were cultured in DMEM (Life Technologies, Grand Island, NY) supplemented with 10 IU/ml penicillin, 0.1g/ml streptomycin, 1 mM sodium pyruvate, 2 mg/ml L-glutamine, and 10% FBS.

Donor	Diagnosis	Sex	Ethnicity	Disease duration (years)	RF	Medications	Origin of cells
RA-1	RA	Female	White	3	+	NSAID	A
RA-2	RA	Male	Hispanic	<1	+	Prednisone, DMARD	A
RA-3	RA	Female	White	<1	+	NSAID	A
RA-4	RA	Female	White	12	+	NSAID, prednisone	A
RA-5	RA	Female	Hispanic	2	+	DMARD, NSAID	FITDP
RA-6	RA	Female	White	21	+	Prednisone, DMARD	FITDP
RA-7	RA	Female	White	30	+	Prednisone, DMARD	FITDP
RA-8	RA	Female	White	20	+	Etanercept, prednisone	FITDP
RA-9	RA	Female	White	21	+	Leflunomide, etanercept, prednisone	FITDP
RA-10	RA	Male	White	15	+	NSAID, prednisone, adalimumab	FITDP
RA-11	RA	Female	African American	11	+	Hydroxychloroquine, prednisone	FITDP
RA-12	RA	Male	White	>10	+	Etanercept	FITDP
RA-13	RA	Female	Hispanic	>10	+	Methotrexate, prednisone	FITDP
RA-14	RA	Female	White	3	+	Prednisone, methotrexate	FITDP
OA-1	OA	Female	White	12	-	None	A
OA-2	OA	Male	White	16	-	None	A
OA-3	OA	Male	White	25	N/A	None	FITDP
OA-4	OA	Male	White	78	N/A	None	FITDP

Table 2. Characteristics of the subjects who donated FLS for this study.

DMARD: disease-modifying antirheumatic drug, A: Asterand, FITDP: Feinstein Institute Tissue Donation Program, N/A: not available, NSAID: non-steroidal anti-inflammatory drug, OA: osteoarthritis, RA: rheumatoid arthritis, RF: rheumatoid factor. Patients with RA were 58 ± 10 years old, and patients with OA were 57 ± 5 years old

4.7. Reverse transcription (RT) and quantitative polymerase chain reaction (qPCR)

Total RNA was isolated from approximately 5×10^5 cells using TRIzol (Life Technologies). Reverse transcription was performed with Superscript III reverse transcriptase and random hexamer primers (Life Technologies), according to the manufacturer's protocol. The resulting cDNA was used as a template for qPCR primers (Table 3.) designed from the National Institutes of Health qPrimerDepot (<http://primerdepot.nci.nih.gov/>), or designed manually and tested by PrimerBlast (<http://www.ncbi.nlm.nih.gov/tools/primer-blast/>). Amplicon sizes were between 70 and 250 bp in all cases. qPCR reactions were conducted in final volumes of 10 μ L using the following components: diluted cDNA (1:10) 4 μ L; and oligo forward and reverse primers (2.5 μ M each) in 6 μ L of iTAQ SYBR Green supermix (Bio-Rad, Hercules, CA). Reactions were run in a ViiA™ 7 Real-Time PCR System (Life Technologies), detecting the accumulation of the fluorescent signal. The cycling conditions were: 20 s at 95°C, 40 cycles at 95°C for 1 s and 60°C for 20 s, 95°C for 15 s, 60°C for 1 min, and a gradient from 60°C to 95°C for 15 min. The results were analyzed using the ViiA™ 7 Software.

Subunit	Accession number	Sense (forward) 5'-3'	Antisense (reverse) 3'-5'	bp
α	NM_002247	GCTCAAGTACCTGTGGACCG	CTGGTTTGAGAGTGCCATCC	104
β 1	NM_004137	CTGTACCACACGGAGGACAC	GCTCTGACCTTCTCCACGTC	107
β 2a	NM_181361	ATTAAGCGTGGCTTTTGAGG	GTITGGTCCAGGGTCTCCTTT	98
β 2b	NM_005832	GAGAAAGAGCAACAAAGCGG	TTAGCAAATCCCAGACATTGC	107
β 3a	NM_171828	AAATCACACTTCAGGGCAGC	GCACATCTAGTGGGTCTCCA	105
β 3b	NM_171829	TCTGAGTGTGAGGGGCTCTT	GCACATCTAGTGGGTCTCCA	105
β 3c	NM_171830	CCATGATGGGCTTCTCAGTC	GCAGTGCAGGTCGATTCTTC	100
β 3d	NM_014407	AGGGACGTGCAATATCCCTG	GAAAGGCTGTCTGTGTCTCGT	351
β 3e	NM_001163677	ACCCGTGTCTTCAGGTGTTT	TCTGTAACATCACGCTTGGGA	107
β 4	NM_014505	CTGAGTCCAACCTCTAGGGCG	GATTTTCTCTTACAGGGAGGG	96
GAPDH	NM_002046	AAGGTGAAGGTCGGAGTCAA	AATGAAGGGGTCATTGATGG	108

Table 3. Primers used for qPCR.

For data analysis, we attained the cycle threshold (cT) values, defined as the number of cycles required for the fluorescent signal to cross the background level. Therefore, a lower cT value indicates greater amount of target nucleic acid in the sample, and in our case greater gene expression. Each cT value was subtracted by the cT of the loading control, yielding the Δ cT. Finally, for relative comparison of gene expression, we subtracted each Δ cT value with the Δ cT of the reference housekeeping gene GAPDH, noted as Δ cT- Δ cT_{GAPDH}. Moreover, due to exponential nature of PCR, the α to β ratio was calculated as:

$$\text{Eq. 4.} \quad \frac{\alpha}{\beta} = 2^{\frac{\Delta cT - \Delta cT_{GAPDH}}{\Delta cT_{KCa1.1\alpha} - \Delta cT_{GAPDH}}}$$

4.8. SDS-PAGE and Western blotting

RA-FLS and healthy Lewis rat testes (Baylor College of Medicine, Houston, USA) were lysed in RIPA buffer (Sigma, Saint Louis, MO) containing 1% protease inhibitors. Protein levels were measured using the Bradford assay. Equal amounts of protein (20 μ g) were loaded and separated by SDS-PAGE (Life Technologies), then transferred onto nitrocellulose membranes (Bio-Rad), according to manufacturer's guidelines. Blots were incubated overnight in a blocking solution consisting of 4% Blotto non-fat milk (Santa Cruz Biotechnology, Santa Cruz, CA). Blots were probed using antibodies specific for the human KCa1.1 channel α and β subunits (Table 1). Each primary antibody was diluted 1:500 in blocking solution. As loading controls, we used anti-actin antibodies. After overnight incubation and wash followed by 2 hours probing with IR-680 or IR-800 labeled secondary antibodies (Table 1) for 1 h at room temperature. The membranes were washed 3 times for 15 min with PBS + 0.1% Tween-20. Visualization was performed with a Li-Cor Odyssey Scanner, and data analyzed with ImageJ (National Institutes of Health).

4.9. Transfection of small interfering RNA (siRNA)

The mix of three different constructs of GAPDH, KCNMB1, or KCNMB3-specific small interfering RNA were mixed with DharmaFect transfection reagent (Dharmacon, Lafayette, CO) and added to 35 mm petri dishes containing cells at \approx 80% confluency according to the manufacturer's instruction. RA-FLS were kept in serum-free medium for 24 h prior to siRNA treatment with DharmaFect siRNA transfection reagent (192). Cells were used 40-80 hrs following transfection of electrophysiological, flow cytometry, and transwell invasion experiments.

4.10. Transwell invasion assay

The ex vivo invasiveness of FLS was assayed in a transwell system using collagen-rich Matrigel-coated inserts (BD Biosciences) as described in the literature (191, 192, 198). Briefly, at the start of the experiment, FLS -containing inserts in serum free medium were placed on 10% serum +DMEM containing wells. The FLS aimed to reach into the serum-rich environment, but had to digest the Matrigel along the way. Moreover, they needed to migrate actively through their environment to reach the bottom of the insert, that the cells were not able to penetrate. After 24 hours, we carefully discarded the Matrigel layer and stained the FLS using crystal violet and counted the cells on the bottom of the inserts.

4.11. Electrophysiology

4.11.1. Whole-cell patch-clamp

Standard whole-cell patch-clamp techniques were used in voltage-clamp configuration, as described previously (224). Pipettes were pulled from GC 150 F-15 borosilicate glass capillaries (Clark Biomedical Instruments, Pangbourne, UK) to gain electrodes of 2-5 M Ω resistance in the bath. Series resistance compensation up to 85% was used to minimize voltage errors and achieve optimal voltage clamp conditions.

Cells were plated on glass coverslips or petri dishes and allowed to adhere. When indicated, cells were incubated for 15 min at room temperature with fluorophore-conjugated anti-CD44 antibodies (Table 1), washed, and CD44^{high} and CD44^{low} cells were immediately assessed for K⁺ currents (225). Total K⁺ currents were recorded using the patch clamp technique in the whole-cell configuration, as described (191, 192, 226). When measuring Kv1.3 in lymphocytes, the internal solution contained 140 mM KF, 5 mM NaCl, 11 mM K₂EGTA, 2 mM MgCl₂, and 10 mM HEPES (pH 7.20, ~295 mOsm). When measuring KCa1.1, the internal solution contained 10 mM EGTA, 5 mM HEPES and 5 μ M free Ca²⁺, calculated using Maxchelator (<http://maxchelator.stanford.edu/CaEGTA-TS.htm>). The external solution contained 160 mM NaCl, 4.5 mM KCl, 2 mM CaCl₂, 1 mM MgCl₂, and 10 mM HEPES, pH 7.4 in both cases. Experiments were performed at room temperature (20-22°C).

Current density was calculated by dividing whole cell peak currents by the cell capacitance. Lymphocyte cell capacitances varied from 2-9 pF. Whole-cell measurements of T lymphocytes were carried out using Axopatch-200B amplifiers connected to personal computers using Axon Instruments Digidata 1440 data acquisition boards (Molecular Devices, Sunnyvale, CA). For data acquisition and analysis, the pClamp10 software package (Molecular Devices, Sunnyvale, CA) were used. RA-FLS cell capacitances ranged from 9 to 17 pF. Results were analyzed using Igor Pro software (WaveMetrics, Lake Oswego, OR) when measuring RA-FLS and OA-FLS.

4.11.2. Activation and inactivation kinetics of the K⁺ current

To assess the activation time constants of the Kv1.3 and KCa1.1 channels, the membrane was depolarized to +50 mV for 15 ms and +140 mV for 50 ms, respectively, from a holding potential of -120 mV and -100 mV, respectively. Current traces were fitted with a single exponential function rising to the maximum according to the Hodgkin-Huxley model ($I(t) = I_a \times (1 - \exp(-t/\tau_a))^4 + C$, where I_a is the amplitude of the activating curve component; τ_a is the activation time constant of the current; C: current amplitude at -120 mV).

To study the inactivation of Kv1.3 and KCa1.1 channels, pulses were evoked to +50 mV for 2 s and +140 mV for 200 s, respectively, from a holding potential -120mV and -100mV, respectively. The decaying part of the current traces was fitted with a single exponential function ($I(t) = I_0 \times \exp(-t/\tau_{in,i}) + C$, I_0 : amplitude of current, $\tau_{in,i}$: inactivation time constant for different groups, C: steady-state current of the whole-cell record at the end of the depolarizing pulse) to attain the inactivation time constant.

4.11.3. Test substances

We used altogether four different substances to assess the pharmacological properties of the KCa1.1 channels.

- **LCA**, that enhances KCa1.1 currents only when the channel contains the $\beta 1$ subunit (40, 41, 227); a stock of LCA (Sigma) was prepared in 1:10 solution of dimethyl sulfoxide (DMSO) and 70% ethanol.
- **AA**, that enhances KCa1.1 currents only when the channel contains $\beta 2$ or $\beta 3$ subunits (42, 227); a stock of AA (Sigma) was prepared in DMSO.
- **Paxilline**, that blocks KCa1.1 channels regardless of β subunit expression (49, 191, 228); a stock of paxilline (Fermentek, Jerusalem, Israel) was prepared in DMSO.
- **ChTx**, that blocks all KCa1.1 channels unless they contain the $\beta 4$ subunit (31, 227, 229); a stock of ChTx (Peptides International, Louisville, KY) was prepared in P6N buffer (10 mM NaHPO₄, 0.8% NaCl, 0.05% Tween-20, pH 6.0) (219, 230, 231).

The stock solutions were further diluted with electrophysiology bath solution immediately before use so that final DMSO concentrations did not exceed 0.05%.

4.12. Statistical evaluation and plotting the results

Flow cytometry data were collected using the BD CellQuest software. For data analysis, we used the freeware program Cyflogic 1.2.1 and the Flowjo X software. The analyzed data was exported to Microsoft Office Excel. For statistical evaluation of our results we used the program SigmaPlot 12.0 and GraphPad Prism 5, where all data is represented as mean \pm S.E.M. To compare different treatments to the control cell population, we applied one-way analysis of variance (ANOVA) test and as post hoc analysis, the Holm-Sidak test. Also, when the data was not normally distributed, as was the case in the very heterogeneous RA-FLS population, we performed non-parametric ANOVA on ranks test (also known as Kruskal-Wallis test), followed by Dunn's post-hoc test, to calculate statistical significance of our results. We marked the level of significance with * if p was <0.05 , with **, if p was <0.01 , and with ***, if p was <0.001 .

5. RESULTS

5.1. The anti-proliferative effect of cation channel blockers in T lymphocytes depends on the strength of mitogenic stimulation

5.1.1. Dose-dependence of mitogen-induced proliferation

Firstly, we aimed to determine which mode of T lymphocyte activation creates the most homogenous cell population in regards of ion channel expression. Therefore, we measured Kv1.3 membrane expression by whole-cell patch clamp and subsequent calculation of current density after treatment of PHA; PMA and ionomycin; α -CD3; α -CD3 and α -CD28 used in combination (Fig. 5.1.).

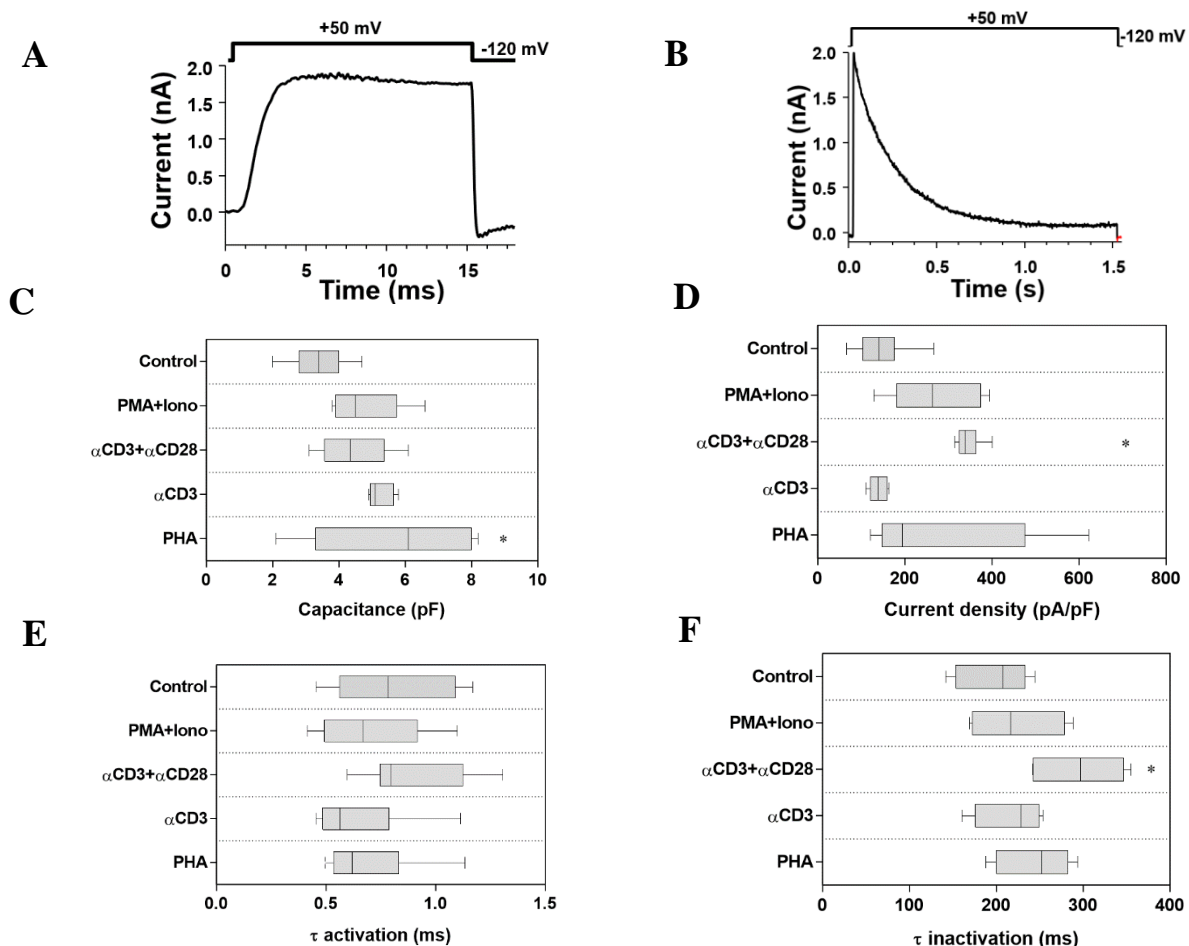


Figure 5.1.: Kv1.3 expression and biophysical properties upon T lymphocyte activation

A-B) Whole-cell recordings of T lymphocytes following depolarization to 50 mV for 15 ms and 2 s, respectively. **C-F)** Whole-cell capacitance, Kv1.3 current density, activation kinetics and inactivation kinetics, respectively, of T lymphocytes upon the following forms of stimulation: control: unstimulated; PMA+Iono: 1 μ M PMA together with 1 μ M ionomycin; α CD3+ α CD28: 1 μ M and 1 μ M; PHA: 1 μ M. Boxes represent quartiles and whiskers represent 10.-90. percentiles, * $p < 0.05$

In case of all treatments, cell division index was $>80\%$ (calculated by Eq.3., see 4.4). Our results indicate that both PHA and anti-CD3 plus anti-CD28 stimulation lead to significant increase in Kv1.3 current density, however, in case of PHA, the population was extremely heterogeneous compared to other modes of stimulation in regards of capacitance as well as current density (Fig. 5.1.). The biophysical characteristics of the Kv1.3 channel did not change significantly upon stimulation, only the inactivation kinetics slowed upon stimulation with combined anti-CD3 and anti-CD28.

After choosing our preferred mode of stimulation, our first step was to achieve multiple levels of selective T lymphocyte stimulation using anti-CD3 and anti-CD28 monoclonal antibodies.

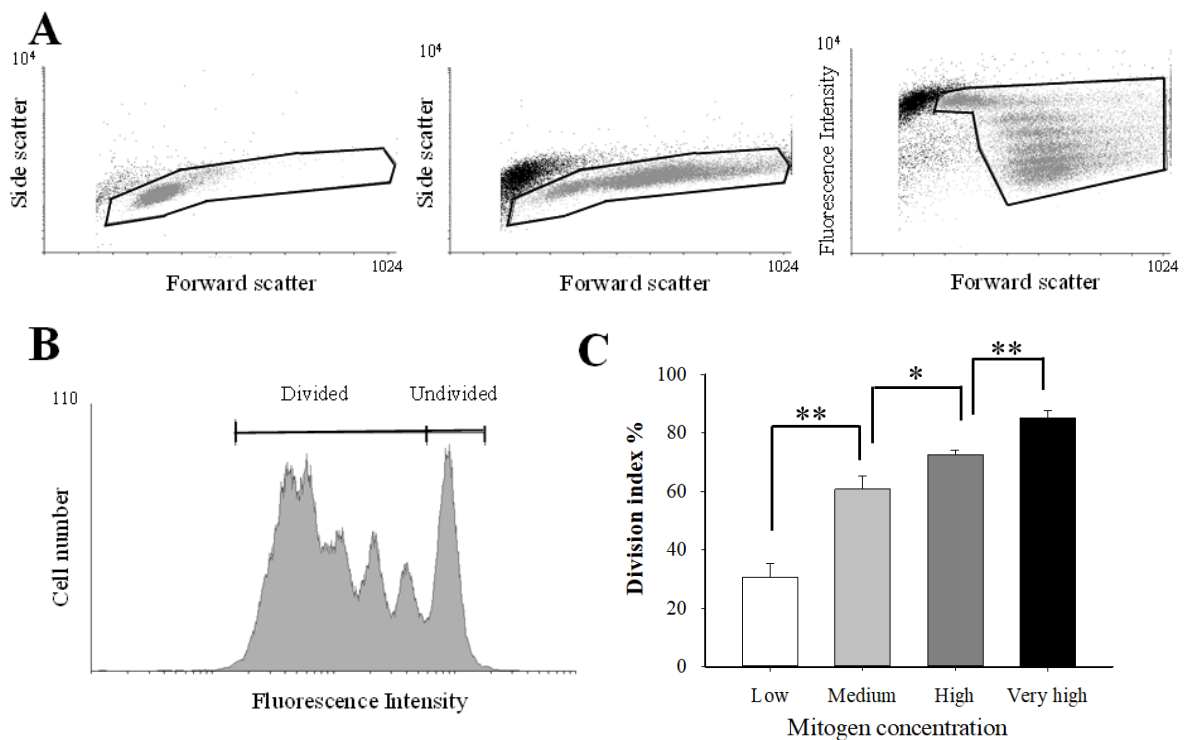


Figure 5.2.: Cell proliferation at different mitogen concentrations.

A) The left and middle dot plots show stimulated PBMC populations stimulated by $1 \mu\text{g/ml}$ anti-CD3 and anti-CD28 monoclonal antibodies on day 0 and day 5, respectively. Solid black line polygons indicate the position of the gates. The dot plot on the right shows the FSC/ Fluorescence intensity of the same population as on the middle dot plot, **B)** The fluorescence intensity histogram shows CFSE fluorescence intensity obtained from the gated population of the dot plot on the right in panel A. The marker above the histogram indicates the divided and the undivided cell populations, and the ratio of divided cells to all gated cells was calculated yielding the division index (DI, see Materials and Methods). **C)** DI of the cells stimulated by anti-CD3 and anti-CD28 at various mitogen concentrations, calculated by Eq.3 in chapter 4.4. The DIs of these populations are shown in Fig 5.3. as positive controls (Pos.) and the DI of inhibitor treatments were normalized to this data.

In our preliminary experiments, we did not find significant differences between CD3⁺ T cells and PBMCs regarding the extent of proliferation or in the proliferation-inhibiting effect of AnTx at K_d and $10K_d$ concentrations. Therefore, we used whole PBMC population in our main experiments.

Fig. 5.2.C shows that comparing the division indices (DI) of stimulated PBMC populations 5 days following mitogen stimulus, four levels of the mitogen effect could be distinguished: low concentration (200 ng/ml or 1 bead:200 cells) of the mitogen led to a relatively low amount of proliferation, while the medium (500 ng/ml or 1 bead:50 cells), high (1 μ g/ml or 1 bead:10 cells) and very high concentrations (3 μ g/ml or 1 bead:1 cells) resulted in markedly high rates of cell division. Pairwise comparison of the observed proliferation rates indicated a significant increase with each subsequent increase in mitogen concentration.

5.1.2. Ion channel blockers and rapamycin alone and in combination inhibit lymphocyte proliferation

The effect of ion channel inhibitors on cell proliferation was tested at a concentration corresponding to the dissociation constant of the drug on the relevant channel ($1 \times K_d$) and at ten times higher concentration ($10 \times K_d$). Rapamycin was used at the lowest IC_{50} obtained from the relevant literature (214, 215), and at ten times higher concentration. Fig. 5.3.A-D panels show representative fluorescence histograms of the CFSE dilution assay recorded in the absence or in the presence of the blockers in two concentrations. The markedly reduced peaks of the gray-shaded histogram relative to the control light-gray line in Fig. 5.3.A qualitatively show that the Kv1.3 K⁺ channel blocker AnTx at $10 \times K_d$ concentration inhibited proliferation when the cells were stimulated at low mitogen concentration. Quantitative analysis using normalized DIs (Fig. 5.3.E and F) showed that AnTx at $1 \times K_d$ and $10 \times K_d$ concentration inhibited proliferation at low, but not at very high mitogen concentration.

The nearly superimposable fluorescence histograms in Fig. 5.3.B show that the KCa3.1 inhibitor TRAM-34, regardless of its concentration, caused only a minor reduction of the proliferation of T cells stimulated by low mitogen concentration. The statistical analysis of the DIs (Fig. 5.3.E and F) showed that TRAM-34 failed to inhibit cell proliferation both at $1 \times K_d$ and at $10 \times K_d$ concentrations regardless of the mitogen concentration used. The gray-shaded histogram in Fig. 5.3.C shows qualitatively that at low mitogen stimulation the CRAC channel

modulator, 2-Aminoethoxydiphenyl borate (2-Apb) applied at $10\times K_d$ blocker concentration inhibited cell proliferation whereas $1\times K_d$ blocker concentration was ineffective. Fig. 5.3.F shows that at very high mitogen concentration 2-Apb did not inhibit T cell proliferation even at $10\times K_d$ concentration.

The representative histograms in Fig. 5.3.D shows that the mTOR inhibitor rapamycin, applied at both $1\times IC_{50}$ and $10\times IC_{50}$ concentrations markedly inhibits the proliferation of T cells stimulated with low mitogen concentration. This effect was confirmed by the statistical analysis shown in Fig. 5.3.E. As opposed to the ion channel blockers AnTx and 2-Apb, rapamycin alone inhibited proliferation even at very high mitogen concentration both at $1\times IC_{50}$ and $10\times IC_{50}$ doses. As shown in Fig. 5.3.G, using the combination of all ion channel blockers at $10\times K_d$ concentration led to a marked inhibition of cell proliferation, which did not differ from the blocking potential of $10\times IC_{50}$ rapamycin. The inhibitory effect of ion channel blockers combined with rapamycin proved to be the most effective treatment, resulting in complete blockage of cell division. In the latter case proliferation was not significantly different from the negative control group, which was not stimulated by mitogens.

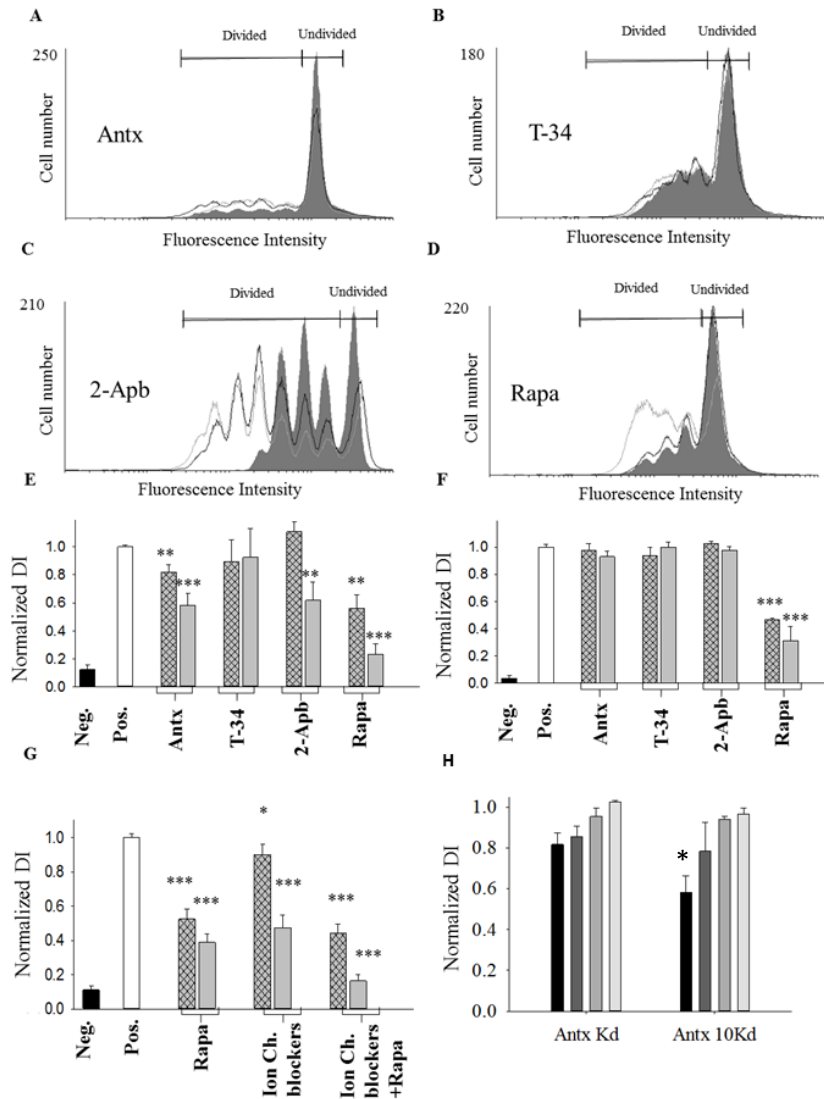


Figure 5.3.: Effect of ion channel blockers and rapamycin on cell proliferation.

A-D) The representative fluorescence histograms corresponding to the CFSE dilution assay (see methods) show the effect of four inhibitors on T cell proliferation. Light gray lines in the histograms indicate the positive control population (Pos.) treated solely with mitogens, black lines and gray filled histograms indicate data obtained in the presence of a blocker at $1 \times K_d$ and $10 \times K_d$ concentrations, respectively (concentrations see in text). Cells were stimulated with low mitogen concentration in each case. **E-F)** Proliferation, represented by DI (see Figure 5.2.), at low (Fig. 5.2.E) or very high (Fig. 5.2.F) mitogen concentrations in the presence of $1 \times K_d$ (cross-hatched bars) and $10 \times K_d$ (gray) blocker concentrations. Neg. indicates the negative control population, where cells were not stimulated by mitogens, but were stained with CFSE. The DIs of samples treated with different blockers were normalized to the average DI of the Pos. sample. **G)** Comparison of the effectiveness of treatment combinations as compared to the pos. control. During the combined treatments, each blocker was applied at its $1 \times K_d$ (cross-hatched) or $10 \times K_d$ (gray) concentration, data obtained for different mitogen concentrations were pooled for the analysis. **H)** Mitogen-dependence of the inhibition of cell proliferation. The DIs were determined in the presence of AnTx at $1 \times K_d$ (left) or $10 \times K_d$ (right), at low (black), medium (dark gray), high (gray) and very high (light gray) mitogen concentrations (see legend to Fig. 5.2). Error bars indicate S.E.M, asterisks indicate significance (* if p was <0.05 , with **, if p was <0.01 , and with ***, if p was <0.001)

Data above showed that the Kv1.3 blocker AnTx and the CRAC channel blocker 2-Apb interfered with T cell proliferation only if cells were stimulated at low mitogen concentration but were ineffective if cells were stimulated with very high mitogen concentration. To further explore this phenomenon, we measured the normalized DI at varying mitogen concentrations (low, medium, high and very high, see above) in the presence of $1 \times K_d$ (Fig. 5.3.H left panel) or $10 \times K_d$ (Fig. 5.3.H right panel) concentrations of AnTx. As shown in Fig. 5.3.H right panel a marked inhibition of cell division was observed when the combination of low mitogen and $10 \times K_d$ blocker concentration (black bar) was used. At medium, high and very high mitogen concentrations the inhibition of proliferation was not statistically significant as compared to the positive control, but a clear decreasing trend is seen in the effectiveness of the blockers with increasing mitogen concentration. The same tendency could be observed if AnTx was applied at $1 \times K_d$ concentration (Fig. 5.3.H left panel). The inhibition of proliferation was statistically significant only if low mitogen concentration was used whereas at medium, high, and very high mitogen concentrations the inhibition of proliferation did not prove to be significant.

5.1.3. Cell viability is not affected by the inhibitors of T cell proliferation

The reduced proliferation in the presence of the ion channel blockers and rapamycin (see above, Fig. 5.3.) might be induced by a decrease in the viability of the cells in the presence of these compounds. This was tested in the experiments shown in Fig. 5.4. using a propidium iodide uptake assay. The dot-plots in Fig. 5.4.A show the threshold discriminating viable and non-viable cells using the combination of forward scatter and PI fluorescence. The corresponding fluorescence histograms in Fig 5.4.B show that stimulation of the cells increased the proportion of the viable cells. The proportion of viable cells was not altered either by the channel blockers or rapamycin alone, or in their various combinations regardless of the concentration of the compounds (Fig. 5.4.C).

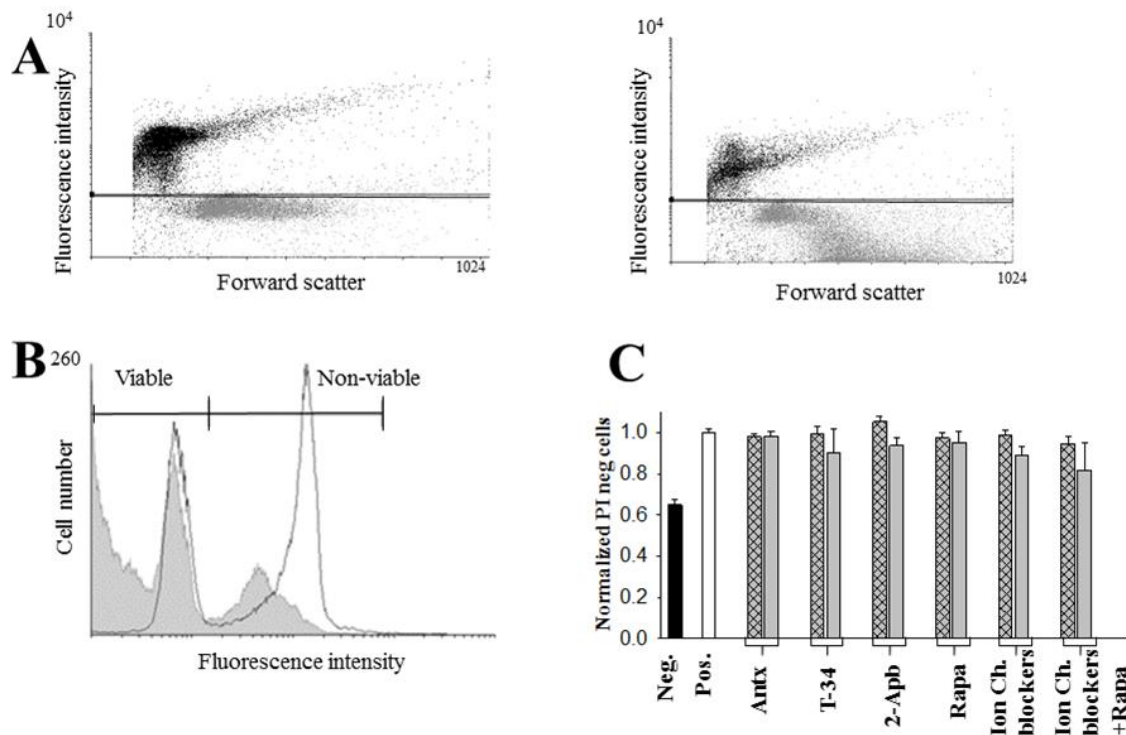


Figure 5.4.: Effect of ion channel blockers and rapamycin on the cellular viability.

A) The dot plots show the standard gating strategy for propidium iodide (PI) staining. The left panel indicates non-stimulated (Neg.), the right panel shows the stimulated population (Pos.) after 5 days of incubation with superparamagnetic bead-conjugated anti-CD3 and anti-CD28 monoclonal antibodies at 1 bead:1 cells ratio. The horizontal black line indicates the threshold for discriminating live and non-live cells. **B)** The fluorescence histograms were generated from the dot plots shown in A, the bar and the markers indicate the PI negative viable and the PI positive non-viable cells in the Neg. (black line) and Pos. (gray fill) samples. **C)** Viability of the cell populations in the presence of inhibitors. The number of PI negative cells in the presence of various compounds was normalized to that of the untreated, but activated cells (Pos. sample). Cross-hatched and gray bars show data obtained in the presence of 1×Kd and 10×Kd concentrations of the indicated compounds alone or in mixtures (T-34: TRAM-34, Rapa: rapamycin). Mixtures of ion channel blockers contained each blocker at 1×Kd or 10×Kd (Ion Ch. blockers) whereas in the Ion Ch. Blockers+Rapa samples the ion channel blocker mixture is supplemented with the corresponding concentrations of rapamycin (1×IC50 or 10×IC50). Error bars indicate S.E.M.

5.1.4. Cytokine production of T cells can be reduced by ion channel blockers

We investigated the effect of channel blockers and rapamycin on the secretion of the anti-inflammatory IL-10 and the pro-inflammatory IFN- γ cytokines by ELISA. Increasing the mitogen concentration from low to very high induced approximately 4-fold and 10-fold increases in secreted IL-10 and IFN- γ levels, respectively (Fig. 5.5. A and B, Pos.). IFN- γ as well as IL-10 secretion was significantly inhibited at low mitogen stimulation by all inhibitors and combinations at both applied concentrations (Fig. 5.5.A and B, left panels). At very high mitogenic stimulation IFN- γ secretion was inhibited by AnTx, rapamycin and combination treatments at $10\times K_d$ and by 2-Apb and the ion channel blocker combination at $1\times K_d$ (Fig. 5.5.A right panel). IL-10 production was only inhibited by $10\times K_d$ of 2-Apb, rapamycin and combination treatments (Fig 5.5.B right panel).

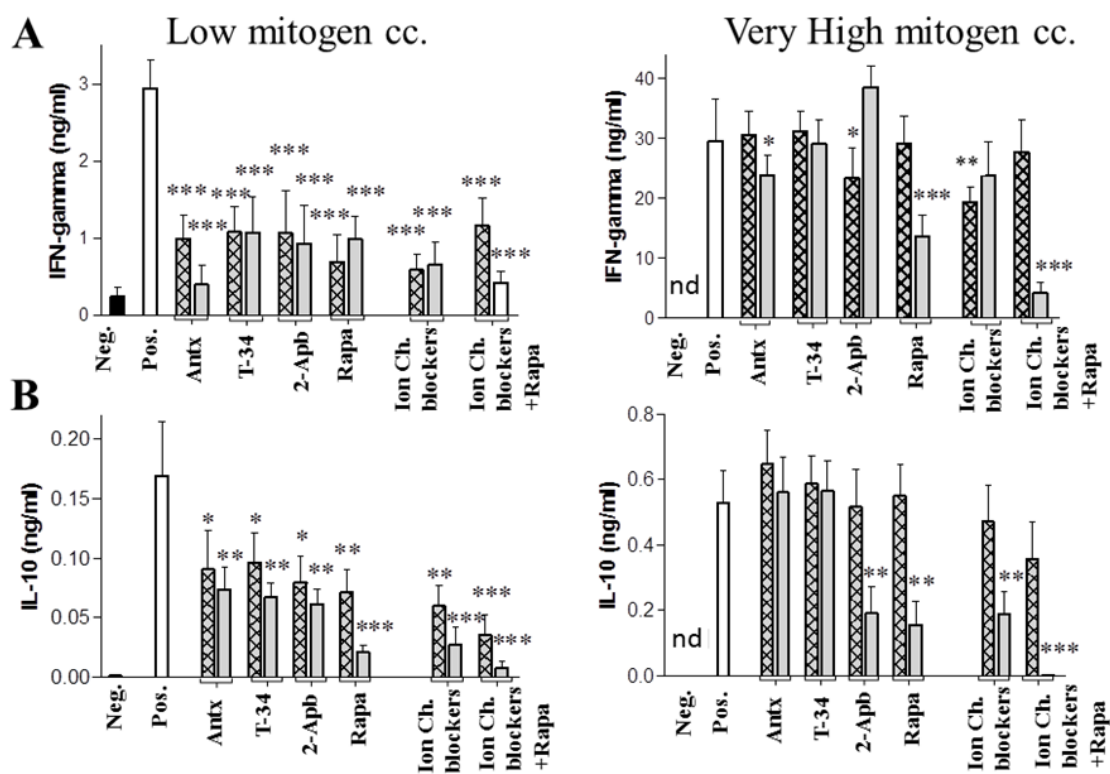


Figure 5.5.: Inhibition of cytokine secretion by ion channel blockers and rapamycin.

A) IFN- γ and **B)** IL-10 secretion were measured using ELISA (OptEIA kit) at different mitogen concentrations. Left and right panels refer to data obtained at low and very high mitogen concentrations. Neg. indicates the unstimulated control cell population whereas Pos. indicates the mitogen-stimulated cell population in the absence of ion channel blockers and/or rapamycin. The blockers are represented at $1\times K_d$ (cross-hatched), $10\times K_d$ (gray) or in case of rapamycin $1\times IC_{50}$ and $10\times IC_{50}$ concentrations, respectively. Error bars indicate S.E.M, asterisks indicate significance (* if p was <0.05 , with **, if p was <0.01 , and with ***, if p was <0.001), and n.d. indicates “not detectable” where values are too low to be shown.

5.2. Different Expression of β Subunits of the KCa1.1 Channel by Invasive and Non-Invasive Human Fibroblast-Like Synoviocytes

5.2.1. RA-FLS express multiple β subunits at the mRNA and protein levels

We found the marked expression of KCa1.1 α subunit in RA-FLS, described thoroughly in a previous article (191). Analysis of mRNA levels by qPCR in RA-FLS showed expression of most KCa1.1 β subunits compared to the housekeeping gene GAPDH (Fig. 5.6.A), albeit at very low levels for β 2b and β 3d. When compared to the expression levels of the KCa1.1 pore-forming α subunit, the highest relative mRNA expression levels were found for three splice variants of the β 3 subunit (β 3b, β 3c, and β 3e) and for β 4 subunits (Fig. 5.6.B).

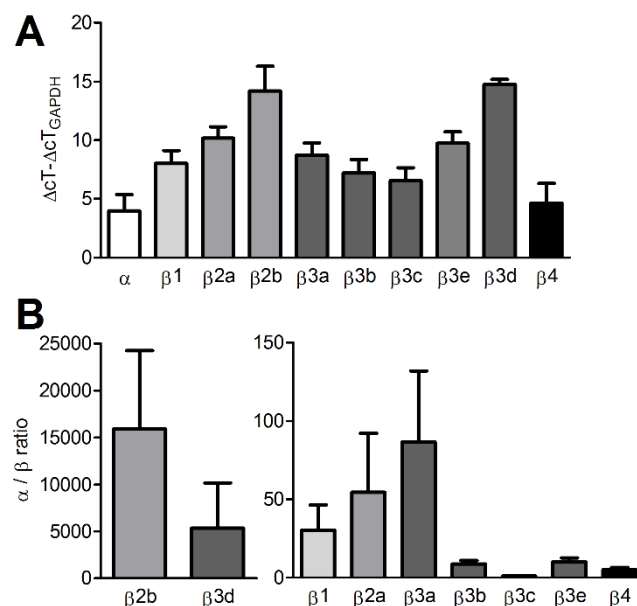


Figure 5.6.: RA-FLS express mRNA of multiple KCa1.1 β subunits.

A) expression fold measurements were conducted by RT-qPCR, compared to GAPDH expression ($n = 6$ donors with 3 independent repeats). Each bar shows expression of a different KCa1.1 subunit, the letters a-e represent different transcript variants. A lower $\Delta C_T - \Delta C_T_{GAPDH}$ value indicates higher relative expression of the target gene, as detailed in 4.7. **B)** α to β ratio (see Eq. 4.) showing the amount of KCa1.1 α subunits expressed for each single β subunit. Note the different scales of the y-axis in B. Error bars indicate S.E.M.

Since mRNAs are not always translated into proteins, we used Western blotting to determine protein levels of the different β subunits. Analysis of the total cellular protein content shows variable amounts of all β subunits of KCa1.1 in different RA-FLS donors compared to

the loading control actin. Whereas expression of $\beta 1$, $\beta 2$, and $\beta 4$ was only detectable in the cell lysates from some donors, $\beta 3$ subunits were consistently identified in all donors but one (Fig. 5.7.).

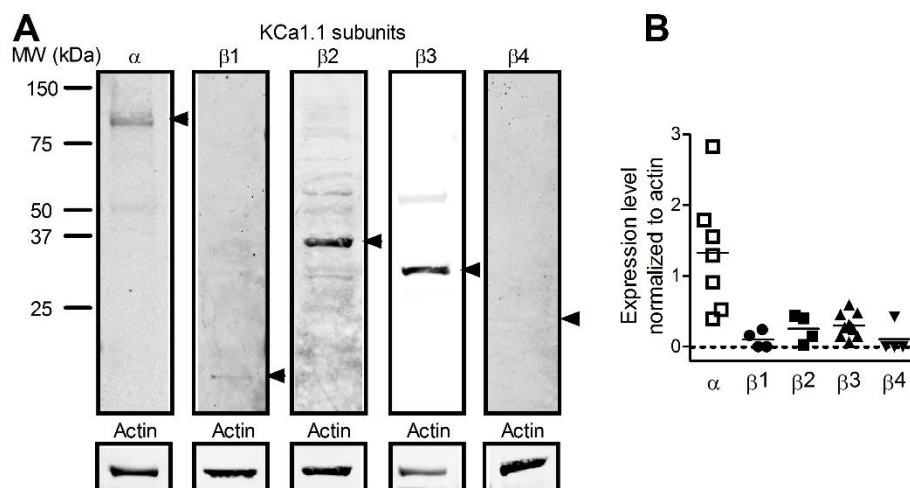


Figure 5.7.: RA-FLS express proteins of multiple KCa1.1 β subunits

A) Representative Western Blot from a gel loaded with proteins from one RA-FLS donor with different lanes probed with antibodies against different subunits of KCa1.1 (top) and actin (bottom). **B**) Intensity of KCa1.1 α and β subunit protein bands normalized to actin expression levels in RA-FLS; each symbol on the scatter plot represents results from a different donor. The horizontal bar represents the mean for each subunit.

5.2.2. RA-FLS express either $\beta 1$ or $\beta 3b$ subunits at their plasma membrane

The pore-forming α subunits of KCa1.1 can be detected at the plasma membrane and in the nucleus of RA-FLS (191). Since our focus here is on the channels expressed at the plasma membrane and since co-expression of β subunits with α subunits affects the kinetics and pharmacology of K^+ currents through the KCa1.1 channel, we used patch-clamp electrophysiology to assess the expression of functional β subunits at the plasma membrane of RA-FLS. Of the 51 RA-FLS from 5 different donors patch-clamped, 47 (92%) exhibited a K^+ current (Fig. 5.8.A and Table 4.) as previously described (191). Addition of paxilline, a blocker of the KCa1.1 α subunits regardless of β subunit expression (49, 191, 228), completely blocked the K^+ current in all 14 cells tested (Fig. 5.8.A and B and Table 4.), further confirming that the K^+ channel observed is KCa1.1, as previously demonstrated (191). In 70% of the cells analyzed, the current displayed little or no inactivation (Fig. 5.8.A and Table 4.). Since $\beta 2a$, $\beta 3a$, $\beta 3c$, and $\beta 3e$ subunits have all been shown to induce inactivation of KCa1.1 (205, 227, 229, 232, 233),

the lack of inactivation suggest these subunits are not involved in the KCa1.1 channel in RA-FLS.

Finding	Eliminated β subunit	Possible β subunit	References
Electrophysiology			
92% of RA-FLS display a K ⁺ current	None	None, β 1, β 2a, β 2b, β 3a, β 3b, β 3c, β 3d, β 3e, β 4	(191)
The K ⁺ current in 100% of RA-FLS is sensitive to paxilline	None	None, β 1, β 2a, β 2b, β 3a, β 3b, β 3c, β 3d, β 3e, β 4	(49, 191, 228)
70% of RA-FLS KCa1.1 currents are non-inactivating	β 2a, β 3a, β 3c, β 3e	None, β 1, β 3b, β 3c, β 3d, β 4	(205, 227, 229, 232, 233)
100% of RA-FLS KCa1.1 currents are sensitive to ChTX	β 4	None, β 1, β 3b, β 3d	(31, 227)
36% of RA-FLS KCa1.1 current are sensitive to LCA	β 2a, β 2b, β 3a, β 3b, β 3c, β 3d, β 3e, β 4	β1	(40, 41, 227)
65% of RA-FLS KCa1.1 currents are sensitive to AA	β 1, β 4	β 3b, β 3d	(42, 227)
Western blotting			
Band detected with pan- β 3 antibody	None	β 3b, β 3d	
No band detected with antibody selective for β 3a, β 3c, β 3d, and β 3e	β 3a, β 3c, β 3d, β 3e	β3b	

Table 4. Summary of findings from the electrophysiology and Western blot assays for identification of the functional β subunits expressed by RA-FLS.

To further identify the β subunits associated with the KCa1.1 channels in RA-FLS, we used KCa1.1 openers and blockers known to exert different effects on the channel depending on its β subunit composition. First, we tested the effects of the scorpion venom toxin ChTx on RA-FLS K⁺ currents as it can only block KCa1.1 channels that do not contain the β 4 subunit (31, 227, 229). ChTx inhibited the currents at 100 nM in all cells tested (Fig. 5.8.A and B and Table 4.), demonstrating the absence of β 4 subunits in KCa1.1 channels of RA-FLS. We next tested the effects of LCA, known to enhance currents through KCa1.1 channels only in the presence of β 1 subunits (40, 41, 227). This increase in current was observed in only 36% of RA-FLS tested (Fig. 5.8.A and B and Table 4.), demonstrating that KCa1.1 channels are formed of α and β 1 subunits in approximately a third of RA-FLS. To identify the β subunit in the remainder of the RA-FLS, we used AA, known to increase KCa1.1 currents in the presence of β 2 and β 3 subunits (42, 227). Such an increase was observed in 65% of cells tested (Fig. 5.8.A and B and Table 4). Since the kinetics data above had already eliminated the possibility of β 2a,

$\beta 3a$, $\beta 3c$, or $\beta 3e$ subunits (Fig. 5.8.A and Table 4), this result with AA suggests that the majority of RA-FLS express a $\beta 3$ subunit, either $\beta 3b$ or $\beta 3d$ (Table 4). To discriminate between these two splice variants of $\beta 3$, we performed Western blot experiments using two types of antibodies. The first antibody is directed to a conserved region of the $\beta 3$ subunit, common to all five splice variants, and leads to a band of the correct molecular weight (Fig. 5.7.A and 5.8.C and Table 4.). The second antibody used was raised against the N-terminus of $\beta 3$ and therefore detects all splice variants of $\beta 3$ other than $\beta 3b$.

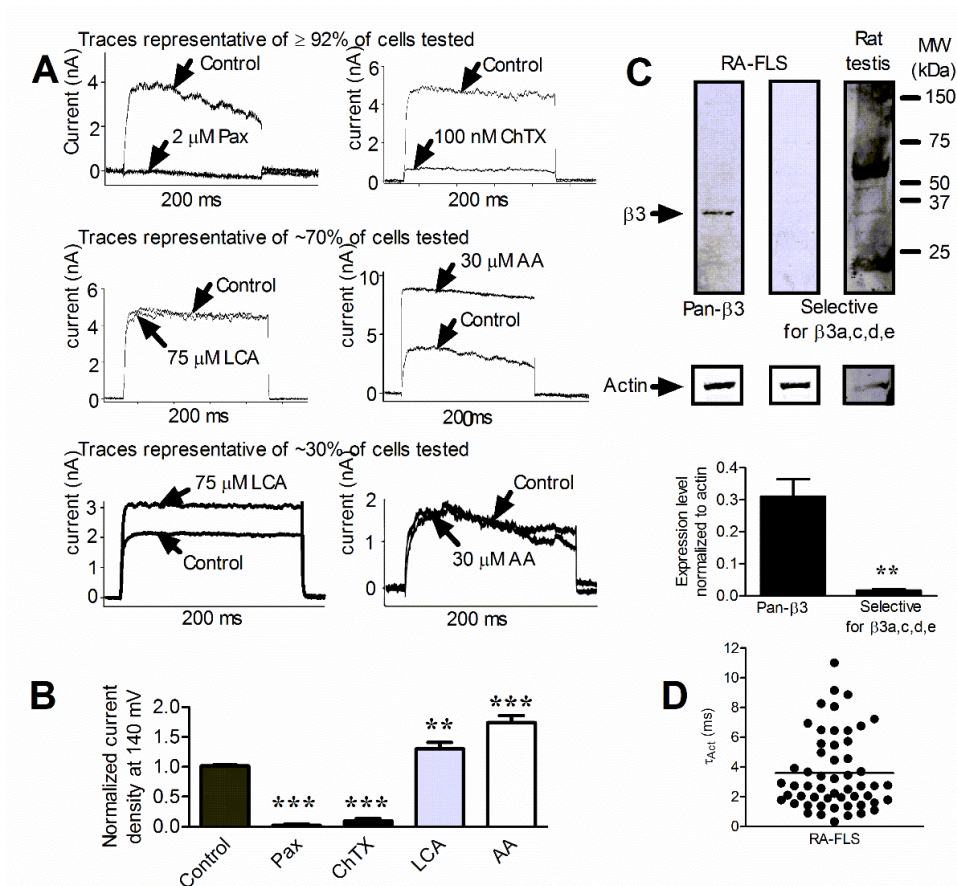


Figure 5.8 Functional $KCa1.1$ $\beta 3b$ subunits are present on the plasma membrane of RA-FLS.

A) Representative traces of whole-cell $KCa1.1$ currents elicited by 140 mV pulses for 200 ms with 5 μM Ca^{2+} in the internal solution before (control) and after applying 2 μM paxilline (Pax), 100 nM ChTx, 30 μM AA or 75 μM LCA. **B)** Peak $KCa1.1$ currents after different treatments normalized to the control levels. Mean \pm S.E.M.; $n = 5$ different donors. **C)** Representative Western Blot from a gel loaded with proteins from one RA-FLS donor with different lanes probed with antibodies against all splice variants of $KCa1.1$ $\beta 3$ (pan- $\beta 3$) or against $KCa1.1$ $\beta 3a,c,d,e$ only (top) and intensity of $KCa1.1$ $\beta 3$ protein bands normalized to actin expression levels. Mean \pm S.E.M.; $n = 6$ different donors. **D)** Activation kinetics of RA-FLS K^+ currents; each symbol on the scatter plot represents a different cell; $n = 5$ different donors; $**p \leq 0.01$, $***p \leq 0.001$.

Although this antibody detected a band of the correct molecular weight (about 32 kDa) in rat testis extracts, the only tissue with known $\beta 3$ expression (234), it yielded no detectable band with RA-FLS extracts (Fig 5.8.C and Table 4), suggesting that RA-FLS express the $\beta 3b$ subunit of KCa1.1. Since $\beta 1$, but not $\beta 3b$, subunits slow the activation kinetics (τ_{Act}) of KCa1.1 channels (235), we measured these kinetics in RA-FLS and found a spread in τ_{Act} with only 17 of the 54 cells assessed (31%) having a $\tau_{Act} > 4$ ms and 69% of RA-FLS having a $\tau_{Act} \leq 4$ ms (Fig. 5.8.D). These results reinforce the finding that different individual RA-FLS cells within a line express different β subunits.

5.2.3 Expression of KCa1.1 $\beta 3b$ is associated with higher levels of KCa1.1 α and CD44

Since invasiveness is an important feature of aggressive FLS during RA, we wanted to test whether invasiveness is associated with differential expression of KCa1.1 β subunits by the cells. In the absence of antibodies that recognize an extracellular epitope of either $\beta 1$ or $\beta 3$ subunits, we searched for a surrogate marker with an extracellular epitope to allow for isolation of live cells. Elevated expression of CD44, a type I transmembrane glycoprotein that binds hyaluronan and other extracellular and cell surface ligands, by FLS and other cells was observed in RA (236, 237). Interestingly, an elevated CD44 expression correlates with enhanced invasiveness of cancer cells (238, 239). To determine whether expression of $\beta 1$ or $\beta 3$ subunits correlates with CD44 expression levels and invasiveness in RA-FLS, we first showed a correlation between elevated expression of KCa1.1 α and of CD44 (Fig. 5.9.A). We next used flow cytometry to sort CD44^{high} and CD44^{low} RA-FLS and performed invasion assays. CD44^{high} RA-FLS were significantly more invasive than CD44^{low} cells (Fig. 5.9.B). Since FLS invasiveness has also been associated with expression of podoplanin, cadherin-11, and MMP-2 (240, 241), we assessed expression levels of these three markers within the CD44^{low} and CD44^{high} populations of RA-FLS. We observed an association between elevated expression of CD44 and all three markers (Fig. 5.9.C).

We then stained cells for expression of CD44 and performed whole-cell patch-clamp to assess K⁺ current densities and activation kinetics in CD44^{high} and CD44^{low} cells (Fig. 5.9.C). CD44^{high} RA-FLS exhibited higher current densities and faster activation rates than did CD44^{low}

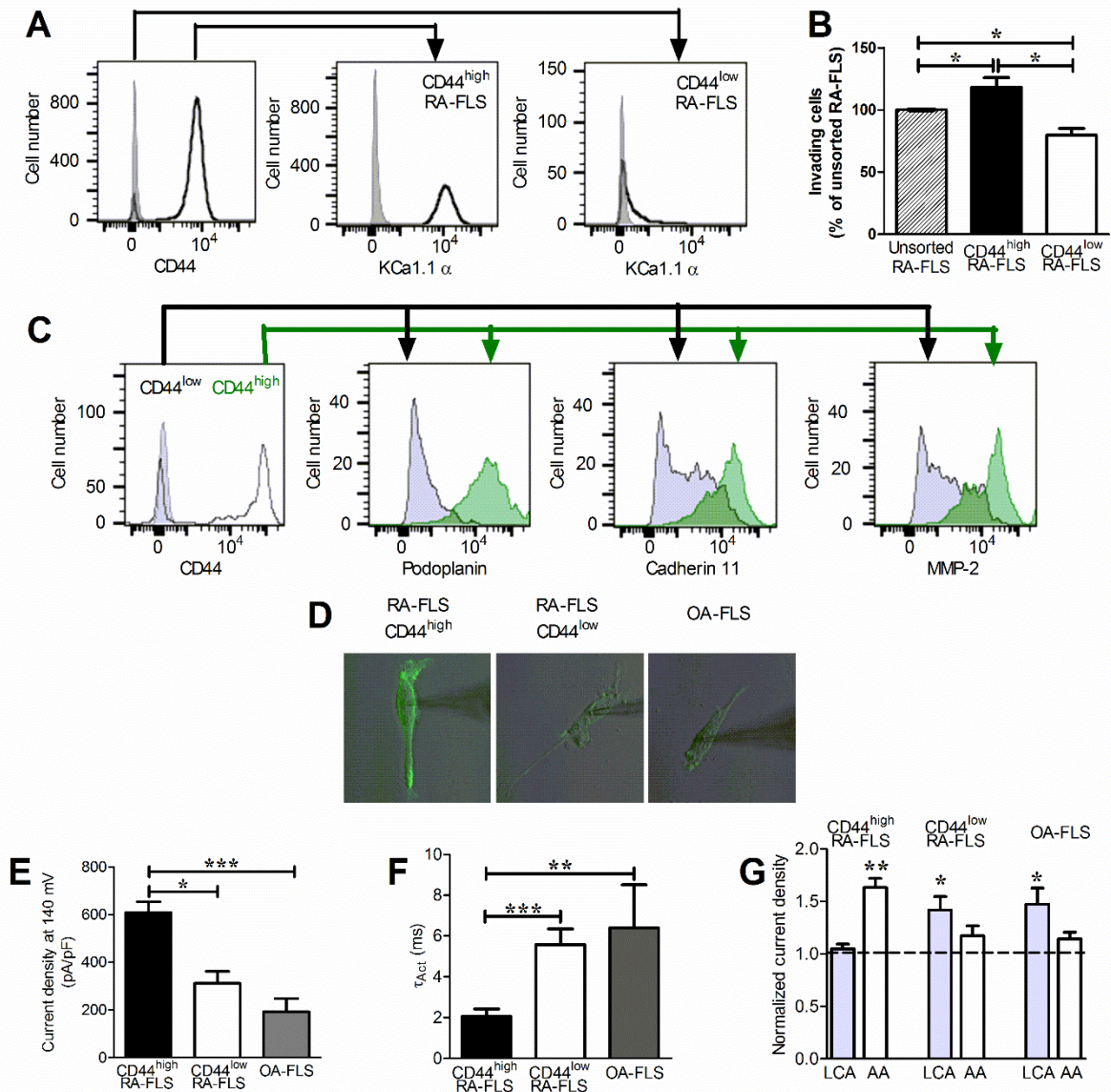


Figure 5.9.: The *KCa1.1* $\beta 3$ subunit is expressed by *CD44*^{high} RA-FLS whereas the $\beta 1$ subunit is expressed by *CD44*^{low} RA-FLS and OA-FLS.

A) Representative flow cytometry histograms showing expression of *KCa1.1* α by *CD44*^{high} and *CD44*^{low} RA-FLS. Gray shading represents control staining; black lines represent *CD44* (left) or *KCa1.1* α (middle and right) staining. **B)** Invasiveness of unsorted RA-FLS and RA-FLS from the same donors sorted by flow cytometry into *CD44*^{low} and *CD44*^{high} populations. Mean \pm SEM; $n = 3$ RA-FLS donors. The line for the error bar for the control was thickened compared with other plots to make it visible. **C)** Representative flow cytometry histograms showing expression of podoplanin, cadherin-11, and matrix metalloproteinase (MMP)-2 by *CD44*^{high} (green) and *CD44*^{low} (gray) RA-FLS. In the left panel, gray shading represents control staining and black lines represent *CD44* staining. **D)** Individual RA-FLS stained for *CD44*. The patch-clamp pipette's shadow is visible on the right of each image. **E)** K^+ current density elicited at 140 mV in *CD44*^{high} RA-FLS, *CD44*^{low} RA-FLS, and OA-FLS. Mean \pm SEM; $n = 5$ RA-FLS donors and 4 OA-FLS donors. **F)** Activation kinetics (τ_{Act}) of K^+ currents elicited at 140 mV in *CD44*^{high} RA-FLS, *CD44*^{low} RA-FLS, and OA-FLS. Mean \pm SEM; $n = 5$ RA-FLS donors and 4 OA-FLS donors. **G)** K^+ current density after treatment of *CD44*^{high} RA-FLS, *CD44*^{low} RA-FLS, and OA-FLS with 75 μ M lithocholic acid (LCA) or 30 μ M arachidonic acid (AA) and normalized to current densities before treatment (horizontal dashed line). Mean \pm SEM; $n = 5$ RA-FLS donors and 4 OA-FLS donors. * $p \leq 0.05$, ** $p \leq 0.01$, *** $p \leq 0.001$.

cells, suggesting expression of $\beta 1$ subunits by CD44^{low} cells and of $\beta 3b$ subunits by CD44^{high} cells (Fig. 5.9.D and E). These results were further confirmed by assessing the effects of AA and LCA on the two cell subsets as CD44^{high} cells displayed sensitivity to AA but not LCA whereas CD44^{low} cells displayed sensitivity to LCA and not AA (Fig. 5.9.F). As a control, we used minimally invasive FLS obtained from patients with OA. OA-FLS exhibited low current densities at 140 mV, fast τ_{Act} , and sensitivity to LCA but not AA, similarly to CD44^{low} RA-FLS (Fig. 5.9.D-F).

5.2.4 Knocking down the $\beta 3$ subunit of KCa1.1 decreases cell surface expression of the pore-forming α subunit of KCa1.1

We used a pool of siRNA to selectively inhibit gene expression of the $\beta 3$ subunit. In whole-cell patch-clamp assays, RA-FLS became less sensitive to treatment with the $\beta 3$ agonist AA after transfection with $\beta 3$, but not control siRNA, demonstrating the effectiveness of the siRNA. Neither control nor $\beta 3$ siRNA affected the cells' response to LCA showing a lack of effect on $\beta 1$ subunits (Fig. 5.10.A). Flow cytometry measurements showed that $\beta 3$ silencing induced a 20% reduction in expression of the KCa1.1 α subunit (Fig. 5.10.B). Moreover, whole cell KCa1.1 current densities at voltages above 50 mV were significantly decreased after KCa1.1 $\beta 3$ subunit silencing (Fig. 5.10.C), suggesting lower surface expression of the α subunit of KCa1.1.

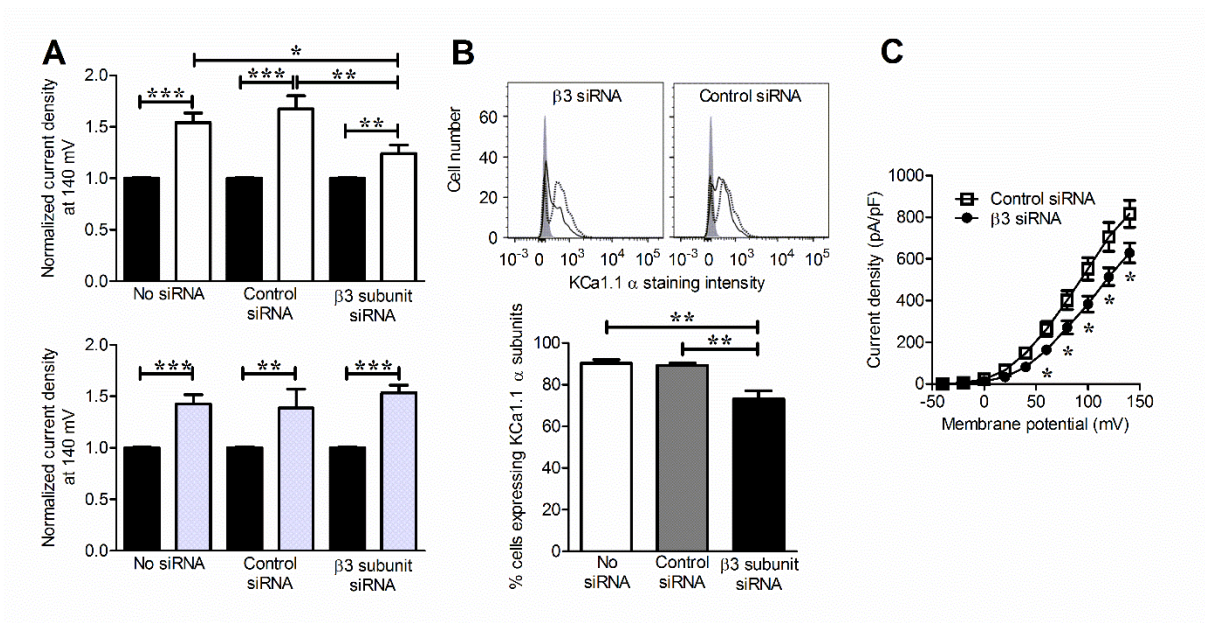


Figure 5.10.: Silencing KCa1.1 $\beta 3$ expression reduces cell surface expression of KCa1.1 α

A) K^+ current density of untransfected RA-FLS and RA-FLS transfected with control siRNA or with siRNA against KCa1.1 $\beta 3$ before (black) and after treatment with 30 μ M AA (white; top plot) or 75 μ M LCA (grey; bottom plot) and normalized to current densities before treatment; Mean \pm S.E.M.; $n = 4$ RA-FLS donors. **B)** Representative flow cytometry histograms showing background staining (grey shaded), expression levels of KCa1.1 α in untransfected RA-FLS (dotted line) and RA-FLS transfected with siRNA against KCa1.1 $\beta 3$ (solid black line; left histogram) or with control siRNA (solid black line; right histogram). The bar graph below shows the percentage of cells expressing KCa1.1 α calculated from the flow cytometric profiles of 3 RA-FLS samples; Mean \pm S.E.M. **C)** K^+ current densities of RA-FLS transfected with control siRNA (\square) or with siRNA against KCa1.1 $\beta 3$ (\bullet) and pulsed stepwise from -40 to 140 mV in 20 mV increments; Mean \pm S.E.M.; $n = 4$ RA-FLS donors. * $p \leq 0.05$, ** $p \leq 0.01$, *** $p \leq 0.001$.

5.2.5 Knocking down the $\beta 3$, but not the $\beta 1$, subunit of KCa1.1 attenuates the ex vivo invasiveness of RA-FLS

Reducing the expression or function of the α subunit of KCa1.1 inhibits the invasiveness of FLS (191, 192); we therefore assessed the effects of silencing the $\beta 3$ subunit of KCa1.1 on RA-FLS invasiveness using Matrigel invasion assays. We also used a pool of siRNA to inhibit the expression of the $\beta 1$ subunit of KCa1.1 and used the channel's sensitivity to LCA to demonstrate the effectiveness of the siRNA as control siRNA did not affect RA-FLS response to LCA whereas $\beta 1$ siRNA reduced it (Fig. 5.11.A). Whereas $\beta 3$ siRNA reduced the invasiveness of RA-FLS, silencing the $\beta 1$ subunit of KCa1.1 did not affect this invasiveness (Fig. 5.11.B).

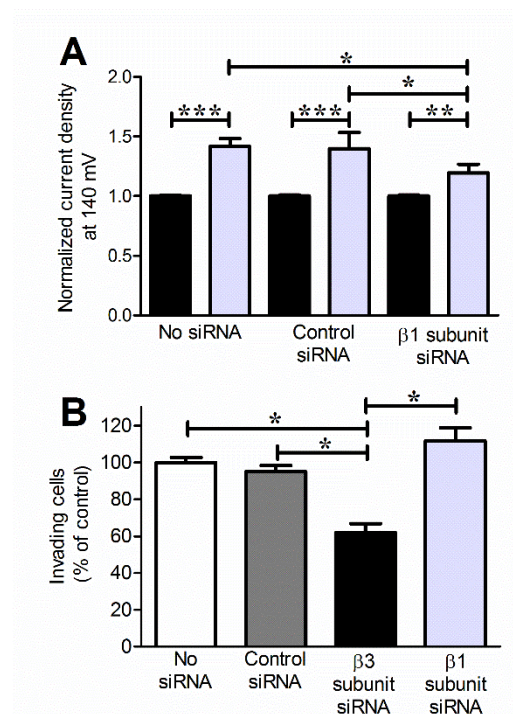


Figure 5.11.: Silencing KCa1.1 $\beta 3$ but not KCa1.1 $\beta 1$ expression reduces inhibits the invasiveness of RA-FLS

A) K^+ current density of untransfected RA-FLS and RA-FLS transfected with control siRNA or with siRNA against KCa1.1 $\beta 1$ before (black) and after treatment with 75 μ M LCA (grey) and normalized to current densities before treatment; Mean \pm S.E.M.; n = 3 RA-FLS donors. **B)** Invasiveness of untransfected RA-FLS and RA-FLS transfected with control siRNA, with siRNA against KCa1.1 $\beta 3$, or with siRNA against KCa1.1 $\beta 1$; Mean \pm S.E.M.; n = 4 RA-FLS donors. * $p \leq 0.5$, ** $p \leq 0.01$, *** $p \leq 0.001$.

6. DISCUSSION

6.1 The anti-proliferative effect of cation channel blockers in T lymphocytes depends on the strength of mitogenic stimulation

Altered T cell homeostasis is involved in the pathogenesis of autoimmune diseases such as MS (242) and systemic lupus erythematosus (243). To maximize anti-proliferative effects and to reduce potential side effects, immunosuppressive drugs are commonly used in combinations (244). One group of the most promising candidates for future therapy is the family of Kv1.3 inhibitors, because this ion channel is found only in a few tissues and it can be inhibited selectively (124). Before applying ion channel blockers in therapy, it is crucial to investigate how they interact with other immunosuppressive agents. However, original research data about the pharmacodynamics of combinations of traditional immunosuppressive and novel drugs such as ion channel blockers are scarce and they usually lack functional comparison. Therefore, in our recent experiments, we approached this problem from multiple aspects and have found an additive interaction between rapamycin and the ion channel blockers when using them in combination.

The effects of ion channel blockers exerted on T cell functions have already been described (69). However, to the best of our knowledge, no data comparing the proliferative effects of Kv1.3, KCa3.1 and CRAC channel blockers applied alone or in combination at identical experimental conditions are currently available. Moreover, the synergy between the effects of ion channel inhibitors and the mTOR inhibitor rapamycin has not been investigated to date. In our study we were the first to describe the mitosis-inhibiting effect of AnTx, a high affinity scorpion toxin blocker of Kv1.3 (63) both at high ($10 \times K_d$) and low ($1 \times K_d$) concentrations. The observed effect of 2-Apb correlated well with past literature, as it was proposed that 2-Apb has a bimodal effect. At low blocker concentrations (K_d), 2-Apb promotes Ca^{2+} signaling, which ultimately results in enhanced cell proliferation, whereas at higher concentrations, in our case at $10 \times K_d$, it effectively inhibits the CRAC channel, ultimately blocking cellular proliferation (245).

Even low mitogen concentrations, which corresponded to 1:200 bead-to-cell ratio produced an unexpectedly high amount of polyclonal lymphocyte proliferation, as over 30% of the cells have undergone cell division. This phenomenon may be explained by the fact that there is a large number of anti-CD3 and anti-CD28 molecules on a single bead, and that lymphocytes form a rosette-like structure around beads. Therefore, numerous lymphocytes are activated

simultaneously by a single bead, and this effect could be further enhanced by autocrine and paracrine cytokine secretion of the activated T cells (246, 247).

Our most intriguing finding in this research was that increasing the mitogen concentration markedly decreased the anti-proliferative effect of ion channel blockers that ultimately completely disappeared when cells were stimulated with very high concentration of the mitogens (Fig. 5.3.H). A possible explanation may be that at low mitogen concentrations the few, initially highly localized Ca^{2+} signals are suppressed by the blocked ion channels in their immediate vicinity (248). However, at very high mitogen concentration when most TCRs are likely to be activated, the number of localized signaling loci is sufficiently high so that even a very low fraction of unblocked ion channels is sufficient to maintain the downstream activation cascade upon TCR activation. Moreover, it is reasonable to assume that lymphocytes redirect their activation pathways to other, Ca^{2+} -independent directions. As several intracellular signaling pathways, e.g. mTOR activation, do not essentially involve ion channels (146, 147), these processes may become overly active upon applying very high mitogen concentrations. However, to the best of our knowledge no study has ever addressed this question and thus it warrants further experiments.

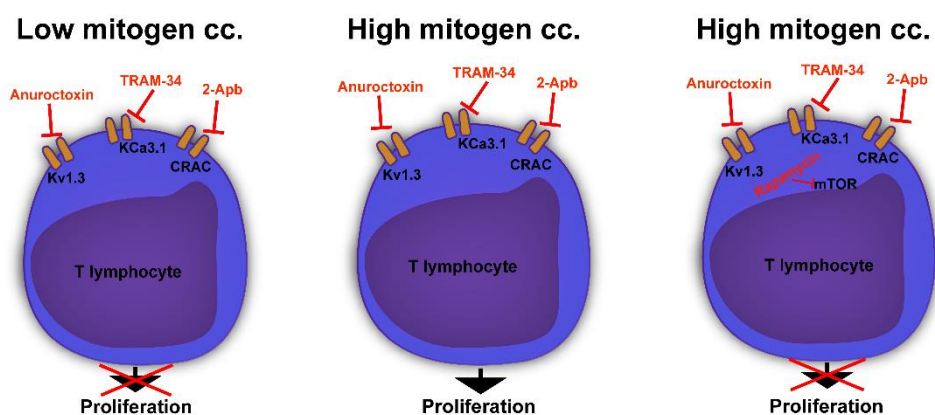


Figure 6.1. Increasing stimulation disrupts the anti-proliferative effect of the blockers

Ion channel blockers inhibit T lymphocyte proliferation at low mitogen concentrations. This effect fades upon using higher mitogen concentrations, but can be rescued by combining ion channel blockers with other immunopharmacological agents such as the mTOR inhibitor rapamycin.

At very high mitogen concentrations we could achieve significant blockage of proliferation only by using rapamycin or its combination with ion channel blockers acting on a different pathway that ultimately leads to permanent changes in cellular signaling (Fig. 6.1.).

This may indicate that co-treatment of T cells with rapamycin and ion channel blockers may be a more feasible therapeutic approach than using these drugs separately.

Previous studies have shown that blocking Kv1.3 channels without affecting the KCa3.1 channels inhibited IFN- γ expression in T_{EM} (249). Moreover, the blockage of CRAC channels with SKF 96365 decreased both IL-10 and IFN- γ production (176). In line with these studies our data showed that treatment of T-cells with various inhibitors (Fig. 5.5) significantly decreased both anti-inflammatory IL-10 and inflammatory IFN- γ cytokine production but only at low mitogenic stimulation. In accordance with the literature TRAM-34 strongly suppressed cytokine production despite the fact that it did not inhibit proliferation (77, 161). At very high mitogen concentration the effect of the ion channel blockers on cytokine production diminished. Although some of them caused statistically significant reductions in cytokine production, these changes are not likely to be biologically relevant as the remaining concentration of IFN- γ still remained in the ng/ml range and therefore was sufficient to promote cell proliferation, so division rate was unaffected. In contrast, rapamycin and the combination treatments applied at $10 \times K_d$ concentration caused a more robust decrease, which was also reflected in the suppressed proliferation of these cells.

Since IL-10 and IFN- γ levels were affected in a qualitatively comparable manner by the inhibitors both at low and very high mitogen concentrations, it is safe to assume that these treatments did not alter the proportion of T cell subtypes specifically (i.e. CD4⁺ T_H1 and CD8⁺ cytotoxic T cells vs. T_H2 T cells and regulatory CD4⁺/CD25⁺/FoxP3⁺ T_{reg} cells), but rather were affecting globally the entire T cell population.

In summary, the greatest level of inhibition of T-cell proliferation and the production of selected cytokines could be achieved by rapamycin, and this effect could be further potentiated by using it in combination with cation channel blockers. This may indicate an additive effect of Ca²⁺-dependent and Ca²⁺-independent inhibitory mechanisms involved in T-cell activation. Finally, we found that upon increasing the concentration of the mitogenic antibodies, the anti-proliferative effect of ion channel blockers faded. The increased *in vitro* antiproliferative potency of rapamycin and ion channel blocker combination presented in this study urges for *in vivo* experiments whereby the therapeutic benefit of the combined treatment can be assessed.

6.2 Different Expression of β Subunits of the KCa1.1 Channel by Invasive and Non-Invasive Human Fibroblast-Like Synoviocytes

In the second part of this work we focused on the KCa1.1 channel, that has been proposed as a therapeutic target to treat RA (191, 192). However, the wide tissue distribution of the pore-forming α subunit of the channel precludes the use of antagonists targeted to this subunit alone due to the risk of severe side effects in multiple organ systems (195-197). KCa1.1 does however remain an attractive target for therapy because the regulatory β subunits of KCa1.1 have restricted tissue distribution (30, 32). Here, we demonstrated that RA-FLS express functional $\beta 1$ and $\beta 3$ subunits of KCa1.1 at their plasma membrane and that expression of $\beta 3$ is higher on CD44^{high} RA-FLS and is associated with higher expression levels of KCa1.1 α . Silencing $\beta 3$, but not $\beta 1$, significantly reduced the invasiveness of RA-FLS. In addition, silencing $\beta 3$ reduced the expression level of KCa1.1 α .

Analysis by qPCR showed expression of most β subunits in RA-FLS at the mRNA level. Low mRNA expression levels of β accessory subunits were described in the majority of tissues, therefore it was not surprising to find similar results in RA-FLS (234). In addition, mRNA are not always translated into proteins, requiring the detection of the proteins themselves. Western blots detected $\beta 3$ subunits in all samples analyzed but other β subunits were also detectable at the mRNA and protein levels in some samples. Determination of the kinetics and pharmacological profile of KCa1.1 currents of RA-FLS by single-cell electrophysiology demonstrated the expression of functional $\beta 1$ and $\beta 3$ subunits at the plasma membrane. Previous work has also shown the expression of the α subunit of KCa1.1 in the nucleus of RA-FLS and in several organelles in different cell types (250). This raises the possibility that β subunits of the channel may also be expressed by organelles and play a role not yet understood in FLS.

Levels of the β subunits were lower than those of the α subunit as measured at the mRNA and protein levels by qPCR and Western blot, respectively. It is therefore likely that each α subunit tetramer is associated with fewer than 4 β subunits. The ratio of β and α subunits required to modify current kinetics and pharmacological response of KCa1.1 channels remains unclear; our electrophysiology results demonstrate that the numbers of $\beta 1$ or $\beta 3$ expressed by RA-FLS is sufficient to affect the function of the KCa1.1 channels at their plasma membrane.

The majority of RA-FLS had characteristic whole cell KCa1.1 K⁺ currents sensitive to paxilline, except for approximately 8% of the cells that displayed no K⁺ currents under the conditions used, confirming our previous study (191). No single assay is sufficient to identify the β subunits associated with α subunits to form KCa1.1 channels; we have therefore used a

combination of patch-clamp electrophysiology to measure activation and inactivation kinetics of the currents and test the effects of well-characterized pharmacological agents and of Western blots using antibodies raised against different epitopes of the $\beta 3$ subunit. When examining the pharmacological response to the perfused agents, we used the bile acid derivate LCA, which, at concentrations of 50-150 μM acts as a potent reversible potentiator of KCa1.1 currents only in the presence of $\beta 1$ subunits (40, 251). A minority of cells responded to LCA, indicating functional $\beta 1$ subunit expression on some RA-FLS. In contrast, treating the RA-FLS with 30 μM AA, known to enhance KCa1.1 currents only in the presence of $\beta 2$ or $\beta 3$ subunits (42), induced an increase in current amplitude in the majority of the cells. We tested ChTx that blocks KCa1.1 channels associated with $\beta 1$, $\beta 2$, and $\beta 3$, but not $\beta 4$ subunits, (31) leading to current block in 100% of the RA-FLS assayed and thus demonstrating the absence of $\beta 4$ subunits as components of KCa1.1 at the plasma membrane of these cells. A phenotype of non-inactivating KCa1.1 currents blocked by both paxilline and ChTx, and potentiated by AA, but not by LCA, leads to the conclusion, that the majority of RA-FLS mainly express functional KCa1.1 α and $\beta 3$ subunits. Western blots using antibodies specific to different $\beta 3$ epitopes indicate that RA-FLS express the $\beta 3b$ isoform.

Our data correlate with the expression of KCa1.1 channels formed of α and $\beta 3$ subunits and high current densities with a high expression of CD44, previously shown in RA synovial tissues (236, 237) whereas the $\alpha\beta 1$ phenotype correlated with a low expression of CD44 and lower current densities. Since we had previously shown an increased expression of KCa1.1 α in invasive FLS (192), this raised the possibility that a differential expression of β subunits could underlie the different expression levels of the α subunit of KCa1.1. Indeed, silencing of the $\beta 3$ subunit did decrease the expression levels of KCa1.1 α and reduced the K^+ current densities, suggesting that $\beta 3$ may participate in the cell surface expression of the channel as has been described in other systems with $\beta 1$, $\beta 2$, and $\beta 4$ (33, 34, 39).

To our knowledge, association between high expression levels of potassium channels and CD44 has not directly been reported. However, CD44 expression has long been associated with cancer cell metastasis (239). More recently, the expression of various potassium channels, including KCa1.1, has also been linked to enhanced metastatic potential in cancer (252). Further work needs to be done to determine whether CD44 and potassium channels share any signaling pathways leading to their concomitant upregulation in highly motile cells and to assess whether their expression or function is interdependent in these cells. Additional work is also required to determine whether the switch from KCa1.1 $\beta 1$ to $\beta 3b$ expression in RA-FLS is a consequence, an initiating event, or an independent event in the upregulation of CD44 by these cells. Finally,

it will be interesting to establish whether KCa1.1 and CD44 play synergistic roles in regulating the invasiveness of RA-FLS.

The work presented here focused on the regulatory β subunits of KCa1.1. In the last few years, γ subunits of KCa1.1 have also been identified in various tissues (16, 35). These subunits are structurally different from β subunits but, like β subunits, affect the function of the KCa1.1 channels with which they are co-expressed. It is possible that FLS express γ subunits of KCa1.1 in addition to the β subunits we have identified, either at the plasma membrane or in organelles.

The KCa1.1 channel formed of α and β_3 subunits expressed by RA-FLS represents an attractive therapeutic target for RA. The mRNA for β_3 is expressed only in very low quantity in most tissues, with the highest levels detected in the testis (234). The incidence of RA is higher in women than in men (183-185); in the majority of patients there would therefore not be a concern about male reproductive organ toxicity. Furthermore, the testes are protected by the blood-testis barrier that prevents access from many drugs (253). It is therefore possible to design KCa1.1 blockers that cannot cross this barrier.

In addition to this restricted tissue distribution, the presence of β subunits alters the pharmacology of the channel. Indeed, several scorpion venom peptides affect KCa1.1 channels differently depending on the β subunit expressed. ChTx and iberiotoxin both block KCa1.1 channels containing β_1 , β_2 , and β_3 , but not β_4 subunits, (31, 254). Martentoxin blocks KCa1.1 formed of $\alpha\beta_4$ whereas it opens KCa1.1 formed of $\alpha\beta_1$ and is yet to be tested on KCa1.1 containing β_2 or β_3 subunits (255). It is therefore conceivable that venom peptides that selectively target KCa1.1 $\alpha\beta_3$ could be identified or that existing KCa1.1-blocking peptides could be engineered to enhance their selectivity for this channel as was done successfully with other K^+ channel-blocking peptides (45, 169, 256). A peptide selective for KCa1.1 $\alpha\beta_3$ that cannot cross the blood-testis barrier would be attractive to target KCa1.1 on invasive RA-FLS without the severe side effects induced by the blockade of all KCa1.1 channels regardless of β subunit expression.

7. SUMMARY

Ion channels are key regulators of the inflammatory process, in regards of T lymphocytes as well as of fibroblast like synoviocytes in rheumatoid arthritis, RA-FLS. It is still necessary to deepen our understanding on these topics to be able to treat autoimmune diseases using ion channel inhibitors.

As a major concern, it was not clear how ion channel inhibition correlated with inhibition of cell proliferation as there was an obvious variability in the literature regarding this topic. Our results showed that ion channel blockers and rapamycin inhibit cytokine secretion and cell division in T cells in a dose-dependent manner, while not impairing cell viability. Our key finding was that upon increasing the extent of mitogenic stimulation, the anti-proliferative effect of the ion channel blockers diminished and at very high concentrations it disappeared. Also, this antiproliferative effect can be recovered by combining ion channel blockers with immunopharmacological agents such as the mTOR inhibitor rapamycin. Our findings thus may indicate synergy among the various activation pathways and wishes for *in vivo* experiments where the benefit of the combined treatment can be assessed in autoimmune diseases.

Furthermore, we aimed to improve our understanding considering novel therapeutic opportunities involving ion channel inhibition in rheumatoid arthritis. As RA-FLS, the major effector cells responsible for cartilage destruction in RA, express mainly KCa1.1 channels as potassium channels, these channels can be regarded as an attractive target for RA treatment. As the pore-forming subunit is ubiquitously expressed in the human body, tissue-restricted accessory subunits are the best targets in blocking these channels without any significant side effects. We identified KCa1.1 β 1 and β 3 regulatory subunits expressed in RA-FLS. KCa1.1 β 3 subunits were expressed by in the vast majority of the cells and were associated with highly invasive CD44^{high} RA-FLS, whereas minimally invasive CD44^{low} RA-FLS and FLS from patients with osteoarthritis expressed either β 1 or no regulatory β subunits. Furthermore, we showed that silencing the β 3 but not the β 1 subunit with siRNA reduces KCa1.1 channel density at the plasma membrane of RA-FLS and inhibits RA-FLS invasiveness. These findings suggest that the KCa1.1 channel, composed of α and β 3 subunits in RA-FLS is an attractive therapeutic target for RA, and future efforts are desired to develop a specific KCa1.1 β 3 inhibitor.

In conclusion, we lifted former mysteries involving the functional role of ion channels in both physiological and pathological conditions and by pointing out novel therapeutic opportunities we authenticated future efforts in the aspect of ion channels and disease.

8. ÖSSZEFOGLALÁS

Az ioncsatornák a gyulladásos folyamatok kulcsfontosságú szabályozói, mind T-limfocitákon, mind pedig effektor sejteken (pl.: RA-FLS). További ismeretek szükségesek a fenti témával kapcsolatosan, hogy képesek legyünk autoimmun betegségeket ioncsatorna gátlószerekkel kezelni.

Többek között nem volt világos, hogyan függ össze az ioncsatornagátlás a sejtproliferáció gátlásával, mivel a szakirodalom nagy mértékű szórást mutatott ezen adatokban. Eredményeink azt mutatták, hogy az ioncsatornablokkolók és a rapamicin dóziszfüggő módon gátolják a T-sejtek citokin-szekréciónját és osztódását, miközben nem csökkentik ezen sejtek életképességét. Legfontosabb megállapításunk az volt, hogy a mitogén stimulus mértékének növelésekor az ioncsatornagátlók antiproliferatív hatása csökkent, és nagyon magas koncentrációban el is tűnt. Ezt az proliferációt gátló hatást vissza lehetett állítani oly módon, hogy az ioncsatornablokkolókat egyéb anyagokkal, például mTOR gátló rapamicinnel kombináltuk. Eredményeink tehát szinergiát mutattak a különböző aktivációs utak között és további *in vivo* kísérletek szükségesek, hogy az együttes kezelés előnyeit autoimmun betegségekből fel lehessen mérni.

Ezen túlmenően a reumatoid artritiszben ioncsatornagátlással járó új terápiás lehetőségek tekintetében bővítettük ismereteinket. Mivel az RA-FLS-k, a RA-ban a porc pusztulásáért felelős fő effektor sejtek, K^+ csatornaként főként a KCa1.1 csatornát fejezik ki, ezek a csatornák vonzó célpontok a RA kezelésben. Mivel a pórusképző alegység mindenütt jelen van az emberi szervezetben, a szövetileg behatárolt járulékos alegységek a legmegfelelőbb célpontok ezen csatornák blokkolásában, hogy kiküszöböljük a lehetséges jelentős mellékhatásokat. A RA-FLS-ekben KCa1.1 $\beta 1$ és $\beta 3$ szabályozó alegységeket azonosítottuk. A KCa1.1 $\beta 3$ alegységet a sejtek túlnyomó többsége expresszálta, és erősen invazív CD44^{high} RA-FLS-sel társult, míg az osteoarthritisben szenvedő betegek vagy a minimálisan invazív CD44^{low} RA-FLS-el $\beta 1$ alegységet vagy semmilyen β -t se fejeztek ki. Továbbá azt mutattuk ki, hogy a $\beta 3$ alegység siRNS-sel történő csendesítésével csökkent a KCa1.1 csatorna sűrűsége az RA-FLS membránjában, és csökkent az RA-FLS invazivitása. Ezek az eredmények arra utalnak, hogy az RA-FLS α - és $\beta 3$ -alegységéből álló KCa1.1-csatorna vonzó terápiás célpont RA-ban, és a jövőben erőfeszítésekre van szükség egy specifikus KCa1.1. $\beta 3$ -inhibitor kifejlesztéséhez.

Összefoglalva elmondhatjuk, hogy az ioncsatornák funkcionális szerepe mind fiziológias, mind kóros körülmények között számottevő, és betegségekből, új terápiás lehetőségként kiemelt jelentőségűek lehetnek az ioncsatornák.

9. REFERENCES

1. Zheng J, Trudeau MC. Handbook of ion channels. Boca Raton: CRC Press,, 2015:1 online resource (xx, 671 pages).
2. Benarroch EE. Potassium channels: brief overview and implications in epilepsy. *Neurology*.2009;72:664-669.
3. Rettinger Jr, Schwarz S, Schwarz W, Ohio Library and Information Network. *Electrophysiology : basics, modern approaches and applications*.
4. Alexander SP, et al. The Concise Guide to PHARMACOLOGY 2013/14: overview. *Br J Pharmacol*.2013;170:1449-1458.
5. Gutman GA, et al. International Union of Pharmacology. LIII. Nomenclature and molecular relationships of voltage-gated potassium channels. *Pharmacol Rev*.2005;57:473-508.
6. Lee US, Cui J. BK channel activation: structural and functional insights. *Trends Neurosci*.2010;33:415-423.
7. Berkefeld H, Fakler B, Schulte U. Ca²⁺-activated K⁺ channels: from protein complexes to function. *Physiol Rev*.2010;90:1437-1459.
8. Morales P, Garneau L, Klein H, Lavoie MF, Parent L, Sauve R. Contribution of the KCa3.1 channel-calmodulin interactions to the regulation of the KCa3.1 gating process. *J Gen Physiol*.2013;142:37-60.
9. Horrigan FT, Aldrich RW. Coupling between voltage sensor activation, Ca²⁺ binding and channel opening in large conductance (BK) potassium channels. *J Gen Physiol*.2002;120:267-305.
10. Derler I, Jardin I, Romanin C. Molecular mechanisms of STIM/Orai communication. *American journal of physiology Cell physiology*.2016;310:C643-662.
11. Prakriya M. The molecular physiology of CRAC channels. *Immunol Rev*.2009;231:88-98.
12. Zheng H, et al. Differential roles of the C and N termini of Orai1 protein in interacting with stromal interaction molecule 1 (STIM1) for Ca²⁺ release-activated Ca²⁺ (CRAC) channel activation. *The Journal of biological chemistry*.2013;288:11263-11272.
13. Jegla TJ, Zmasek CM, Batalov S, Nayak SK. Evolution of the human ion channel set. *Comb Chem High Throughput Screen*.2009;12:2-23.
14. Dolphin AC. Voltage-gated calcium channels and their auxiliary subunits: physiology and pathophysiology and pharmacology. *J Physiol*.2016;594:5369-5390.
15. Barrallo-Gimeno A, Gradogna A, Zanardi I, Pusch M, Estevez R. Regulatory-auxiliary subunits of CLC chloride channel-transport proteins. *J Physiol*.2015;593:4111-4127.
16. Zhang J, Yan J. Regulation of BK channels by auxiliary γ subunits. *Front Physiol*.2014;5:401.
17. Tseng TT, et al. Sodium channel auxiliary subunits. *J Mol Microbiol Biotechnol*.2007;12:249-262.
18. Pongs O, Schwarz JR. Ancillary subunits associated with voltage-dependent K⁺ channels. *Physiol Rev*.2010;90:755-796.
19. Kline CF, Mohler PJ. Defective interactions of protein partner with ion channels and transporters as alternative mechanisms of membrane channelopathies. *Biochim Biophys Acta*.2014;1838:723-730.
20. Marionneau C, et al. The sodium channel accessory subunit Navbeta1 regulates neuronal excitability through modulation of repolarizing voltage-gated K(+) channels. *J Neurosci*.2012;32:5716-5727.
21. Wang YW, Ding JP, Xia XM, Lingle CJ. Consequences of the stoichiometry of Slo1 alpha and auxiliary beta subunits on functional properties of large-conductance Ca²⁺-activated K⁺ channels. *J Neurosci*.2002;22:1550-1561.

22. Ding JP, Li ZW, Lingle CJ. Inactivating BK channels in rat chromaffin cells may arise from heteromultimeric assembly of distinct inactivation-competent and noninactivating subunits. *Biophys J*.1998;74:268-289.
23. Majumder K, De Biasi M, Wang Z, Wible BA. Molecular cloning and functional expression of a novel potassium channel beta-subunit from human atrium. *FEBS Lett*.1995;361:13-16.
24. England SK, Uebele VN, Shear H, Kodali J, Bennett PB, Tamkun MM. Characterization of a voltage-gated K⁺ channel beta subunit expressed in human heart. *Proc Natl Acad Sci U S A*.1995;92:6309-6313.
25. Scott VE, et al. Primary structure of a beta subunit of alpha-dendrotoxin-sensitive K⁺ channels from bovine brain. *Proc Natl Acad Sci U S A*.1994;91:1637-1641.
26. Bähring R, et al. Coupling of voltage-dependent potassium channel inactivation and oxidoreductase active site of Kvbeta subunits. *The Journal of biological chemistry*.2001;276:22923-22929.
27. Heinemann SH, Rettig J, Graack HR, Pongs O. Functional characterization of Kv channel beta-subunits from rat brain. *J Physiol*.1996;493 (Pt 3):625-633.
28. Heinemann SH, Rettig J, Wunder F, Pongs O. Molecular and functional characterization of a rat brain Kv beta 3 potassium channel subunit. *FEBS Lett*.1995;377:383-389.
29. Sanguinetti MC, et al. Coassembly of K(V)LQT1 and minK (IsK) proteins to form cardiac I(Ks) potassium channel. *Nature*.1996;384:80-83.
30. Brenner R, Jegla TJ, Wickenden A, Liu Y, Aldrich RW. Cloning and functional characterization of novel large conductance calcium-activated potassium channel beta subunits, hKCNMB3 and hKCNMB4. *J Biol Chem*.2000;275:6453-6461.
31. Meera P, Wallner M, Toro L. A neuronal beta subunit (KCNMB4) makes the large conductance, voltage- and Ca²⁺-activated K⁺ channel resistant to charybdotoxin and iberiotoxin. *Proc Natl Acad Sci USA*.2000;97:5562-5567.
32. Orio P, Rojas P, Ferreira G, Latorre R. New disguises for an old channel: MaxiK channel β-subunits. *News Physiol Sci*.2002;17:156-161.
33. Shruti S, Urban-Ciecko J, Fitzpatrick JA, Brenner R, Bruchez MP, Barth AL. The brain-specific beta4 subunit downregulates BK channel cell surface expression. *PloS one*.2012;7:e33429.
34. Toro B, et al. KCNMB1 regulates surface expression of a voltage and Ca²⁺-activated K⁺ channel via endocytic trafficking signals. *Neuroscience*.2006;142:661-669.
35. Yan J, Aldrich RW. BK potassium channel modulation by leucine-rich repeat-containing proteins. *Proc Natl Acad Sci USA*.2012;109:7917-7922.
36. Li Q, Yan J. Modulation of BK Channel Function by Auxiliary Beta and Gamma Subunits. *Int Rev Neurobiol*.2016;128:51-90.
37. Yan J, Aldrich RW. LRRC26 auxiliary protein allows BK channel activation at resting voltage without calcium. *Nature*.2010;466:513-516.
38. Almassy J, Begenisich T. The LRRC26 protein selectively alters the efficacy of BK channel activators. *Molecular pharmacology*.2012;81:21-30.
39. Zarei MM, et al. Endocytic trafficking signals in KCNMB2 regulate surface expression of a large conductance voltage and Ca²⁺-activated K⁺ channel. *Neuroscience*.2007;147:80-89.
40. Bukiya AN, Vaithianathan T, Toro L, Dopico AM. Channel β2-4 subunits fail to substitute for β1 in sensitizing BK channels to lithocholate. *Biochem Biophys Res Commun*.2009;390:995-1000.
41. Bukiya AN, Liu J, Toro L, Dopico AM. β1 (KCNMB1) subunits mediate lithocholate activation of large-conductance Ca²⁺-activated K⁺ channels and dilation in small, resistance-size arteries. *Mol Pharmacol*.2007;72:359-369.
42. Sun X, Zhou D, Zhang P, Moczydlowski EG, Haddad GG. β-subunit-dependent modulation of hslow BK current by arachidonic acid. *J Neurophysiol*.2007;97:62-69.
43. Panyi G, Possani LD, Rodriguez de la Vega RC, Gaspar R, Varga Z. K⁺ channel blockers: novel tools to inhibit T cell activation leading to specific immunosuppression. *Curr Pharm Des*.2006;12:2199-2220.
44. Hille B. Ion channels of excitable membranes. Third edition ed.

45. Beeton C. Targets and therapeutic properties of venom peptides. In: Kastin AJ, ed. *The handbook of peptides*, 2nd edition: Elsevier, 2012:473-482.
46. Zhou Y, Lingle CJ. Paxilline inhibits BK channels by an almost exclusively closed-channel block mechanism. *J Gen Physiol*.2014;144:415-440.
47. Sanchez M, McManus OB. Paxilline inhibition of the alpha-subunit of the high-conductance calcium-activated potassium channel. *Neuropharmacology*.1996;35:963-968.
48. Knaus HG, et al. Tremorgenic indole alkaloids potently inhibit smooth muscle high-conductance calcium-activated potassium channels. *Biochemistry*.1994;33:5819-5828.
49. Zhou Y, Lingle CJ. Paxilline inhibits BK channels by an almost exclusively closed-channel block mechanism. *J Gen Physiol*.2014;144:415-440.
50. Dutertre S, Lewis RJ. Use of venom peptides to probe ion channel structure and function. *The Journal of biological chemistry*.2010;285:13315-13320.
51. Aiyar J, et al. Topology of the pore-region of a K⁺ channel revealed by the NMR-derived structures of scorpion toxins. *Neuron*.1995;15:1169-1181.
52. Leonard RJ, Garcia ML, Slaughter RS, Reuben JP. Selective blockers of voltage-gated K⁺ channels depolarize human T lymphocytes: mechanism of the antiproliferative effect of charybdotoxin. *Proc Natl Acad Sci U S A*.1992;89:10094-10098.
53. Ahern C, Pless S, Ohio Library and Information Network. Novel chemical tools to study ion channel biology.
54. Hite RK, Tao X, MacKinnon R. Structural basis for gating the high-conductance Ca²⁺-activated K⁺ channel. *Nature*.2017;541:52-57.
55. Hite RK, MacKinnon R. Structural Titration of Slo2.2, a Na⁺-Dependent K⁺ Channel. *Cell*.2017;168:390-399 e311.
56. Su M, et al. Structural basis for conductance through TRIC cation channels. *Nat Commun*.2017;8:15103.
57. James ZM, et al. CryoEM structure of a prokaryotic cyclic nucleotide-gated ion channel. *Proc Natl Acad Sci U S A*.2017;114:4430-4435.
58. Egelman EH. The Current Revolution in Cryo-EM. *Biophys J*.2016;110:1008-1012.
59. Banerjee A, Lee A, Campbell E, Mackinnon R. Structure of a pore-blocking toxin in complex with a eukaryotic voltage-dependent K(+) channel. *Elife*.2013;2:e00594.
60. Chen X, Wang Q, Ni F, Ma J. Structure of the full-length Shaker potassium channel Kv1.2 by normal-mode-based X-ray crystallographic refinement. *Proc Natl Acad Sci U S A*.2010;107:11352-11357.
61. Long SB, Campbell EB, Mackinnon R. Crystal structure of a mammalian voltage-dependent Shaker family K⁺ channel. *Science*.2005;309:897-903.
62. Bartok A, et al. An engineered scorpion toxin analogue with improved Kv1.3 selectivity displays reduced conformational flexibility. *Sci Rep*.2015;5:18397.
63. Bagdany M, et al. Anuroctoxin, a new scorpion toxin of the alpha-KTx 6 subfamily, is highly selective for Kv1.3 over IKCa1 ion channels of human T lymphocytes. *Molecular pharmacology*.2005;67:1034-1044.
64. Varga Z, et al. Vm24, a natural immunosuppressive peptide, potently and selectively blocks Kv1.3 potassium channels of human T cells. *Molecular pharmacology*.2012;82:372-382.
65. Papp F, et al. Tst26, a novel peptide blocker of Kv1.2 and Kv1.3 channels from the venom of *Tityus stigmurus*. *Toxicon*.2009;54:379-389.
66. Corzo G, et al. A selective blocker of Kv1.2 and Kv1.3 potassium channels from the venom of the scorpion *Centruroides suffusus suffusus*. *Biochem Pharmacol*.2008;76:1142-1154.
67. Choi KL, Aldrich RW, Yellen G. Tetraethylammonium blockade distinguishes two inactivation mechanisms in voltage-activated K⁺ channels. *Proc Natl Acad Sci U S A*.1991;88:5092-5095.
68. Grissmer S, Cahalan M. TEA prevents inactivation while blocking open K⁺ channels in human T lymphocytes. *Biophys J*.1989;55:203-206.
69. Cahalan MD, Chandy KG. The functional network of ion channels in T lymphocytes. *Immunological reviews*.2009;231:59-87.

70. Cahalan MD, Wulff H, Chandy KG. Molecular properties and physiological roles of ion channels in the immune system. *Journal of clinical immunology*.2001;21:235-252.
71. Luik RM, Lewis RS. New insights into the molecular mechanisms of store-operated Ca²⁺ signaling in T cells. *Trends in molecular medicine*.2007;13:103-107.
72. Varga Z, Hajdu P, Panyi G. Ion channels in T lymphocytes: an update on facts, mechanisms and therapeutic targeting in autoimmune diseases. *Immunology letters*.2010;130:19-25.
73. Logsdon NJ, Kang J, Togo JA, Christian EP, Aiyar J. A novel gene, hKCa4, encodes the calcium-activated potassium channel in human T lymphocytes. *The Journal of biological chemistry*.1997;272:32723-32726.
74. Begeisich T, et al. Physiological roles of the intermediate conductance, Ca²⁺-activated potassium channel Kcnn4. *The Journal of biological chemistry*.2004;279:47681-47687.
75. Melzer N, Hicking G, Gobel K, Wiendl H. TRPM2 cation channels modulate T cell effector functions and contribute to autoimmune CNS inflammation. *PLoS one*.2012;7:e47617.
76. Lewis RS, Ross PE, Cahalan MD. Chloride channels activated by osmotic stress in T lymphocytes. *The Journal of general physiology*.1993;101:801-826.
77. Schoenborn JR, Wilson CB. Regulation of interferon-gamma during innate and adaptive immune responses. *Adv Immunol*.2007;96:41-101.
78. Wulff H, et al. The voltage-gated Kv1.3 K(+) channel in effector memory T cells as new target for MS. *The Journal of clinical investigation*.2003;111:1703-1713.
79. Szilagyi O, Boratko A, Panyi G, Hajdu P. The role of PSD-95 in the rearrangement of Kv1.3 channels to the immunological synapse. *Pflugers Archiv : European journal of physiology*.2013;465:1341-1353.
80. Robert V, Triffaux E, Savignac M, Pelletier L. [Calcium signaling in T lymphocytes]. *Medecine sciences : M/S*.2012;28:773-779.
81. Santoni G, et al. The role of transient receptor potential vanilloid type-2 ion channels in innate and adaptive immune responses. *Front Immunol*.2013;4:34.
82. Schmitz C, Dorovkov MV, Zhao X, Davenport BJ, Ryazanov AG, Perraud AL. The channel kinases TRPM6 and TRPM7 are functionally nonredundant. *The Journal of biological chemistry*.2005;280:37763-37771.
83. King LB, Freedman BD. B-lymphocyte calcium influx. *Immunol Rev*.2009;231:265-277.
84. Wulff H, Knaus HG, Pennington M, Chandy KG. K⁺ channel expression during B cell differentiation: implications for immunomodulation and autoimmunity. *Journal of immunology*.2004;173:776-786.
85. Feske S, Skolnik EY, Prakriya M. Ion channels and transporters in lymphocyte function and immunity. *Nat Rev Immunol*.2012;12:532-547.
86. Feske S, Wulff H, Skolnik EY. Ion channels in innate and adaptive immunity. *Annu Rev Immunol*.2015;33:291-353.
87. Kis-Toth K, et al. Voltage-gated sodium channel Nav1.7 maintains the membrane potential and regulates the activation and chemokine-induced migration of a monocyte-derived dendritic cell subset. *Journal of immunology*.2011;187:1273-1280.
88. Zsiros E, et al. Developmental switch of the expression of ion channels in human dendritic cells. *Journal of immunology*.2009;183:4483-4492.
89. Mullen KM, et al. Potassium channels Kv1.3 and Kv1.5 are expressed on blood-derived dendritic cells in the central nervous system. *Ann Neurol*.2006;60:118-127.
90. Bittner S, Meuth SG. Targeting ion channels for the treatment of autoimmune neuroinflammation. *Ther Adv Neurol Disord*.2013;6:322-336.
91. Sumoza-Toledo A, Penner R. TRPM2: a multifunctional ion channel for calcium signalling. *J Physiol*.2011;589:1515-1525.
92. Barbet G, et al. The calcium-activated nonselective cation channel TRPM4 is essential for the migration but not the maturation of dendritic cells. *Nat Immunol*.2008;9:1148-1156.

93. Toth BI, Benko S, Szollosi AG, Kovacs L, Rajnavolgyi E, Biro T. Transient receptor potential vanilloid-1 signaling inhibits differentiation and activation of human dendritic cells. *FEBS Lett.*2009;583:1619-1624.
94. Song MG, Hwang SY, Park JI, Yoon S, Bae HR, Kwak JY. Role of aquaporin 3 in development, subtypes and activation of dendritic cells. *Mol Immunol.*2011;49:28-37.
95. Wang GF, Dong CL, Tang GS, Shen Q, Bai CX. Membrane water permeability related to antigen-presenting function of dendritic cells. *Clin Exp Immunol.*2008;153:410-419.
96. Mutini C, et al. Mouse dendritic cells express the P2X7 purinergic receptor: characterization and possible participation in antigen presentation. *Journal of immunology.*1999;163:1958-1965.
97. Szteyn K, et al. Expression and functional significance of the Ca(2+)-activated Cl(-) channel ANO6 in dendritic cells. *Cell Physiol Biochem.*2012;30:1319-1332.
98. Szteyn K, Yang W, Schmid E, Lang F, Shumilina E. Lipopolysaccharide-sensitive H+ current in dendritic cells. *American journal of physiology Cell physiology.*2012;303:C204-212.
99. Tong J, et al. Acid-sensing ion channels contribute to the effect of acidosis on the function of dendritic cells. *Journal of immunology.*2011;186:3686-3692.
100. Craner MJ, et al. Sodium channels contribute to microglia/macrophage activation and function in EAE and MS. *Glia.*2005;49:220-229.
101. Shaw PJ, Feske S. Physiological and pathophysiological functions of SOCE in the immune system. *Front Biosci (Elite Ed).*2012;4:2253-2268.
102. Jin SW, et al. Close functional coupling between Ca2+ release-activated Ca2+ channels and reactive oxygen species production in murine macrophages. *Mediators Inflamm.*2006;2006:36192.
103. Painter RG, et al. The role of chloride anion and CFTR in killing of *Pseudomonas aeruginosa* by normal and CF neutrophils. *J Leukoc Biol.*2008;83:1345-1353.
104. Demaurex N, El Chemaly A. Physiological roles of voltage-gated proton channels in leukocytes. *J Physiol.*2010;588:4659-4665.
105. Bromley SK, et al. The immunological synapse. *Annu Rev Immunol.*2001;19:375-396.
106. Badou A, Jha MK, Matza D, Flavell RA. Emerging roles of L-type voltage-gated and other calcium channels in T lymphocytes. *Front Immunol.*2013;4:243.
107. Zweifach A, Lewis RS. Mitogen-regulated Ca2+ current of T lymphocytes is activated by depletion of intracellular Ca2+ stores. *Proc Natl Acad Sci U S A.*1993;90:6295-6299.
108. Prakriya M, Lewis RS. CRAC channels: activation, permeation, and the search for a molecular identity. *Cell Calcium.*2003;33:311-321.
109. Hoth M, Penner R. Depletion of intracellular calcium stores activates a calcium current in mast cells. *Nature.*1992;355:353-356.
110. Hoth M, Penner R. Calcium release-activated calcium current in rat mast cells. *The Journal of physiology.*1993;465:359-386.
111. Cahalan MD, Wulff H, Chandy KG. Molecular properties and physiological roles of ion channels in the immune system. *Journal of clinical immunology.*2001;21:235-252.
112. Drachman DB, Angus CW, Adams RN, Michelson JD, Hoffman GJ. Myasthenic antibodies cross-link acetylcholine receptors to accelerate degradation. *The New England journal of medicine.*1978;298:1116-1122.
113. Lennon VA. Immunology of the acetylcholine receptor. *Immunological communications.*1976;5:323-344.
114. RamaKrishnan AM, Sankaranarayanan K. Understanding autoimmunity: The ion channel perspective. *Autoimmun Rev.*2016;15:585-620.
115. Gultekin SH, Rosenfeld MR, Voltz R, Eichen J, Posner JB, Dalmau J. Paraneoplastic limbic encephalitis: neurological symptoms, immunological findings and tumour association in 50 patients. *Brain : a journal of neurology.*2000;123 (Pt 7):1481-1494.
116. Shillito P, et al. Acquired neuromyotonia: evidence for autoantibodies directed against K+ channels of peripheral nerves. *Annals of neurology.*1995;38:714-722.
117. Myers KA, Baker SK. Late-onset seropositive Isaacs' syndrome after Guillain-Barre syndrome. *Neuromuscul Disord.*2009;19:288-290.

118. Srivastava R, et al. Potassium channel KIR4.1 as an immune target in multiple sclerosis. *N Engl J Med.*2012;367:115-123.
119. Romi F, Suzuki S, Suzuki N, Petzold A, Plant GT, Gilhus NE. Anti-voltage-gated potassium channel Kv1.4 antibodies in myasthenia gravis. *J Neurol.*2012;259:1312-1316.
120. Moritoki Y, et al. AMA production in primary biliary cirrhosis is promoted by the TLR9 ligand CpG and suppressed by potassium channel blockers. *Hepatology.*2007;45:314-322.
121. Proks P, de Wet H, Ashcroft FM. Molecular mechanism of sulphonylurea block of K(ATP) channels carrying mutations that impair ATP inhibition and cause neonatal diabetes. *Diabetes.*2013;62:3909-3919.
122. Proks P. Neonatal diabetes caused by activating mutations in the sulphonylurea receptor. *Diabetes Metab J.*2013;37:157-164.
123. Toldi G, et al. Lymphocyte activation in type 1 diabetes mellitus: the increased significance of Kv1.3 potassium channels. *Immunol Lett.*2010;133:35-41.
124. Beeton C, et al. Kv1.3 channels are a therapeutic target for T cell-mediated autoimmune diseases. *Proceedings of the National Academy of Sciences of the United States of America.*2006;103:17414-17419.
125. Wulff H, et al. The voltage-gated Kv1.3 K(+) channel in effector memory T cells as new target for MS. *The Journal of clinical investigation.*2003;111:1703-1713.
126. Beeton C, Chandy KG. Potassium channels, memory T cells, and multiple sclerosis. *The Neuroscientist : a review journal bringing neurobiology, neurology and psychiatry.*2005;11:550-562.
127. Gilhar A, Bergman R, Assay B, Ullmann Y, Etzioni A. The beneficial effect of blocking Kv1.3 in the psoriasiform SCID mouse model. *J Invest Dermatol.*2011;131:118-124.
128. Lian YT, et al. Curcumin serves as a human kv1.3 blocker to inhibit effector memory T lymphocyte activities. *Phytother Res.*2013;27:1321-1327.
129. Hansen LK. The role of T cell potassium channels, KV1.3 and KCa3.1, in the inflammatory cascade in ulcerative colitis. *Dan Med J.*2014;61:B4946.
130. Wulff H, Castle NA. Therapeutic potential of KCa3.1 blockers: recent advances and promising trends. *Expert Rev Clin Pharmacol.*2010;3:385-396.
131. Strobaek D, et al. NS6180, a new K(Ca) 3.1 channel inhibitor prevents T-cell activation and inflammation in a rat model of inflammatory bowel disease. *Br J Pharmacol.*2013;168:432-444.
132. Mazza C, Malissen B. What guides MHC-restricted TCR recognition? *Seminars in immunology.*2007;19:225-235.
133. Samelson LE. Signal transduction mediated by the T cell antigen receptor: the role of adapter proteins. *Annual review of immunology.*2002;20:371-394.
134. Levinson W. *Review of medical microbiology and immunology.* New York: McGraw-Hill Education, 2016.
135. Lan RY, Ansari AA, Lian ZX, Gershwin ME. Regulatory T cells: development, function and role in autoimmunity. *Autoimmun Rev.*2005;4:351-363.
136. Jabeen R, Kaplan MH. The symphony of the ninth: the development and function of Th9 cells. *Curr Opin Immunol.*2012;24:303-307.
137. Binger KJ, Corte-Real BF, Kleinewietfeld M. Immunometabolic Regulation of Interleukin-17-Producing T Helper Cells: Uncoupling New Targets for Autoimmunity. *Front Immunol.*2017;8:311.
138. Hemdan NY, et al. Interleukin-17-producing T helper cells in autoimmunity. *Autoimmun Rev.*2010;9:785-792.
139. Larbi A, Pawelec G, Wong SC, Goldeck D, Tai JJ, Fulop T. Impact of age on T cell signaling: a general defect or specific alterations? *Ageing research reviews.*2011;10:370-378.
140. Purtilo B, Pitcher LA, van Oers NS, Wulffing C. T cell receptor (TCR) clustering in the immunological synapse integrates TCR and costimulatory signaling in selected T cells. *Proceedings of the National Academy of Sciences of the United States of America.*2005;102:2904-2909.
141. Lenschow DJ, Walunas TL, Bluestone JA. CD28/B7 system of T cell costimulation. *Annual review of immunology.*1996;14:233-258.

142. Jiang H, Chess L. Regulation of immune responses by T cells. *The New England journal of medicine*.2006;354:1166-1176.
143. Dustin ML. The immunological synapse. *Cancer Immunol Res*.2014;2:1023-1033.
144. Crabtree GR. Generic signals and specific outcomes: signaling through Ca²⁺, calcineurin, and NF-AT. *Cell*.1999;96:611-614.
145. Rao A, Luo C, Hogan PG. Transcription factors of the NFAT family: regulation and function. *Annu Rev Immunol*.1997;15:707-747.
146. Chen J, Fang Y. A novel pathway regulating the mammalian target of rapamycin (mTOR) signaling. *Biochemical pharmacology*.2002;64:1071-1077.
147. Gingras AC, Raught B, Sonenberg N. Regulation of translation initiation by FRAP/mTOR. *Genes & development*.2001;15:807-826.
148. Saunders RN, Metcalfe MS, Nicholson ML. Rapamycin in transplantation: a review of the evidence. *Kidney international*.2001;59:3-16.
149. Abbas AK, Lichtman AH, Pillai S. *Cellular and molecular immunology*. 7th ed. Philadelphia: Saunders/Elsevier, 2012.
150. Frauwirth KA, Thompson CB. Activation and inhibition of lymphocytes by costimulation. *J Clin Invest*.2002;109:295-299.
151. Trickett A, Kwan YL. T cell stimulation and expansion using anti-CD3/CD28 beads. *Journal of immunological methods*.2003;275:251-255.
152. DeCoursey TE, Chandy KG, Gupta S, Cahalan MD. Voltage-gated K⁺ channels in human T lymphocytes: a role in mitogenesis? *Nature*.1984;307:465-468.
153. Wulff H, Beeton C, Chandy KG. Potassium channels as therapeutic targets for autoimmune disorders. *Current opinion in drug discovery & development*.2003;6:640-647.
154. Castaneda O, et al. Characterization of a potassium channel toxin from the Caribbean Sea anemone *Stichodactyla helianthus*. *Toxicon*.1995;33:603-613.
155. Matheu MP, et al. Imaging of effector memory T cells during a delayed-type hypersensitivity reaction and suppression by Kv1.3 channel block. *Immunity*.2008;29:602-614.
156. Tarcha EJ, et al. Safety and pharmacodynamics of dalazatide, a Kv1.3 channel inhibitor, in the treatment of plaque psoriasis: A randomized phase 1b trial. *PloS one*.2017;12:e0180762.
157. Chen J, Fang Y. A novel pathway regulating the mammalian target of rapamycin (mTOR) signaling. *Biochem Pharmacol*.2002;64:1071-1077.
158. Gingras AC, Raught B, Sonenberg N. Regulation of translation initiation by FRAP/mTOR. *Genes Dev*.2001;15:807-826.
159. Witkowski JM, Siebert J, Lukaszuk K, Trawicka L. Comparison of effect of a panel of membrane channel blockers on the proliferative, cytotoxic and cytoadherence abilities of human peripheral blood lymphocytes. *Immunopharmacology*.1993;26:53-63.
160. Jensen BS, Odum N, Jorgensen NK, Christophersen P, Olesen SP. Inhibition of T cell proliferation by selective block of Ca(2+)-activated K(+) channels. *Proceedings of the National Academy of Sciences of the United States of America*.1999;96:10917-10921.
161. Wulff H, Miller MJ, Hansel W, Grissmer S, Cahalan MD, Chandy KG. Design of a potent and selective inhibitor of the intermediate-conductance Ca²⁺-activated K⁺ channel, IKCa1: a potential immunosuppressant. *Proceedings of the National Academy of Sciences of the United States of America*.2000;97:8151-8156.
162. Schmitz A, et al. Design of PAP-1, a selective small molecule Kv1.3 blocker, for the suppression of effector memory T cells in autoimmune diseases. *Molecular pharmacology*.2005;68:1254-1270.
163. Pegoraro S, et al. Inhibitors of potassium channels KV1.3 and IK-1 as immunosuppressants. *Bioorganic & medicinal chemistry letters*.2009;19:2299-2304.
164. Grgic I, Wulff H, Eichler I, Flothmann C, Kohler R, Hoyer J. Blockade of T-lymphocyte KCa_{3.1} and Kv1.3 channels as novel immunosuppression strategy to prevent kidney allograft rejection. *Transplant Proc*.2009;41:2601-2606.

165. Pennington MW, Harunur Rashid M, Tajhya RB, Beeton C, Kuyucak S, Norton RS. A C-terminally amidated analogue of ShK is a potent and selective blocker of the voltage-gated potassium channel Kv1.3. *FEBS Lett.*2012;586:3996-4001.
166. Beeton C, et al. Targeting effector memory T cells with a selective peptide inhibitor of Kv1.3 channels for therapy of autoimmune diseases. *Molecular pharmacology.*2005;67:1369-1381.
167. Ghanshani S, et al. Up-regulation of the IKCa1 potassium channel during T-cell activation. Molecular mechanism and functional consequences. *The Journal of biological chemistry.*2000;275:37137-37149.
168. Koo GC, et al. Blockade of the voltage-gated potassium channel Kv1.3 inhibits immune responses in vivo. *Journal of immunology.*1997;158:5120-5128.
169. Chi V, et al. Development of a sea anemone toxin as an immunomodulator for therapy of autoimmune diseases. *Toxicon.*2012;59:529-546.
170. Schmitz A, et al. Design of PAP-1, a selective small molecule Kv1.3 blocker, for the suppression of effector memory T cells in autoimmune diseases. *Molecular pharmacology.*2005;68:1254-1270.
171. Vennekamp J, et al. Kv1.3-blocking 5-phenylalkoxypsoralens: a new class of immunomodulators. *Molecular pharmacology.*2004;65:1364-1374.
172. Shah K, Tom Blake J, Huang C, Fischer P, Koo GC. Immunosuppressive effects of a Kv1.3 inhibitor. *Cell Immunol.*2003;221:100-106.
173. Dreker T, Hamm S, Tasler S. Effects of Small Molecule Kv1.3 and K(Ca)3.1 Inhibitors on T_{EM}-Cell Proliferation. *Biophysical Journal*;98:535a.
174. Verheugen JA, Le Deist F, Devignot V, Korn H. Enhancement of calcium signaling and proliferation responses in activated human T lymphocytes. Inhibitory effects of K⁺ channel block by charybdotoxin depend on the T cell activation state. *Cell calcium.*1997;21:1-17.
175. Toldi G, et al. Lymphocyte calcium influx kinetics in multiple sclerosis treated without or with interferon beta. *J Neuroimmunol.*2011;237:80-86.
176. Ye Y, et al. The anti-inflammatory effect of the SOCC blocker SK&F 96365 on mouse lymphocytes after stimulation by Con A or PMA/ionomycin. *Immunobiology.*2011;216:1044-1053.
177. Chen G, et al. Characterization of a novel CRAC inhibitor that potently blocks human T cell activation and effector functions. *Mol Immunol.*2013;54:355-367.
178. Nordstrom T, Nevanlinna HA, Andersson LC. Mitosis-arresting effect of the calcium channel inhibitor SK&F 96365 on human leukemia cells. *Exp Cell Res.*1992;202:487-494.
179. Weir MR, Peppler R, Gomolka D, Handwerker BS. Calcium channel blockers inhibit cellular uptake of thymidine, uridine and leucine: the incorporation of these molecules into DNA, RNA and protein in the presence of calcium channel blockers is not a valid measure of lymphocyte activation. *Immunopharmacology.*1993;25:75-82.
180. Bottini N, Firestein GS. Duality of fibroblast-like synoviocytes in RA: passive responders and imprinted aggressors. *Nat Rev Rheumatol.*2013;9:24-33.
181. Bartok B, Firestein GS. Fibroblast-like synoviocytes: key effector cells in rheumatoid arthritis. *Immunol Rev.*2010;233:233-255.
182. Large RJ, et al. Ionic currents in intimal cultured synoviocytes from the rabbit. *American journal of physiology Cell physiology.*2010;299:C1180-1194.
183. Gregersen PK, Plenge RM, Gulko PS. Genetics of rheumatoid arthritis. In: Firestein G, Panayi G, Wollheim FA, eds. *Rheumatoid arthritis.* New York: Oxford University Press, 2006:3-14.
184. Gulko PS, Winchester RJ. Rheumatoid arthritis. In: Austen KF, Frank MM, Atkinson JP, Cantor H, eds. *Samter's immunologic diseases.* Baltimore: Lippincott, Williams & Wilkins, 2001:427-463.
185. Gibofsky A. Overview of epidemiology, pathophysiology, and diagnosis of rheumatoid arthritis. *Am J Manag Care.*2012;18:S295-S302.
186. Noss EH, Brenner MB. The role and therapeutic implications of fibroblast-like synoviocytes in inflammation and cartilage erosion in rheumatoid arthritis. *Immunol Rev.*2008;223:252-270.

187. Laragione T, Brenner M, Mello A, Symons M, Gulko PS. The arthritis severity locus Cia5d is a novel genetic regulator of the invasive properties of synovial fibroblasts. *Arthritis Rheum.*2008;58:2296-2306.
188. Tolboom TC, van der Helm-Van Mil AH, Nelissen RG, Breedveld FC, Toes RE, Huizinga TW. Invasiveness of fibroblast-like synoviocytes is an individual patient characteristic associated with the rate of joint destruction in patients with rheumatoid arthritis. *Arthritis Rheum.*2005;52:1999-2002.
189. Kahlenberg JM, Fox DA. Advances in the medical treatment of rheumatoid arthritis. *Hand Clin.*2011;27:11-20.
190. Fidder HH, M.M. S, van der Have M, Oldenburg B, van Oijen MG. Low rates of adherence for tumor necrosis factor- α inhibitors in Crohn's disease and rheumatoid arthritis: results of a systematic review. *World J Gastroenterol.*2013;19:4344-4450.
191. Hu X, et al. KCa1.1 potassium channels regulate key pro-inflammatory and invasive properties of fibroblast-like synoviocytes in rheumatoid arthritis. *J Biol Chem.*2012;287:4014-4022.
192. Tanner MR, et al. KCa1.1 inhibition attenuates fibroblast-like synoviocyte invasiveness and ameliorates rat models of rheumatoid arthritis. *Arthritis Rheumatol.*2015;67:96-106.
193. Saleem F, Rowe ICM, Shipston MJ. Characterization of BK channel splice variants using membrane potential dyes. *Br J Pharmacol.*2009;156:143-152.
194. Sanchez M, McManus OB. Paxilline inhibition of the alpha-subunit of the high-conductance calcium-activated potassium channel. *Neuropharmacol.*1996;35:963-968.
195. Meredith AL, Thorneloe KS, Werner ME, Nelson MT, Aldrich RW. Overactive bladder and incontinence in the absence of the BK large conductance Ca²⁺-activated K⁺ channel. *J Biol Chem.*2004;279:36746-36752.
196. Sausbier M, et al. Elevated blood pressure linked to primary hyperaldosteronism and impaired vasodilation in BK channel-deficient mice. *Circulation.*2005;112:60-68.
197. Sausbier M, et al. Cerebellar ataxia and Purkinje cell dysfunction caused by Ca²⁺-activated K⁺ channel deficiency. *Proc Natl Acad Sci USA.*2004;101:9474-9478.
198. Laragione T, et al. The cation channel Trpv2 is a new suppressor of arthritis severity, joint damage, and synovial fibroblast invasion. *Clin Immunol.*2015;158:183-192.
199. Li X, Wang X, Wang Y, Li X, Huang C, Li J. Inhibition of transient receptor potential melastatin 7 (TRPM7) channel induces RA FLSs apoptosis through endoplasmic reticulum (ER) stress. *Clin Rheumatol.*2014;33:1565-1574.
200. Waldburger JM, Boyle DL, Pavlov VA, Tracey KJ, Firestein GS. Acetylcholine regulation of synoviocyte cytokine expression by the alpha7 nicotinic receptor. *Arthritis Rheum.*2008;58:3439-3449.
201. van Maanen MA, et al. The alpha7 nicotinic acetylcholine receptor on fibroblast-like synoviocytes and in synovial tissue from rheumatoid arthritis patients: a possible role for a key neurotransmitter in synovial inflammation. *Arthritis Rheum.*2009;60:1272-1281.
202. Kolker SJ, et al. Acid-sensing ion channel 3 expressed in type B synoviocytes and chondrocytes modulates hyaluronan expression and release. *Ann Rheum Dis.*2010;69:903-909.
203. Contet C, Goulding SP, Kuljis DA, Barth AL. BK Channels in the Central Nervous System. *Int Rev Neurobiol.*2016;128:281-342.
204. Kaczorowski GJ, Garcia ML. Developing Molecular Pharmacology of BK Channels for Therapeutic Benefit. *Int Rev Neurobiol.*2016;128:439-475.
205. Orio P, Latorre R. Differential effects of beta 1 and beta 2 subunits on BK channel activity. *J Gen Physiol.*2005;125:395-411.
206. Krishnamoorthy G, Sonkusare SK, Heppner TJ, Nelson MT. Opposing roles of smooth muscle BK channels and ryanodine receptors in the regulation of nerve-evoked constriction of mesenteric resistance arteries. *Am J Physiol Heart Circ Physiol.*2014;306:H981-988.
207. Holtzclaw JD, Grimm PR, Sansom SC. Role of BK channels in hypertension and potassium secretion. *Curr Opin Nephrol Hypertens.*2011;20:512-517.

208. Brenner R, Chen QH, Vilaythong A, Toney GM, Noebels JL, Aldrich RW. BK channel beta4 subunit reduces dentate gyrus excitability and protects against temporal lobe seizures. *Nat Neurosci.*2005;8:1752-1759.
209. Du W, et al. Calcium-sensitive potassium channelopathy in human epilepsy and paroxysmal movement disorder. *Nat Genet.*2005;37:733-738.
210. Cheeke PR. Endogenous toxins and mycotoxins in forage grasses and their effects on livestock. *J Anim Sci.*1995;73:909-918.
211. N'Gouemo P. Targeting BK (big potassium) channels in epilepsy. *Expert Opin Ther Targets.*2011;15:1283-1295.
212. Li Y, Kurlander RJ. Comparison of anti-CD3 and anti-CD28-coated beads with soluble anti-CD3 for expanding human T cells: differing impact on CD8 T cell phenotype and responsiveness to restimulation. *Journal of translational medicine.*2010;8:104.
213. Bootman MD, Collins TJ, Mackenzie L, Roderick HL, Berridge MJ, Peppiatt CM. 2-aminoethoxydiphenyl borate (2-APB) is a reliable blocker of store-operated Ca²⁺ entry but an inconsistent inhibitor of InsP₃-induced Ca²⁺ release. *FASEB journal : official publication of the Federation of American Societies for Experimental Biology.*2002;16:1145-1150.
214. Ghez D, et al. Rapamycin for refractory acute graft-versus-host disease. *Transplantation.*2009;88:1081-1087.
215. Wang X, et al. Rapamycin inhibits proteasome activator expression and proteasome activity. *European journal of immunology.*1997;27:2781-2786.
216. Lyons AB, Parish CR. Determination of lymphocyte division by flow cytometry. *Journal of immunological methods.*1994;171:131-137.
217. Lyons AB. Analysing cell division in vivo and in vitro using flow cytometric measurement of CFSE dye dilution. *Journal of immunological methods.*2000;243:147-154.
218. Lyons AB, Blake SJ, Doherty KV. Flow cytometric analysis of cell division by dilution of CFSE and related dyes. *Current protocols in cytometry / editorial board, J Paul Robinson, managing editor [et al].*2013;Chapter 9:Unit9 11.
219. Koshy S, et al. Blocking Kv1.3 channels inhibits Th2 lymphocyte function and treats a rat model of asthma. *J Biol Chem.*2014;289:12623-12632.
220. Beeton C, et al. A novel fluorescent toxin to detect and investigate Kv1.3 channel up-regulation in chronically activated T lymphocytes. *J Biol Chem.*2003;278:9928-9937.
221. Aletaha D, et al. 2010 Rheumatoid arthritis classification criteria: an American College of Rheumatology/European League Against Rheumatism collaborative initiative. *Arthritis Rheum.*2010;62:2569-2581.
222. Chan A, Akhtar M, Brenner M, Zheng Y, Gulko PS, Symons M. The GTPase Rac regulates the proliferation and invasion of fibroblast-like synoviocytes from rheumatoid arthritis patients. *Mol Med.*2007;13:297-304.
223. Laragione T, Gulko PS. mTOR regulates the invasive properties of synovial fibroblasts in rheumatoid arthritis. *Mol Med.*2010;16:352-358.
224. Hamill OP, Marty A, Neher E, Sakmann B, Sigworth FJ. Improved patch-clamp techniques for high-resolution current recording from cells and cell-free membrane patches. *Pflugers Archiv : European journal of physiology.*1981;391:85-100.
225. Wulff H, et al. The voltage-gated Kv1.3 K⁺ channel in effector memory T cells as new target for MS. *J Clin Invest.*2003;111:1703-1713.
226. Beeton C, et al. Targeting effector memory T cells with a selective peptide inhibitor of Kv1.3 channels for therapy of autoimmune diseases. *Mol Pharmacol.*2005;67:1369-1381.
227. Torres YP, Granados ST, Latorre R. Pharmacological consequences of the coexpression of BK channels α and β subunits. *Front Physiol.*2014;5:383.
228. Strøbaek D, et al. Modulation of the Ca²⁺-dependent K⁺ channel, hsl α , by the substituted diphenylurea NS 1608, paxilline and internal Ca²⁺. *Neuropharmacol.*1996;35:903-914.
229. Wang B, Jaffe DB, Brenner R. Current understanding of iberiotoxin-resistant BK channels in the nervous system. *Front Physiol.*2014;5:382.

230. Chhabra S, et al. Kv1.3 channel-blocking immunomodulatory peptides from parasitic worms: implications for autoimmune diseases. *FASEB J.*2014;28:3952-3964.
231. Tarcha EJ, et al. Durable pharmacological responses from the peptide ShK-186, a specific Kv1.3 channel inhibitor that suppresses T cell mediators of autoimmune diseases. *J Pharmacol Exp Ther.*2012;342:642-653.
232. Hu S, Labuda MZ, Pandolfo M, Goss GG, McDermid HE, Ali DW. Variants of the KCNMB3 regulatory subunit of maxi BK channels affect channel inactivation. *Physiol Genomics.*2003;15:191-198.
233. Wallner M, Meera P, Toro L. Molecular basis of fast inactivation in voltage and Ca²⁺-activated K⁺ channels: a transmembrane beta-subunit homolog. *Proc Natl Acad Sci USA.*1999;96:4137-4142.
234. Behrens R, Nolting A, Reimann F, Schwarz M, Waldschutz R, Pongs O. hKCNMB3 and hKCNMB4, cloning and characterization of two members of the large-conductance calcium-activated potassium channel beta subunit family. *FEBS Lett.*2000;474:99-106.
235. Lee US, Cui J. β subunit-specific modulations of BK channel function by a mutation associated with epilepsy and dyskinesia. *J Physiol.*2009;587:1481-1498.
236. Haynes BF, Hale LP, Patton KL, Martin ME, McCallum RM. Measurement of an adhesion molecule as an indicator of inflammatory disease activity: Up-regulation of the receptor for hyaluronate (CD44) in rheumatoid arthritis. *Arthritis Rheum.*1991;34:1434-1443.
237. Naor D, Nedvetzki S. CD44 in rheumatoid arthritis. *Arthritis Res Ther.*2003;5:105-115.
238. Knudson W. The role of CD44 as a cell surface hyaluronan receptor during tumor invasion of connective tissue. *Front Biosci.*1998;3:d604-615.
239. Jothy S. CD44 and its partners in metastasis. *Clin Exp Metastasis.*2003;20:195-201.
240. Kiener HP, Niederreiter B, Lee DM, Jimenez-Boj E, Smolen JS, Brenner MB. Cadherin 11 promotes invasive behavior of fibroblast-like synoviocytes. *Arthritis Rheum.*2009;60:1305-1310.
241. Ekwall AK, et al. The tumour-associated glycoprotein podoplanin is expressed in fibroblast-like synoviocytes of the hyperplastic synovial lining layer in rheumatoid arthritis. *Arthritis Res Ther.*2011;13:R40.
242. Venken K, Hellings N, Liblau R, Stinissen P. Disturbed regulatory T cell homeostasis in multiple sclerosis. *Trends in molecular medicine.*2010;16:58-68.
243. Tsokos GC, Nambiar MP, Tenbrock K, Juang YT. Rewiring the T-cell: signaling defects and novel prospects for the treatment of SLE. *Trends in immunology.*2003;24:259-263.
244. Nevins TE. Overview of new immunosuppressive therapies. *Current opinion in pediatrics.*2000;12:146-150.
245. Goto J, et al. Two novel 2-aminoethyl diphenylborinate (2-APB) analogues differentially activate and inhibit store-operated Ca(2+) entry via STIM proteins. *Cell calcium.*2010;47:1-10.
246. Kim DT, Rothbard JB, Bloom DD, Fathman CG. Quantitative analysis of T cell activation: role of TCR/ligand density and TCR affinity. *Journal of immunology.*1996;156:2737-2742.
247. Arakaki A, et al. TCR-beta repertoire analysis of antigen-specific single T cells using a high-density microcavity array. *Biotechnology and bioengineering.*2010;106:311-318.
248. Parekh AB. Ca²⁺ microdomains near plasma membrane Ca²⁺ channels: impact on cell function. *J Physiol.*2008;586:3043-3054.
249. Xu R, et al. Kv1.3 channels as a potential target for immunomodulation of CD4⁺ CD28^{null} T cells in patients with acute coronary syndrome. *Clin Immunol.*2012;142:209-217.
250. Singh H, Stefani E, Toro L. Intracellular BK_{Ca} (iBK_{Ca}) channels. *J Physiol.*2012;590:5937-5947.
251. Bukiya AN, McMillan J, Parrill AL, Dopico AM. Structural determinants of monohydroxylated bile acids to activate beta 1 subunit-containing BK channels. *J Lipid Res.*2008;49:2441-2451.
252. Comes N, et al. Involvement of potassium channels in the progression of cancer to a more malignant phenotype. *Biochim Biophys Acta.*2015;1848:2477-2492.
253. Quignot N. Modeling bioavailability to organs protected by biological barriers. *In Silico Pharmacol.*2013;31:8.
254. Candia S, Garcia ML, Latorre R. Mode of action of iberiotoxin, a potent blocker of the large conductance Ca²⁺-activated K⁺ channel. *Biophys J.*1992;63:583-590.

255. Tao J, Shi J, Liu ZR, Ji YH. Martenotoxin: a unique ligand of BK channels. *Acta Physiol Sin.*2012;64:355-364.
256. Beeton C, Pennington MW, Norton RS. Analogs of the sea anemone potassium channel blocker ShK for the treatment of autoimmune diseases. *Inflamm Allergy Drug Targets.*2011;10:313-321.

10. LIST OF PUBLICATIONS



UNIVERSITY OF DEBRECEN
UNIVERSITY AND NATIONAL LIBRARY



Registry number: DEENK/271/2017.PL
Subject: PhD Publikációs Lista

Candidate: Zoltán Pethő
Neptun ID: JOG5ED
Doctoral School: Doctoral School of Molecular Medicine
MTMT ID: 10043198

List of publications related to the dissertation

1. **Pethő, Z.**, Tanner, M. R., Tajhya, R. B., Huq, R., Laragione, T., Panyi, G., Gulko, P. S., Beeton, C.: Different expression of [béta] subunits of the KCa1.1 channel by invasive and non-invasive human fibroblast-like synoviocytes.
Arthritis Res. Ther. 18 (1), 103, 2016.
DOI: <http://dx.doi.org/10.1186/s13075-016-1003-4>
IF: 4.121
2. **Pethő, Z.**, Balajthy, A., Bartók, Á., Bene, K., Somodi, S., Szilágyi, O., Rajnavölgyi, É., Panyi, G., Varga, Z.: The anti-proliferative effect of cation channel blockers in T lymphocytes depends on the strength of mitogenic stimulation.
Immunol. Lett. 171, 60-69, 2016.
DOI: <http://dx.doi.org/10.1016/j.imlet.2016.02.003>
IF: 2.86



Address: 1 Egyetem tér, Debrecen 4032, Hungary Postal address: Pf. 39. Debrecen 4010, Hungary
Tel.: +36 52 410 443 Fax: +36 52 512 900/63847 E-mail: publikaciok@lib.unideb.hu Web: www.lib.unideb.hu



List of other publications

3. Pajtás, D., Kónya, K., Kiss-Szikszai, A., Džubák, P., **Pethő, Z.**, Varga, Z., Panyi, G., Patonay, T.:
Optimization of the Synthesis of Flavone-Amino Acid and Flavone-Dipeptide Hybrids via
Buchwald-Hartwig Reaction.
J. Org. Chem. 82 (9), 4578-4587, 2017.
DOI: <http://dx.doi.org/10.1021/acs.joc.7b00124>
IF: 4.849 (2016)
4. Balajthy, A., Somodi, S., **Pethő, Z.**, Péter, M., Varga, Z., Szabó, G., Paragh, G., Vigh, L., Panyi,
G., Hajdu, P.: 7DHC-induced changes of Kv1.3 operation contributes to modified T cell
function in Smith-Lemli-Opitz syndrome.
Pflugers Arch. 468 (8), 1403-1418, 2016.
DOI: <http://dx.doi.org/10.1007/s00424-016-1851-4>
IF: 3.156
5. Somodi, S., Balajthy, A., Szilágyi, O., **Pethő, Z.**, Harangi, M., Paragh, G., Panyi, G., Hajdu, P.:
Analysis of the K⁺ current in human CD4⁺ T lymphocytes in hypercholesterolemic state.
Cell. Immunol. 281 (1), 20-26, 2013.
DOI: <http://dx.doi.org/10.1016/j.cellimm.2013.01.004>
IF: 1.874

Total IF of journals (all publications): 16,86

Total IF of journals (publications related to the dissertation): 6,981

The Candidate's publication data submitted to the iDEa Tudóstér have been validated by DEENK on
the basis of Web of Science, Scopus and Journal Citation Report (Impact Factor) databases.

01 September, 2017



11. ORAL AND POSTER PRESENTATIONS

I. Oral presentations on conferences

June 21-24. 2010.: 2nd International Student Medical Congress Kosice, Kosice, Slovakia.

- K⁺ current expression and proliferation of human T-lymphocytes induced by various stimuli (oral presentation)

Authors: Pethő Zoltán Dénes, Balajthy András

May 17-20. 2011.: 41. Sümegi Membrán-transzport konferencia, Sümeg, Hungary.

- Limfociták proliferációjának és Kv1.3 kálium ioncsatornáinak vizsgálata hiperkoleszterinémias állapotban (oral presentation)

Authors: Balajthy András, Pethő Zoltán Dénes, Dr. Somodi Sándor, Dr. Hajdú Péter

August 2011.: European Biophysics Societies' Association (EBSA) congress, Budapest, Hungary.

- Analysis of the K⁺ current in human T-cells in hypercholesterinaemic state (oral presentation)

Authors: Balajthy András, Pethő Zoltán Dénes, Dr. Krasznai Zoltán, Dr. Somodi Sándor, Dr. Hajdú Péter

July 18-21. 2013.: International Medical Student Congress Novi Sad IMSCNS, Novi Sad, Serbia.

- Studying the interactions between mesenchymal stem cells and lymphocytes (oral presentation)

Authors: Pethő Zoltán Dénes, Balajthy András, Mészáros Beáta

August 19.-22. 2013.: Veszprémi Magyar Biofizikai Társaság Kongresszusa, Veszprém, Hungary.

- Mesenchymalis őssejtek hatása T-lymphocyták proliferációjára és Kv1.3 ioncsatornáira (oral presentation)

Authors: Pethő Zoltán Dénes, Mészáros Beáta, Balajthy András, Bartók Ádám, Dr. Panyi György

**may 22. 2013. I. Sántha Kálmán Szakkollégiumi Kerekasztal, Debrecen, Hungary
(szakkollégiumi konferencia)**

- Limfociták és mezenhimális őssejtek közötti kölcsönhatások tanulmányozása I. (oral presentation)

Author: Pethő Zoltán Dénes

**december 5. 2013. III. Sántha Kálmán Szakkollégiumi Kerekasztal, Debrecen, Hungary
(szakkollégiumi konferencia)**

- A mezenhimális őssejtek és lehetséges immunomoduláns hatásaik (oral presentation)

Author: Pethő Zoltán Dénes

II. Poster presentations on conferences

april 9-11. 2010.: „Bridges in Life Sciences 5th Annual Scientific Meeting”- Lvov, Ukraine.

- K⁺ current expression and proliferation of human T-lymphocytes induced by various stimuli (poster)

Authors: Pethő Zoltán Dénes, Balajthy András

- Analysis of the K⁺ current in human T cells in hypercholesterinaemic state (poster)

Authors: Balajthy András, Pethő Zoltán Dénes, Somodi Sandor

may 17-20. 2011.: 41. Sümegi Membrán-transzport konferencia, Sümeg, Hungary.

- Kationcsatorna-gátlók hatása mitogénnel stimulált T-limfocitákra (poszter)

Authors: Pethő Zoltán Dénes, Balajthy András, Dr. Varga Zoltán, Dr. Panyi György

august 2011: European Biophysics Societies' Association (EBSA) congress, Budapest, Hungary.

- Effect of ion channel blockers on T-lymphocytes stimulated with anti-CD3 and anti-CD28 (poszter)

Authors: Pethő Zoltán Dénes, Balajthy András, Dr. Krasznai Zoltán, Dr. Varga Zoltán, Dr. Panyi György

october 19-22. 2012.: European medical student conference EMESCO, Debrecen, Hungary.

- Immune cells produce thyroglobulin antibodies in thyroid cancer: a tissue-specific immune response (poszter)

Authors: Pethő Zoltán Dénes, Balajthy András, Christian Bernecker, Margret Ehlers, Dr. Panyi György, Matthias Schott

- Effects of hypercholesterinaemia on Kv1.3 currents (poster)

Authors: Balajthy András, Pethő Zoltán Dénes, Dr. Somodi Sándor, Dr. Hajdú Péter

juli 18-21. 2013.: International Medical Student Congress Novi Sad IMSCNS, Novi Sad, Serbia.

- Inherited disorder of cholesterol biosynthesis (SLO syndrome) modifies the function of Kv1.3 channels and proliferation of lymphocytes (poster)

Authors: Balajthy András, Pethő Zoltán Dénes, Dr. Hajdú Péter

may 21.-24. 2013.: 43. Sümegi Membrán-transzport konferencia, Sümeg, Hungary.

- A Smitz-Leimnitz-Opitz szindróma megváltoztatja a lymphocyták Kv1.3 ioncsatornáinak működését, melyet ciklodextrin/7DHC töltéssel modellezni lehet (másodszerzős poster)

Authors: Balajthy András, Pethő Zoltán Dénes, Dr. Somodi Sándor, Dr. P. Szabó Gabriella, Dr. Hajdú Péter

november 8. 2013.: Semmelweis Symposium 2013, Budapest, Hungary.

- Inherited disorder of cholesterol biosynthesis (SLO syndrome) modifies the function of Kv1.3 channels and proliferation of lymphocytes (poster)

Authors: Balajthy András, Pethő Zoltán Dénes

february 15.-19. 2014.: Biophysical Society 58th Annual meeting (BSM) , San Francisco, USA.

- Altered Gating of Kv1.3 Channels of T Lymphocytes in Smith-Lemli-Opitz Syndrome (poster)

Authors: Andras Balajthy, Sandor Somodi, Maria Peter, Zoltan Denes Petho, Laszlo Vigh, Gyorgy Panyi, Peter Hajdu

february 7.-11. 2015.: Biophysical Society 59th Annual meeting (BSM) , Baltimore, USA.

- KCa1.1 (BK) channels on fibroblast-like synoviocytes: a novel therapeutic target for rheumatoid arthritis (társzerzős poszter)

Authors: Mark R. Tanner, Zoltan Denes Petho, Rajeev B. Tajhya, Redwan Huq, Frank T. Horrigan, Percio S. Gulco, Christine Beeton

- The anti-proliferative effect of cation channel blockers on T lymphocytes stimulated by anti-CD3 and anti-CD28 (társ szerzős poszter)

Authors: Zoltan Varga, Zoltan Denes Petho, Andras Balajthy, Adam Bartok, Sandor Somodi, Orsolya Szilagy, Gyorgy Panyi

may 19.-22. 2015.: 45. Sümegi Membrán-transzport konferencia, Sümeg, Hungary.

- Glioblastoma multiforme KCa1.1 ioncsatornáinak feltérképezése (poster)

Szerző: Pethő Zoltán Dénes, Papp Pál, Balajthy András, Klekner Álmos, Panyi György, Varga Zoltán

february 27.- march 2. 2016: Biophysical Society 60th Annual meeting (BSM) , Los Angeles, USA.

- The effect of membrane cholesterol content on the gating mechanism of voltage gated potassium channels (poster)

Authors: Pal Pap, Zoltan Petho, Gyorgy Panyi, Zoltan Varga

- 7-dehydrocholesterol modifies the operation of Kv1.3 channels in T cells isolated from Smith-Lemli-Opitz syndrome patients (poster)

Authors: Andras Balajthy, Zoltan Petho, Sandor Somodi, Zoltan Varga, Maria Peter, Laszlo Vigh, Gabriella P. Szabó, Gyorgy Paragh, Gyorgy Panyi, Peter Hajdu

february 11.- 15. 2017: Biophysical Society 61th Annual meeting (BSM) , New Orleans, USA.

- KCa1.1 Channel Auxiliary Beta Subunit Composition in Glioblastoma Multiforme (poster)

Authors: Zoltan Denes Petho, Andras Balajthy, Almos Klekner, Laszlo Bogнар, Zoltan Varga, Gyorgy Panyi

may 17.- 19. 2017: Brain Tumor Congress, Berlin, Germany.

- KCa1.1 Channel Auxiliary Beta Subunit Composition in Glioblastoma Multiforme (poster)

Authors: Zoltan Denes Petho, Andras Balajthy, Almos Klekner, Laszlo Bogнар, Zoltan Varga, Gyorgy Panyi

june 23.- 27. 2017: 6th International Ion Channel Conference Qingdao, China.

- The specific fluorescent signal in voltage clamp fluorometry originates from quenching amino acids in the Ci-Hv1 proton channel (poster)

Authors: Zoltán Pethő, György Panyi, Zoltán Varga, Ferenc Papp

III. Student Research Conferences

2009 / 2010. local TDK conference, Debrecen:

- Különböző stimulációk hatására bekövetkező proliferáció- és ionáramváltozás T-limfocitákon (1. prize)

Authors: Pethő Zoltán Dénes, Balajthy András

- Kv1.3 ioncsatornák vizsgálata hypercholesterinaemiás állapotban

Authors: Balajthy András, Pethő Zoltán Dénes

2010 / 2011. local TDK conference, Debrecen:

- Kationcsatorna-gátlók hatása mitogénnel stimulált T-limfocitákra (1. prize)

Authors: Pethő Zoltán Dénes, Balajthy András

- Limfociták proliferációjának és Kv1.3 kálium ioncsatornáinak vizsgálata hiperkoleszterinemiás állapotban (1. prize)

Authors: Balajthy András, Pethő Zoltán Dénes

2011 / 2012. local TDK conference, Debrecen:

- A koleszterin bioszintézis örökletes zavara (SLO szindróma) módosítja a limfociták Kv1.3 csatornáinak működését és proliferációját (1. prize)

Authors: Balajthy András, Pethő Zoltán Dénes

2012 / 2013. local TDK conference, Debrecen:

- Mezenhimális őssejtek és limfociták kölcsönhatásainak vizsgálata (1. prize)

Authors: Pethő Zoltán Dénes, Balajthy András

2013 / 2014. local TDK conference, Debrecen:

-Módosított tenyésztőoldat előállítására K⁺ - csatorna gátlók hatásának optimalizálásához (3. díj)

Authors: Pethő Zoltán Dénes, Balajthy András

2010 / 2011. XXX. National OTDK conference -Debrecen:

- Kationcsatorna-gátlók hatása mitogénnel stimulált T-limfocitákra (2. díj)

Authors: Pethő Zoltán Dénes, Balajthy András

- Limfociták proliferációjának és Kv1.3 kálium ioncsatornáinak vizsgálata hiperkoleszterinémias állapotban (3. díj)

2012 / 2013. XXXI. National OTDK conference-Szeged:

- Mezenhimális őssejtek és limfociták kölcsönhatásainak vizsgálata (különdíj)

Authors: Pethő Zoltán Dénes, Balajthy András

- A koleszterin bioszintézis örökletes zavara (SLO szindróma) módosítja a limfociták Kv1.3 csatornáinak működését és proliferációját (1. díj)

Authors: Balajthy András, Pethő Zoltán Dénes

2014 / 2015. XXXII. National OTDK konferencia-Budapest:

- Módosított tenyésztőoldat előállítására K⁺ - csatorna gátlók hatásának optimalizálásához (2. díj)

Author: Pethő Zoltán Dénes

2013. TDK thesis (diplomamunka):

- Kationcsatorna-gátlók hatása mitogénnel stimulált T-limfocitákra

Author: Pethő Zoltán Dénes

12. KEYWORDS

ion channel

potassium channel

regulatory subunit

patch clamp

electrophysiology

cell proliferation

cell migration

cytokine secretion

T lymphocyte

autoimmune disease

arthritis

KULCSSZAVAK

ioncsatorna

kálium csatorna

járolékos alegység

patch-clamp

elektrofiziológia

sejtproliferáció

sejtmigráció

citokinszekréció

T limfocita

autoimmun betegség

arthritis

13. ACKNOWLEDGEMENTS

First and foremost, I would like to express my deepest gratitude to my supervisor Dr. Zoltán Varga, who has been my mentor throughout my medical studies as well as during my PhD education.

Also, sincerely appreciate the tremendous help from Prof. Dr. György Panyi, the leader of the Electrophysiology Laboratory, who has invited me to the workgroup as a first-year medical student and provided me with invaluable insights both in the scientific and in the everyday life during the last ten years.

Also, am extremely grateful to Dr. Christine Beeton, who has welcomed and accepted me in her lab during my scholarship as a first-year graduate student and her inspirational insights led to an exceptionally productive collaboration between our workgroups.

I would also like to thank the head of the Department of Biophysics and Cell Biology, Prof. Dr. János Szöllősi for allowing me to pursue my research in the department.

Moreover, I cannot even begin to express my appreciation to Dr. András Balajthy, whose help motivated me during the past decade.

The continuous and helpful assistance provided by our lab technicians, Cecília Nagy and Adrienn Bagosi are also greatly appreciated.

I must thank the past and present members of our laboratory: Dr. Zoltán Krasznai, Dr. Sándor Somodi, Dr. Tibor G. Szántó, Dr. Ferenc Papp, Dr. Ádám Bartók, Dr. Orsolya Szilágyi, Dr. Beáta Mészáros, Dr. Ágnes Tóth, Dr. Pál Pap, Dr. Brigitta Domján, Dr. Florina Zákány, Orsolya Vörös, who have not only helped me during my professional life, but have also ensured a great atmosphere to work in.

Also, I am grateful for the members of Christine Beeton's lab, Dr. Rajeev B. Tajhya, Dr. Redwan Huq, and Mark. R. Tanner, who put a lot of effort in helping and training me during my stay at Baylor College of Medicine.

Furthermore, I would like to thank Dr. Pércio S. Gulko and Theresa Laragione, our collaborators from the Icahn School of Medicine at Mount Sinai who provided us with FLS and verified their purity.

Finally, I express my deepest appreciations to my Family and my Fiancée, who never gave up on me and have always supported me.

The experimental work was performed by the support of the TÁMOP-4.2.2.A-11/1-KONV/2012-0025 project and of Baylor College of Medicine fundings,. The doctoral training program was supported by the Campus Hungary Fellowship and the Hungarian National Excellence Program. This research was supported by the European Union and the State of Hungary, co-financed by the European Social Fund in the framework of TÁMOP 4.2.4. A/2-11-1-2012-0001 ‘’ and KTIA_NAP_13-2-2015-0009. Lastly, the work is supported by the GINOP-2.3.2-15-2016-00015 project. The project is co-financed by the European Union and the European Regional Development Fund.